August '94

An Introduction to Wavelet Transforms

P. P. Vaidyanathan and Igor Djokovic

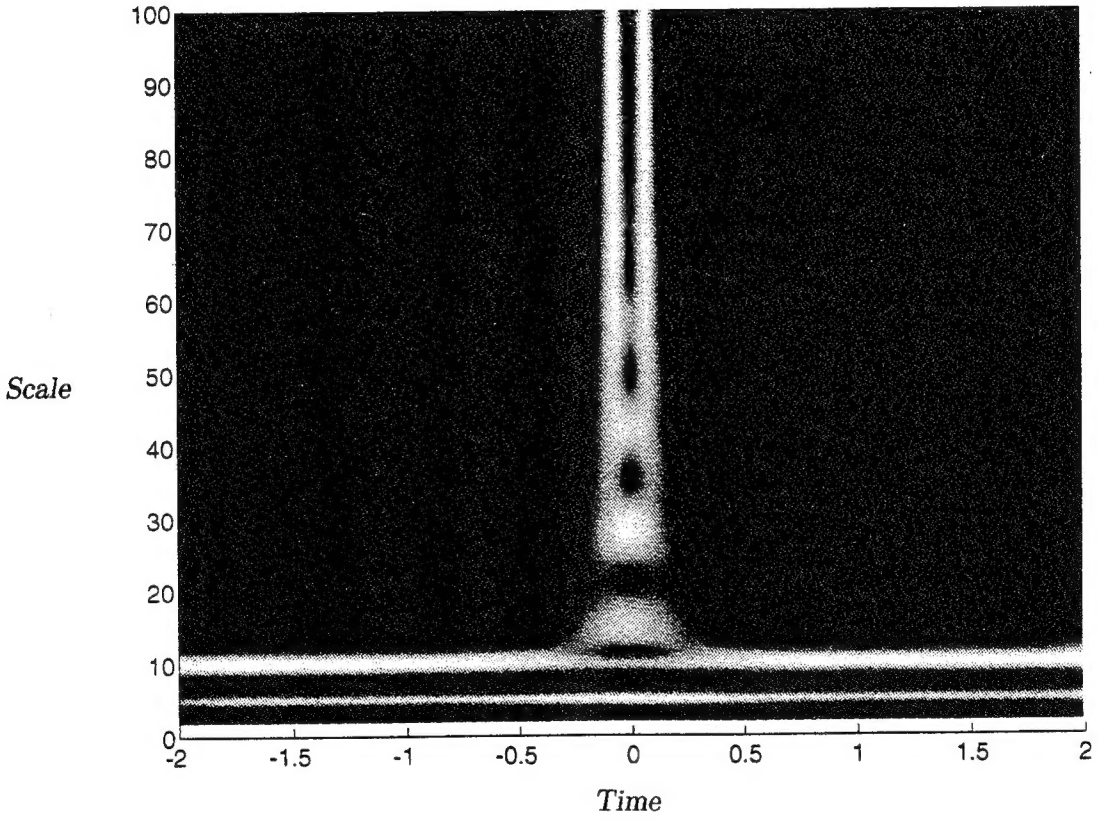

California Institute of Technology
Pasadena, CA 91125

An Introduction to Wavelets

P. P. Vaidyanathan and Igor Djokovic, Caltech, Pasadena, CA 91125

TABLE OF CONTENTS

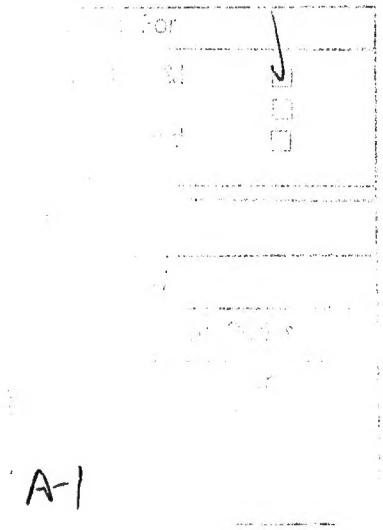

Work supported in parts by Office of Naval Research grant N00014-93-1-0231, Rockwell International, and Tektronix, Inc.

Preface

These notes are meant to provide an introduction to wavelet transforms. The first five sections can be accessed by readers with some exposure to signal processing tools. Sec. 9 – Sec. 13 present advanced material which is at the heart of wavelet research today. While maintaining a mathematically rigorous presentation level, we have attempted to make the presentation accessible to signal processors, and engineers in general. To make this possible, we have included three review sections on mathematics (Sec. 6 – Sec. 8), especially on L^1 and L^2 Fourier transforms, *Frames*, and *Riesz bases* in infinite dimensions.

A slightly reduced version is scheduled to appear in the **Mathematics Section** of the **Circuits and Filters Handbook,** to be published by **CRC Press, Inc.**, next year. There is an appendix on *Distributions* which will probably be deleted from the version to be published.

Remember that this is a handbook chapter, not a text book chapter. Proofs of many standard results are excluded, but with proper citations. We have given *Sketches of Proofs* for some of the recent wavelet results (Sec. 11 – Sec. 13, especially) which brought them to the level of importance they enjoy today. *Comments and suggestions from you, the reader, are most welcome. Enjoy!*

P. P. Vaidyanathan and Igor Djokovic

August 1994

An Introduction to Wavelet Transforms

P. P. Vaidyanathan and Igor Djokovic, Caltech, Pasadena, CA 91125

A new idea is first attacked as absurd; then it is admitted to be true, but obvious; finally it is seen to be so important, that its adversaries claim that they themselves discovered it — William James

1. INTRODUCTION

Transform techniques such as the Fourier and Laplace transforms, and the z-transform have been used in a wide variety of scientific and engineering disciplines for a long time [Van Valkenburg, 1960], [Papoulis, 1962], [Oppenheim, et al., 1983]. In a number of applications where we require a joint time-frequency picture, it is necessary to consider other types of transforms or time-frequency representations. Many such methods have evolved. In particular the wavelet transform technique [Grossman and Morlet, 1984], [Meyer, 1986], [Daubechies, 1992], has some unique advantages over other kinds of time-frequency representations such as the short-time Fourier transform. For historical developments as well as many technical details and original material see [Daubechies, 1992]. In this chapter we will describe some of these representations, and explain the advantages of the wavelet transform, and the reason for its recent popularity.

A subclass of wavelet transforms [Daubechies, 1988], has an intimate connection with the theory of digital filter banks. Filter banks have been known to the signal processing community for over two decades, see [Vaidyanathan, 1993] and references therein, especially [Croisier et al., 1976], [Crochiere and Rabiner, 1983], [Vetterli, 1987], [Akansu and Haddad, 1992] and [Malvar, 1992]. It is this relation that makes it possible to construct in a systematic way a wide family of wavelets with several desirable properties such as compact support (i.e., finite duration), smoothness, good time-frequency localization, and basis-orthonormality (all these terms will be explained later).

The connection between wavelets and filter banks finds beautiful mathematical expression in the theory of multiresolution [Mallat, 1989a]. This enables us to compute the wavelet transform coefficients using the so called *Fast Wavelet Transform (FWT)*, which is essentially a tree structured filter bank. In addition to the practical value, many deep results from several disciplines find a unified home in the theory and development

Work supported in parts by Office of Naval Research grant N00014-93-1-0231, Rockwell International, and Tektronix, Inc.

of the wavelet transform. This includes signal processing, circuit theory, communications, and mathematics. Our emphasis here will be this unification, and the beautiful big picture that it provides. Other tutorials on wavelets with different choices of emphasis can be found in Heil and Walnut [1989], Rioul and Vetterli [1991], Vetterli and Herley [1992], Strang [1993], Vaidyanathan [1993] and Gopinath and Burrus [1993].

Scope and Outline

The literature on wavelets is enormous, and an attempt to do justice to everything would prove to be futile. Even a list of references that is fair to all contributors would be too long. We therefore restrict discussions to really basic, core material. Sections 1–5 give an overview, with the presentation given at a level that can be comprehended by most engineers. The more advanced results on wavelets, which really brought them great attention in recent years, are presented in the last five sections Sec. 9–13. At the heart of these results lie several powerful mathematical tools, which are usually not familiar to engineers. We have therefore presented a fairly extensive math review in three sections (Sec. 6–8). We suggest that the reader go through this review material once and then use it primarily as a reference.

The advanced sections 9-13 are organized such that the main points, summarized as Theorems for convenience of reference, can be appreciated even without the mathematical background material in Sec. 6–8. The mathematical sections do, however, facilitate a deeper understanding. It is our hope that these sections will bring most readers to a point where they can pursue wavelet literature without difficulty.

Why Wavelets?

A commonly asked question is "why wavelets?", that is, "what are the advantages offered by wavelets over other types of transform techniques such as, for example, the Fourier transform?" The answer to this question is fairly sophisticated, and also depends on the level at which we address the question. Several discussions addressing this question are scattered throughout this chapter. A convenient listing of the locations of these discussions is given in the concluding section (Sec. 14) under "Why Wavelets?"

General Notations and Acronyms

1. Bold faced quantities represent matrices and vectors.
2. The notations $\mathbf{A}^T, \mathbf{A}^*$ and $\mathbf{A}^\dagger$ represent, respectively, the transpose, conjugate, and transpose-conjugate of the matrix $\mathbf{A}$.
3. The accent 'tilde' is defined as follows: $\widetilde{\mathbf{H}}(z) = \mathbf{H}^\dagger(1/z^*)$; thus if $\mathbf{H}(z) = \sum_n \mathbf{h}(n)z^{-n}$ then $\widetilde{\mathbf{H}}(z) = \sum_n \mathbf{h}^\dagger(-n)z^{-n}$. On the unit circle $\widetilde{\mathbf{H}}(z) = \mathbf{H}^\dagger(z)$.
4. *Acronyms.* BIBO (Bounded-Input Bounded-Output); FIR (Finite Impulse Response); IIR (Infinite

Impulse Response); LTI (Linear Time Invariant); PR (Perfect Reconstruction); STFT (Short-Time Fourier Transform); WT (Wavelet Transform).

5. For LTI systems, "stability" stands for BIBO stability.
6. $\delta(n)$ denotes the unit pulse or discrete-time impulse, defined such that $\delta(0) = 1$ and $\delta(n) = 0$ otherwise. This should be distinguished from the Dirac delta function [Oppenheim, et al., 1983], which is denoted as $\delta_a(t)$.
7. *Figures.* Sampled versions of continuous time signals are indicated with an arrow on the top (e.g., Fig. 2.10 (a)). The sampled versions are impulse trains of the form $\sum_n c(n)\delta_a(t-n)$, and are functions of continuous t.

2. SIGNAL REPRESENTATION USING BASIS FUNCTIONS

The electrical engineer is very familiar with the Fourier transform (FT) and its role in the study of linear time invariant (LTI) systems or *filters.* For example the frequency response of an LTI system is the FT of its impulse response. The FT is also used routinely in the design and analysis of circuits. As a reminder, the Fourier transform of a signal $x(t)$ is given by the familiar integral $X(\omega) = \int_{-\infty}^{\infty} x(t)e^{-j\omega t}dt$ and the inverse transform by†

$$x(t) = \frac{1}{2\pi}\int_{-\infty}^{\infty} X(\omega)e^{j\omega t}d\omega \tag{2.1}$$

From this equation we can say that $x(t)$ has been expressed as a linear superposition (or linear combination) of an infinite number of functions $g_\omega(t) \triangleq e^{j\omega t}$. Since the frequency ω is a continuous variable, there are uncountably many functions $g_\omega(t)$ to be superimposed. Electrical engineers, in particular signal processors and commnications engineers are also familiar with two special classes of signals which can be regarded as a superposition of *countably* many functions. That is,

$$x(t) = \sum_{n=-\infty}^{\infty} \alpha_n g_n(t), \tag{2.2}$$

where α_n are scalars (possibly complex) uniquely determined by $x(t)$. These two examples are (i) time-limited signals for which we can find a Fourier series (FS), and (ii) bandlimited signals which can be reconstructed from uniformly spaced samples by weighting them with shifted sinc functions (see below).

First consider a time-limited signal $x(t)$ with duration $0 \le t \le 1$ (Fig. 2.1). Under some mild conditions such a signal can be represented in the form (2.2) with $g_n(t) = e^{j2\pi nt}$. The expression (2.2) is then the

† At the moment it is not necessary to worry about the existence, invertibility, and the type (e.g., L^1 or L^2) of the FT. We return to the mathematical subtleties in Sec. 6.3.

Fouier series of $x(t)$, and α_n are the Fourier coefficients. (In contrast we say that (2.1) is the *Fourier integral* of $x(t)$.) The "transform domain" signal $\{\alpha_n\}$ is a sequence, and the transform domain variable is discrete, namely the frequencies $\omega_n \triangleq 2\pi n$. Since $e^{j2\pi nt}$ is periodic in t with period one, the right hand side of (2.2) is periodic, and it represents $x(t)$ only in $0 \leq t \leq 1$. It is sometimes convenient to replace the complex functions $e^{j2\pi nt}$ with the set of real functions $1, \sqrt{2}\cos(2\pi nt), \sqrt{2}\sin(2\pi nt), n > 0$, especially in circuit analysis.

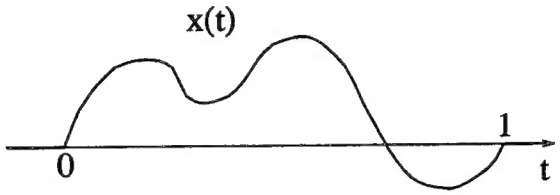

Fig. 2.1. A finite duration signal, with support $0 \leq t \leq 1$.

Next consider a bandlimited signal $x(t)$ with Fourier transform $X(\omega)$ as demonstrated in Fig. 2.2.

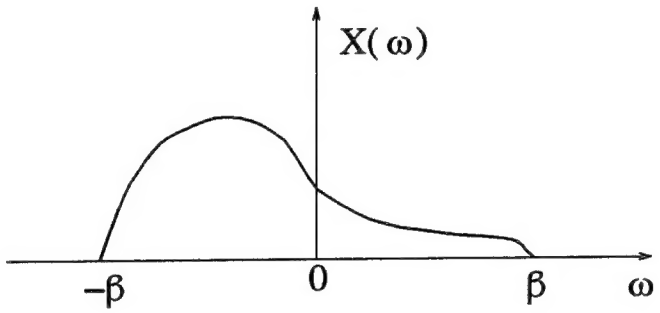

Fig. 2.2. Fourier transform of a signal bandlimited to $|\omega| < \beta$.

If we sample the signal at the Nyquist rate 2β radians/sec (i.e., sampling period $T = \pi/\beta$), then multiple copies of the Fourier transform are generated [Oppenheim, et al., 1983], and we can recover $x(t)$ from the samples by use of an ideal lowpass filter $F(\omega)$ (Fig. 2.3).

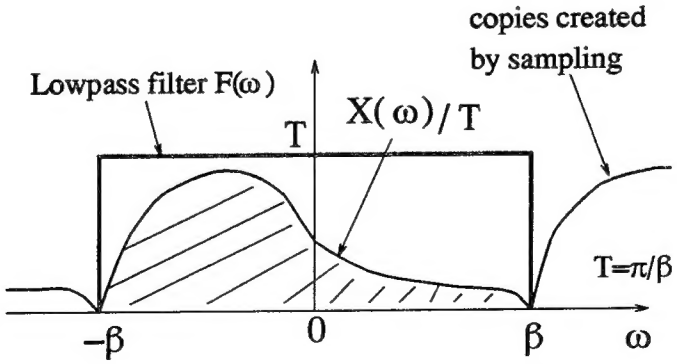

Fig. 2.3. Use of lowpass filter $F(\omega)$ to recover $x(t)$ from its samples.

The impulse response of the filter is the sinc function $f(t) = \frac{\sin \beta t}{\beta t}$ so that the reconstruction formula is

$$x(t) = \sum_{n=-\infty}^{\infty} x(nT) f(t - nT) = \sum_{n=-\infty}^{\infty} x(nT) \frac{\sin \beta(t - nT)}{\beta(t - nT)}, \quad T = \pi/\beta. \tag{2.3}$$

Comparing with (2.2) we see that the "transform domain coefficients" α_n can be regarded as the samples $x(nT)$, whereas the functions $g_n(t)$ are the shifted sinc functions.

If a signal is time-limited or bandlimited, we can therefore express it as a countable linear combination of a set of fundamental functions (called *basis* functions, in fact an orthonormal basis — see below). If the signal is more arbitrary (i.e., not limited in time or bandwidth) can we still obtain such a countable linear combination?

Suppose we restrict $x(t)$ to be a finite energy signal (i.e., $\int |x(t)|^2 dt < \infty$; also called L^2 signals, see Sec. 2.2). Then this is possible. In fact, we can even find an unusual kind of basis called the *wavelet basis,* fundamentally different from the Fourier basis. Representation of $x(t)$ using this basis has, in some applications, some advantages over the Fourier representation or the short-time (windowed) Fourier representation. Wavelet bases also exist for many other classes of signals but we will only consider the L^2 class of signals.

The most common kind of *wavelet representation* takes the form

$$x(t) = \sum_{k=-\infty}^{\infty} \sum_{n=-\infty}^{\infty} c_{kn} \underbrace{2^{k/2} \psi(2^k t - n)}_{\psi_{kn}(t)} \tag{2.4}$$

The functions $\psi_{kn}(t)$ are typically (but not necessarily) linearly independent and form a basis for finite energy signals. The basis is very special in the sense that all the functions $\psi_{kn}(t)$ are derived from a single function $\psi(t)$ called the *wavelet,* by two operations: dilation ($t \to 2^k t$) and time-shift ($t \to t - 2^{-k} n$). The advantage of such a basis is that it allows us to capture the details of a signal at various scales, while providing a time-localization information for these "scales". Examples in future sections will make this idea clearer.

Why Worry About Signal Representations?

A common feature of all the above discussions is that we have taken a signal $x(t)$ and found an equivalent representation in terms of the transform domain quantity $\{\alpha_n\}$ in (2.2), or $\{c_{kn}\}$ in (2.4). If our only aim is to compute α_n from $x(t)$ and then recompute $x(t)$ from α_n, that would be a futile excercise. The motivation in practice is that the transform domain quantities are better suited in some sense. For example in audio coding, decomposition of a signal into frequency components is motivated by the fact that the human ear perceives higher frequencies with less frequency resolution. We can use this information. We can also code the high frequency components with relatively less precision, thereby enabling data compression. In this way we can take into account perceptual information during compression. We could also account for the

fact that the error allowed by the human ear (due to quantization of frequency components) depends on the frequency masking property of the ear, and perform optimum bit allocation for a given bit rate.

Other applications of signal representations using wavelets include numerical analysis, solution of differential equations, and many others [Daubechies, 1992], [Chui, 1992b], [Benedetto and Frazier, 1994].

The main point, in any case, is that we typically perform certain manipulations with the transform domain coefficients α_n [or c_{kn} in (2.4)] before we recombine them to form an approximation of $x(t)$ again. Therefore, we really only have

$$\widehat{x}(t) = \sum_n \widehat{\alpha}_n g_n(t) \tag{2.5}$$

where $\{\widehat{\alpha}_n\}$ approximates $\{\alpha_n\}$. This discussion gives rise to many questions: how best to choose the basis functions $g_n(t)$ for a given application? How to choose the compressed signal $\{\widehat{\alpha}_n\}$ so that for a given data rate the reconstruction error is minimized? What, indeed, is the best way to define the reconstruction error?

These questions are deep and complicated, and will take us too far afield. We will not address them. Our goal is to point out the basic advantages (sometimes) offered by the wavelet transform over other kinds of transforms (e.g., the Fourier transform).

2.1. The ideal bandpass wavelet

Consider a bandpass signal $x(t)$ with Fourier transform as shown in Fig. 2.4.

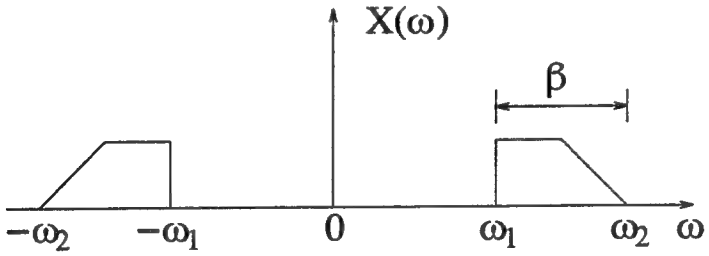

Fig. 2.4. Fourier transform of a bandpass signal.

Such signals arise in communication applications. The bandedges of the signal are ω_1 and ω_2 (and $-\omega_1$ and $-\omega_2$ on the negative side, which is natural if $x(t)$ is real). Viewed as a lowpass signal, the total bandwidth (counting negative frequencies also) is $2\omega_2$. But viewed as a bandpass signal, the total bandwidth is only 2β where $\beta = \omega_2 - \omega_1$. Does it mean that we can sample it at the rate 2β radians/sec (which is the Nyquist rate for the lowpass case)?

In the lowpass case, sampling at Nyquist rate was enough to ensure that the copies of the spectrum created by sampling do not overlap (Fig. 2.3). In the bandpass case, we have two sets of such copies; one created by positive half of the frequency $\omega_1 \le \omega \le \omega_2$ and the other by the negative half $-\omega_2 \le \omega \le -\omega_1$.

This makes the problem somewhat more complicated. It can be shown that for sampling at the rate 2β there is no overlap of images if and only if one of the edges, ω_1 or ω_2, is a multiple of 2β. This is called the *bandpass sampling theorem.* The reconstruction of $x(t)$ from the samples proceeds exactly as in the lowpass case, except that the reconstruction filter $F(\omega)$ is now a bandpass filter (Fig. 2.5) occupying precisely the signal bandwidth. The first part of the expression (2.3) is therefore still valid, i.e., $x(t) = \sum_n x(nT) f(t-nT)$ where $T = \pi/\beta$ again, but the sinc function is replaced with the bandpass impulse response $f(t)$.

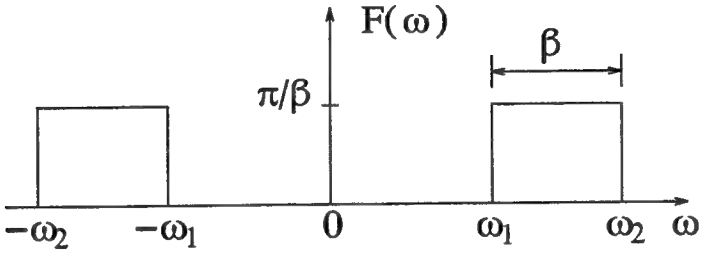

Fig. 2.5. Bandpass filter to be used in the reconstruction of the bandpass signal from its samples.

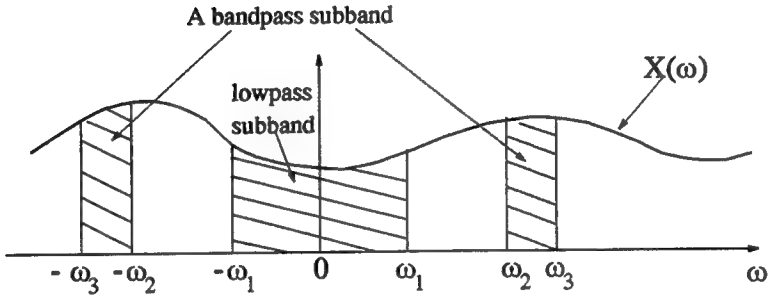

Fig. 2.6. Splitting a signal into frequency subbands.

Given a signal $x(t)$, imagine now that we have split its frequency axis into subbands in some manner (Fig. 2.6). Letting $y_k(t)$ denote the kth subband signal, we can write $x(t) = \sum_k y_k(t)$. This can be visualized as passing $x(t)$ through a bank of filters $\{H_k(\omega)\}$, Fig. 2.7(a), with responses as in Fig. 2.7(b). Note that each subband region is symmetric with respect to zero frequency, and therefore supports positive as well as negative frequencies. If the subband region $\omega_k \leq |\omega| < \omega_{k+1}$ satisfies the bandpass sampling condition, then the bandpass signal $y_k(t)$ can be expressed as a linear combination of its samples as before. Thus, $x(t) = \sum_k y_k(t) = \sum_k \sum_n y_k(nT_k) f_k(t - nT_k)$, where $T_k = \pi/\beta_k$. Here $f_k(t)$ is the impulse response of the reconstruction filter (or synthesis filter) $F_k(\omega)$ shown in Fig. 2.7(c). Fig. 2.7(a) also shows this reconstruction schematic.

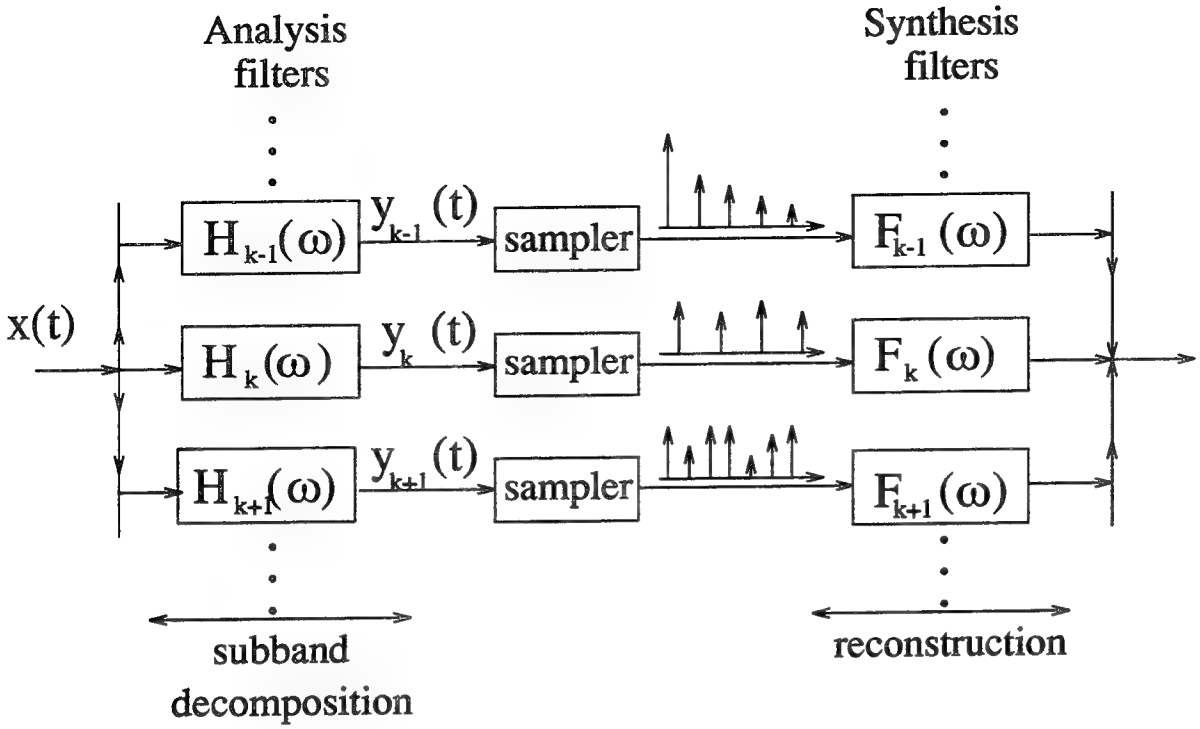

(a)

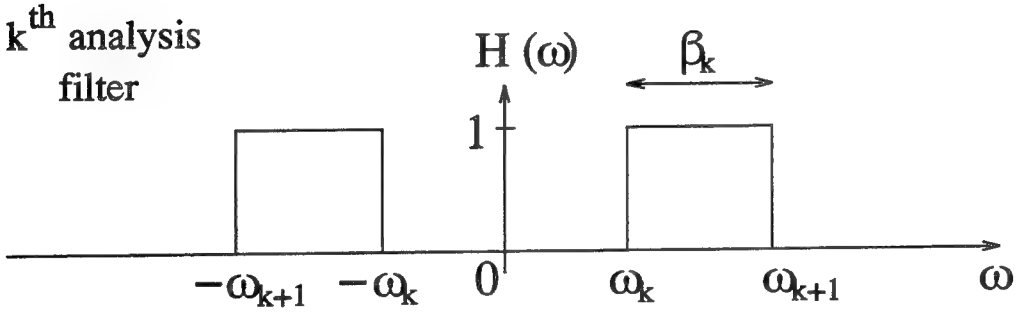

(b)

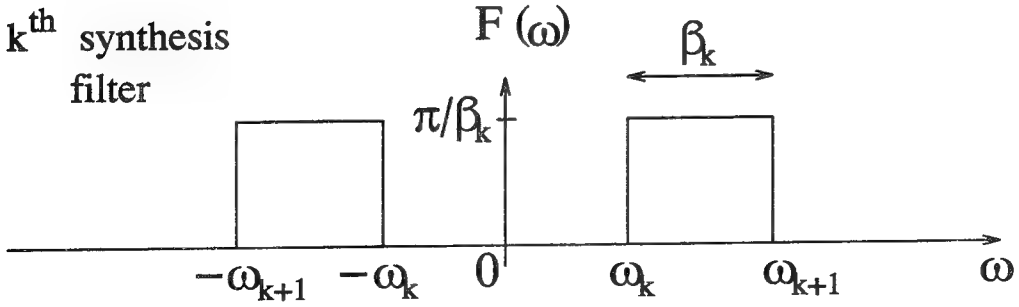

(c)

Fig. 2.7. (a) Splitting a signal into subband signals, sampling and then recombining, (b) response of k^{th} analysis filter and (c) response of k^{th} synthesis filter.

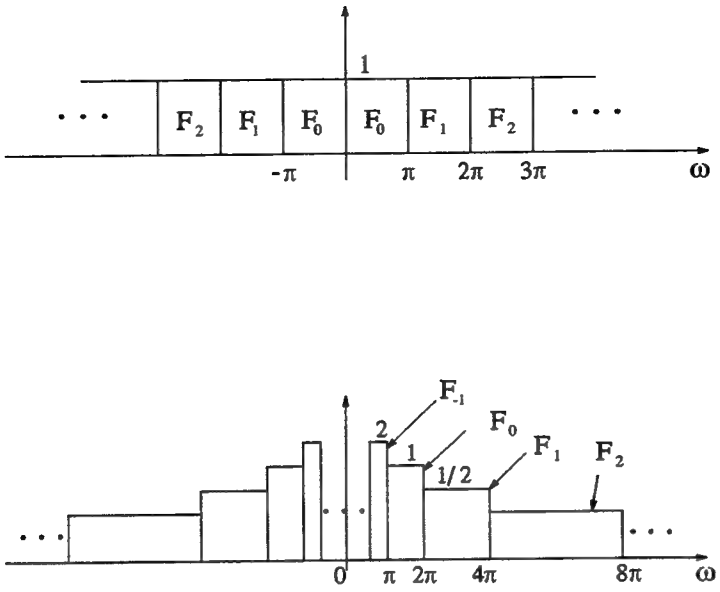

Fig. 2.8. Two possible schemes to decompose a signal into frequency bands.
(a) uniform splitting, and (b) octave band splitting.
The responses shown are those of synthesis filters.

Fig. 2.8 shows the set of synthesis filters $\{F_k(\omega)\}$ for two examples of frequency splitting arrangement, namely uniform splitting and nonuniform (octave) splitting. We will see later that the uniform splitting arrangement gives an example of the short time Fourier transform (STFT) representation (Sec. 3 and 9). In this section we are interested in octave splitting. The bandedges of the filters here are $\omega_k = 2^k\pi$ ($k = \ldots -1, 0, 1, 2, \ldots$). The bandedges are such that $y_k(t)$ is a signal satisfying the bandpass sampling theorem. It has $\beta_k = 2^k\pi$ according to the notation of Fig. 2.7. It can be sampled at period $T_k = \pi/\beta_k = 2^{-k}$ without aliasing, and we can reconstruct it from samples as

$$y_k(t) = \sum_{n=-\infty}^{\infty} y_k(2^{-k}n) f_k(t - 2^{-k}n). \tag{2.6}$$

As k increases, the bandwidths of the filters increase so the sample spacing $T_k = 2^{-k}$ gets finer. Since $x(t) = \sum_k y_k(t)$ we see that $x(t)$ can be expressed as

$$x(t) = \sum_{k=-\infty}^{\infty} \sum_{n=-\infty}^{\infty} y_k(2^{-k}n) f_k(t - 2^{-k}n). \tag{2.7}$$

Our definition of the filters shows that the frequency responses are scaled versions of each other, that is $F_k(\omega) = 2^{-k}\Psi(2^{-k}\omega)$ with $\Psi(\omega)$ as in Fig. 2.9. The impulse responses are therefore related as $f_k(t) = \psi(2^k t)$, and we can rewrite (2.7) as

$$x(t) = \sum_{k=-\infty}^{\infty} \sum_{n=-\infty}^{\infty} y_k(2^{-k}n) \psi(2^k t - n) \tag{2.8}$$

We will write this as $x(t) = \sum_k \sum_n c_{kn}\psi_{kn}(t)$ by defining $c_{kn} = 2^{-k/2}y_k(2^{-k}n)$ and

$$\psi_{kn}(t) = 2^{k/2}\psi(2^k t - n) = 2^{k/2}\psi\Big(2^k(t - 2^{-k}n)\Big) \tag{2.9}$$

Then the functions $\psi_{kn}(t)$ will have the same energy $\int |\psi_{kn}(t)|^2 dt$ for all k, n. From the analysis/synthesis filter bank point of view (Fig. 2.7) this is equivalent to making $H_k(\omega) = F_k(\omega)$ and rescaling as shown in Fig. 2.10. With filters so rescaled, the wavelet coefficients c_{kn} are just samples of the outputs of the analysis filters $H_k(\omega)$.

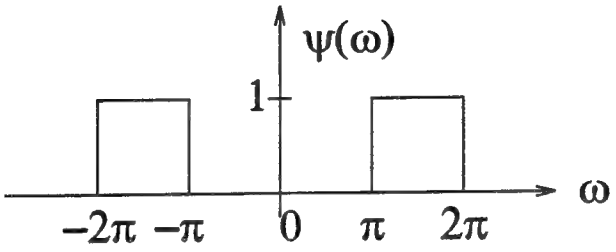

Fig. 2.9. The fundamental bandpass function that generates a bandpass wavelet.

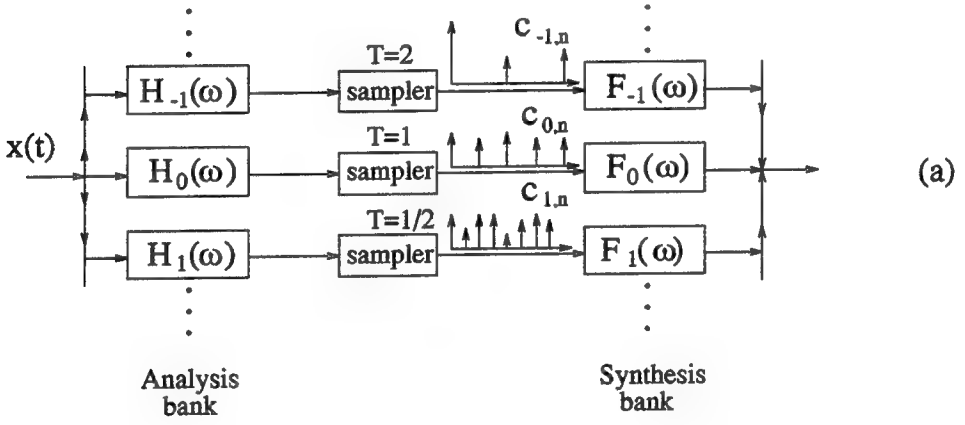

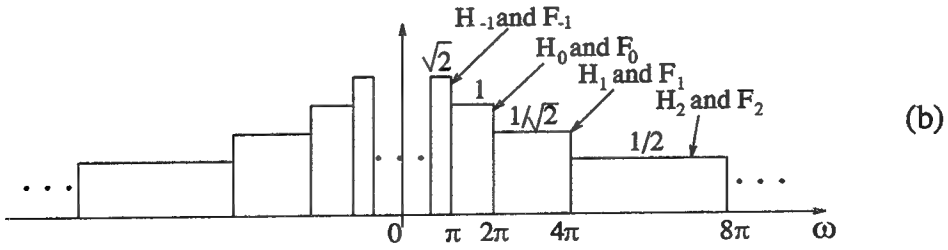

Fig. 2.10. The octave-band splitting scheme. (a) The analysis bank, samples and synthesis bank, and (b) the filter responses.

The function $\psi(2^k t)$ is a dilated version of $\psi(t)$ (squeezed version if $k > 0$ and stretched version if $k < 0$).

The dilation factor 2^k is a power of two, so this is said to be a dyadic dilation. The function $\psi(2^k(t-2^{-k}n))$ is a shifted version of the dilated version. Thus we have expressed $x(t)$ as a linear combination of shifted versions of (dyadic) dilated versions of a single function $\psi(t)$. The shifts $2^{-k}n$ are in integer multiples of 2^{-k} where k governs the dilation. For completeness note that the impulse response $\psi(t)$ corresponding to the function in Fig. 2.9 is given by

$$\psi(t) = \frac{\sin(\pi t/2)}{\pi t/2}\cos(3\pi t/2) \qquad \text{(ideal bandpass wavelet).} \tag{2.10}$$

This is plotted in Fig. 2.11.

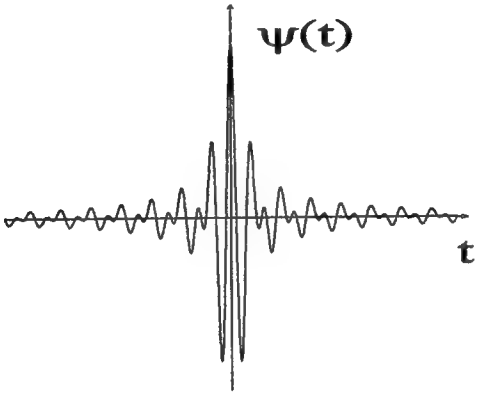

Fig. 2.11. The ideal bandpass wavelet.

In (2.8) we have obtained a wavelet representation for $x(t)$ (compare with (2.4)). The function $\psi(t)$ is called the *ideal bandpass wavelet.* It has also been known as the Littlewood-Paley wavelet. We will now introduce some terminology for convenience and then return to more detailed definitions and discussions of the wavelet transform.

2.2. L^2 spaces, basis functions and orthonormal bases

Most of our discussions will be restricted to the class of L^2 functions or square integrable functions, that is, functions $x(t)$ for which $\int |x(t)|^2 dt$ exists and has a finite value. The norm or L^2 norm of such functions, denoted $\|x(t)\|_2$ is defined as $\|x(t)\|_2 = \left(\int |x(t)|^2 dt\right)^{1/2}$. The notation $L^2[a,b]$ stands for L^2 functions that are zero outside the interval $a \le t \le b$. The set $L^2(R)$ is the class of L^2 functions supported on the real line $-\infty < t < \infty$. We often abbreviate $L^2(R)$ as L^2.

It turns out that the class of L^2 functions forms a (normed) linear vector space, i.e., any linear combination of functions in L^2 is still in L^2. In fact it forms a special linear space such that there exists a countable basis. That is, there is a sequence of linearly independent functions $\{g_n(t)\}$ in L^2 such that any L^2 function $x(t)$ can be expressed as $x(t) = \sum_n \alpha_n g_n(t)$, for a unique set of $\{\alpha_n\}$. We say that $g_n(t)$ are the

basis functions. In fact L^2 spaces have orthonormal bases. For such a basis, the basis functions satisfy

$$\langle g_k(t), g_m(t) \rangle = \delta(k-m) \tag{2.11}$$

where the notation $\langle f(t), g(t) \rangle \triangleq \int f(t) g^*(t) dt$ denotes the inner product between $f(t)$ and $g(t)$. For an orthonormal basis, the coefficients α_n in the expansion $x(t) = \sum_{n=-\infty}^{\infty} \alpha_n g_n(t)$ can thus be computed using the exceptionally simple relation

$$\alpha_n = \langle x(t), g_n(t) \rangle \tag{2.12}$$

We have already seen two examples of orthonormal basis above. The first is the Fourier series expansion of a time limited signal ($0 \le t \le 1$). Here the basis functions $\{e^{j2\pi nt}\}$ are clearly orthonormal (with integrals going from 0 to 1). The second example is the expansion (2.3) of a bandlimited signal; it can be shown that the shifted versions $f(t-nT)$ of the sinc functions form an orthonormal basis for bandlimited signals (integrals going from $-\infty$ to ∞).

Orthogonal projections. Suppose we consider a subset $\{g_{n_k}(t)\}$ of the orthonormal basis $\{g_n(t)\}$. Let $\mathcal{S}$ denote the subspace generated by $\{g_{n_k}(t)\}$ (an accurate statement would be that $\mathcal{S}$ is the "closure of the span of $\{g_{n_k}(t)\}$"; see Sec.7.2). Consider the linear combination $y(t) = \sum_k \alpha_{n_k} g_{n_k}(t)$ where the α_{n_k} are evaluated as above, that is $\alpha_{n_k} = \langle x(t), g_{n_k}(t) \rangle$ for some signal $x(t)$. Then $y(t) \in \mathcal{S}$, and it can be shown that among all functions in $\mathcal{S}$, $y(t)$ is the unique signal closest to $x(t)$ (i.e., $\|x(t) - y(t)\|_2$ is the smallest). We say that $y(t)$ is the orthogonal projection of $x(t)$ onto the subspace $\mathcal{S}$, and write

$$y(t) = P_{\mathcal{S}}[x(t)] \tag{2.13}$$

2.3. Wavelet transforms

If a signal $x(t)$ is in L^2, then its Fourier transform $X(\omega)$ exists in the L^2 sense (Sec. 6.3). We will see in Sec. 6.4 that the discussion which resulted in the expression (2.8) is applicable for any signal $x(t)$ in L^2. Eq. (2.8) means that the signal can be expressed as a linear combination of the form

$$x(t) = \sum_{k=-\infty}^{\infty} \sum_{n=-\infty}^{\infty} c_{kn} \underbrace{2^{k/2} \psi(2^k t - n)}_{\psi_{kn}(t)} \tag{2.14}$$

where $\psi(t)$ is the impulse response (Fig. 2.11) of the bandpass function $\Phi(\omega)$ in Fig. 2.9.† Since the frequency responses for two different values of k do not overlap, the functions $\psi_{kn}(t)$ and $\psi_{mi}(t)$ are orthogonal for

† The above equality, and the convergence of the summation should be interpreted in the L^2 sense, see Sec. 6.2.

$k \neq m$ (use Parseval's relation). For a given k, the functions $\psi_{kn}(t)$ are shifted versions of the impulse responses of the bandpass filter $F_k(\omega)$. From the ideal nature of this bandpass filter we can show that $\psi_{kn}(t)$ and $\psi_{im}(t)$ are also orthonormal for $n \neq m$. Thus, the set of functions $\{\psi_{kn}(t)\}$ with k and n ranging over all integers forms an orthonormal basis for the class of L^2 functions. That is, any L^2 function can be expressed as in (2.14) and furthermore

$$\langle \psi_{kn}(t), \psi_{mi}(t) \rangle = \delta(k-m)\delta(n-i). \tag{2.15}$$

Because of this orthonormality, the coefficients c_{kn} are computed very easily as

$$c_{kn} = \langle x(t), \psi_{kn}(t) \rangle = \int_{-\infty}^{\infty} x(t) 2^{k/2} \psi^*(2^k t - n) dt. \tag{2.16}$$

Defining

$$\eta(t) = \psi^*(-t), \tag{2.17}$$

this takes the form

$$c_{kn} = \langle x(t), \eta_{kn}^*(-t) \rangle = \int_{-\infty}^{\infty} x(t) 2^{k/2} \eta(n - 2^k t) dt \tag{2.18}$$

resembling a convolution.

Wavelet transform definitions. A set of basis functions $\psi_{kn}(t)$ derived from a single function $\psi(t)$ by dilations and shifts of the form

$$\psi_{kn}(t) = 2^{k/2} \psi(2^k t - n) \tag{2.19}$$

is said to be a *wavelet basis,* and $\psi(t)$ is called the *wavelet function.* The coefficients c_{kn} are the *wavelet transform coefficients.* The formula (2.16) which performs the transformation from $x(t)$ to c_{kn} is the *wavelet transform* of the signal $x(t)$. Eqn. (2.14) is the *wavelet representation* or the *inverse wavelet transform.* While this is only a special case of more general wavelet decompositions outlined in Sec. 2.7, it is perhaps the most popular and useful one.

Note that the kth dilated version $\psi(2^k t)$ has the shifted versions $\psi(2^k t - n) = \psi(2^k(t - 2^{-k}n))$, so the amount of shift is in integer multiples of 2^{-k}. Thus the *stretched* versions are shifted by *larger* amounts and squeezed versions by smaller amounts. Even though we developed these ideas based on an example, the above definitions still hold generally for any orthonormal wavelet basis. For the ideal bandpass wavelet, the function $\psi(t)$ is real and symmetric (see (2.10)) so that $\eta(t) = \psi(t)$. For more general orthonormal wavelets we have the relation $\eta(t) = \psi^*(-t)$. We say that $\eta(t)$ is the *analyzing wavelet* (because of (2.18)) and $\psi(t)$ the *synthesis wavelet* (because of (2.14)). For the non orthonormal case we still have the transform and inverse transform equations as above, but the relation between $\psi(t)$ and $\eta(t)$ are not as simple as $\eta(t) = \psi^*(-t)$. We will not discuss this.

Before exploring the properties and usefulness of wavelets let us turn to a distinctly different example. This will show that, unlike the Fourier basis functions $\{e^{j2\pi nt}\}$, the wavelet basis functions can be designed by the user. This makes them more flexible, interesting and useful.

2.4. The Haar wavelet basis

As early as 1910 an orthonormal basis for L^2 functions has been found [Haar, 1910], which satisfies the definition of a wavelet basis given above! That is, the basis functions $\psi_{kn}(t)$ are derived from a single function $\psi(t)$ using dilations and shifts as in (2.19). To explain this system first consider a signal $x(t) \in L^2[0,1]$. The Haar basis is built from two functions called $\phi(t)$ and $\psi(t)$, as described in Fig. 2.12. The basis function $\phi(t)$ is a constant in $[0,1]$. The basis function $\psi(t)$ is constant on each half interval, and its integral is zero. After this, the remaining basis functions are obtained from $\psi(t)$ by dilations and shifts as indicated. It is clear from the figure that any two of these functions are mutually orthogonal. We have an orthonormal set, and it can be shown that this set of functions is an orthonormal basis for $L^2[0,1]$. However, this is not exactly a wavelet basis yet, because of the presence of $\phi(t)$.†

If we eliminate the requirement that $x(t)$ be supported or defined only on $[0,1]$ and consider $L^2(R)$ functions then we can still obtain an orthonormal basis of the above form by including the shifted versions $\{\psi(2^k t - n)\}$ for *all* integer values of n, and also including the shifted versions $\{\phi(t-n)\}$. An alternative to the use of $\{\phi(t-n)\}$ would be to use stretched (i.e., $\psi(2^k t), k < 0$) as well as squeezed (i.e., $\psi(2^k t), k > 0$) versions of $\psi(t)$. The set of functions can thus be written as in (2.19), which has the form of a wavelet basis. It can be shown that this forms an orthonormal basis for $L^2(R)$. The Fourier transform of the Haar wavelet $\psi(t)$ is given by

$$\Psi(\omega) = je^{-j\omega/2}\frac{\sin^2(\omega/4)}{\omega/4} \qquad \text{(Haar wavelet).} \tag{2.20}$$

The Haar wavelet has limited duration in time, whereas the the ideal bandpass wavelet (2.10), being bandlimited, has infinite duration in time.

† We will see in Sec. 10 that the function $\phi(t)$ arises naturally in the context of the fundamental idea of multiresolution.

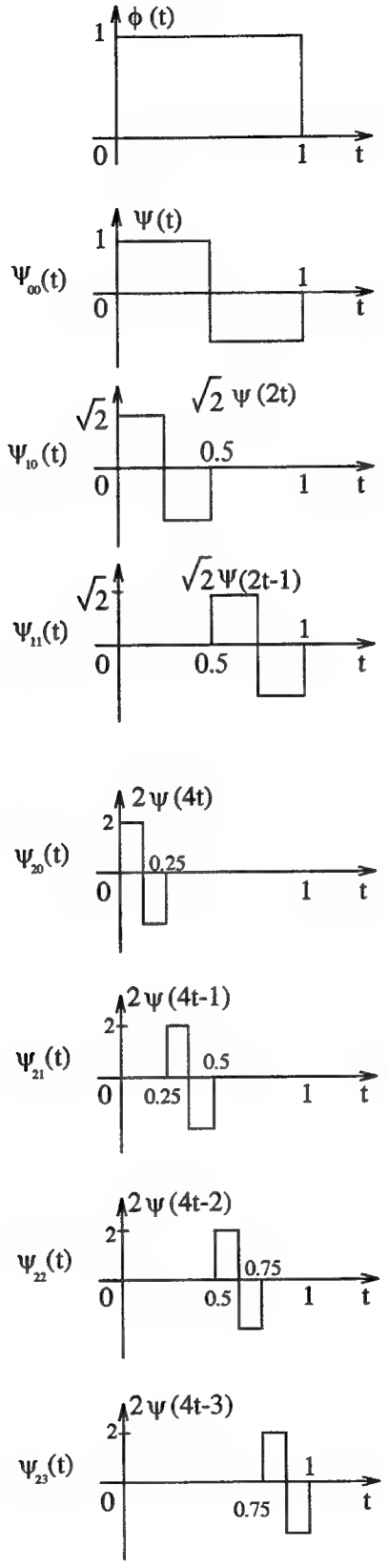

Fig. 2.12. Examples of basis functions in the Haar basis for $L^2[0,1]$.

2.5. Basic properties of wavelet transforms

Based on the definitions and examples provided so far we can already draw some very interesting conclusions about wavelet transforms, and obtain a preliminary comparison with the Fourier transform.

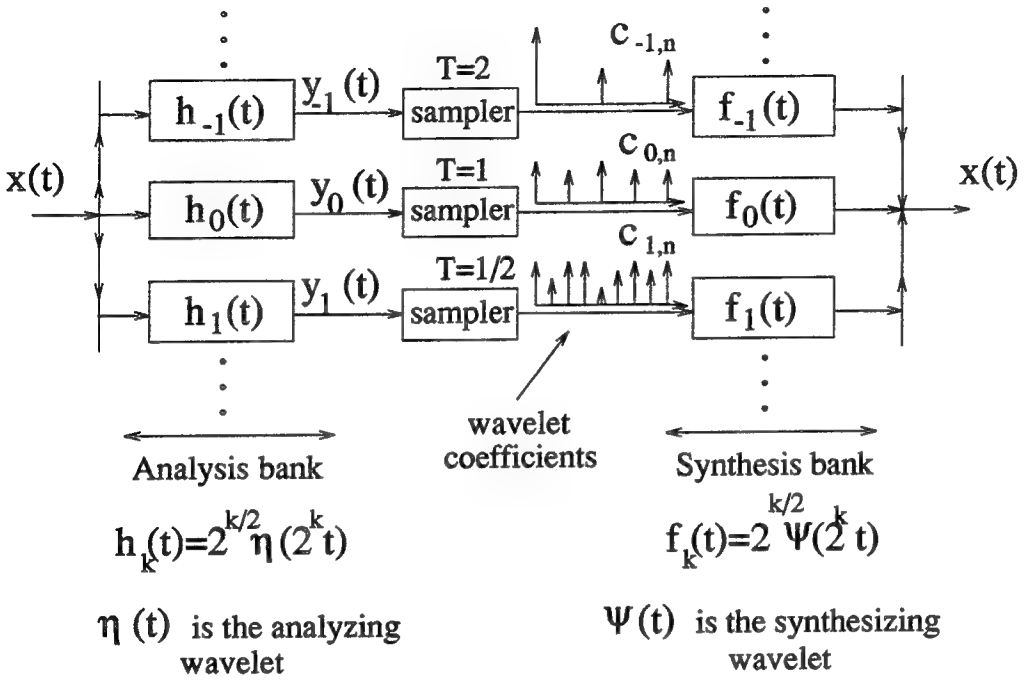

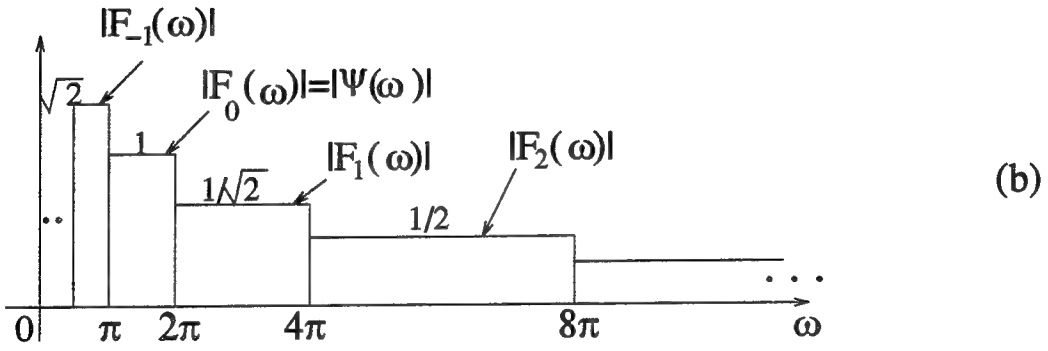

Fig. 2.13. (a) Representing the diadic wavelet transform as an analysis bank followed by samplers, and the inverse transform as a synthesis bank. For the otrhonotmal case, $\psi(t) = \eta^*(-t)$, and $f_k(t) = h_k^*(-t)$.
(b) Filter responses for the example where $\psi(t)$ is the ideal bandpass wavelet.

1. *Concept of scale.* The functions $\psi_{kn}(t)$ are useful to represent finer and finer "variations" in the signal $x(t)$ at various levels. For large k, the function $\psi_{kn}(t)$ looks like a "high frequency signal." This is

especially clear from the plots of the Haar basis functions. (For the bandpass wavelets, see below.) Since these basis functions are not sinusoids, we do not use the term frequency but rather the term "scale". We say that the component $\psi_{kn}(t)$ represents a finer scale for larger k. Accordingly k (sometimes $1/k$) is called the scale variable. Thus, the function $x(t)$ has been represented as a linear combination of component functions that represent variations at different "scales". For instance, consider the Haar basis. If the signal expansion (2.14) has a relatively large value of $c_{4,2}$ this means that the component at scale $k = 4$ has large energy in the interval $[\frac{2}{2^4}, \frac{3}{2^4}]$ (Fig. 2.13).

2. *Localized basis.* The above comment shows that if a signal has energy at a particular scale concentrated in a slot in the time domain, then the corresponding c_{kn} has large value, i.e., $\psi_{kn}(t)$ contributes more to $x(t)$. The wavelet basis therefore provides a *localization information* in time domain as well as in the *scale domain.* For example, if the signal is zero everywhere except in the interval $[\frac{2}{2^4}, \frac{3}{2^4}]$ then the subset of the Harr basis functions which do not have their support in this interval are simply absent in this expansion.

Note that the Haar wavelet has *compact support,* that is the function $\psi(t)$ is zero everywhere outside a closed bounded interval (namely [0,1] here). While the above discussions are motivated by the Haar basis, many of them are typically true, with some obvious modifications, for more general wavelets. Consider for example the ideal bandpass wavelet (Fig. 2.11) obtained from the bandpass filter $\Psi(\omega)$ in Fig. 2.9. In this case the basis functions do not have compact support but are still locally concentrated around $t = 0$. Moreover, the basis functions for large k represent "fine" information, namely the frequency component around the center frequency of the filter $F_k(\omega)$ (Fig. 2.10). The Haar wavelet and the ideal bandpass wavelet are two extreme examples (one is time limited and the other bandlimited). We will find later that many intermediate examples can be constructed.

2.6. Filter Bank Interpretation and Time-Frequency Representation

We know that the wavelet coefficients c_{kn} for the ideal bandpass wavelet can be viewed as the sampled version of the output of a bandpass filter (Fig. 2.10(a)). The same is true for any kind of wavelet transform. For this recall the expression (2.18) for the wavelet coefficients. This can be interpreted as the set of sampled output sequences of a bank of filters $H_k(\omega)$ with impulse response $h_k(t) = 2^{k/2}h_0(2^k t)$ where $h_0(t) = \eta(t)$. Thus the wavelet transform can be interpreted as a *nonuniform continuous-time analysis filter bank,* followed by samplers. The Haar basis and ideal bandpass wavelet basis are two examples of the choice of these bandpass filters!

The wavelet coefficients c_{kn} for a given scale k are therefore obtained by sampling the output $y_k(t)$ of

the bandpass filter $H_k(\omega)$, as indicated in Fig. 2.10(a). The first subscript k (the scale variable) represents the filter number. As k increases by one, the center frequency ω_k increases by a factor of two. The wavelet coefficients c_{kn} at scale k are merely the samples $y_k(2^{-k}n)$. As k increases the filter bandwidth increases, so the samples are spaced by a proportionately finer amount 2^{-k}. The quantity $c_{kn} = y_k(2^{-k}n)$ measures the "amount" of the "frequency component" around the center frequency ω_k of the analysis filter $H_k(\omega)$, localized in *time* around $2^{-k}n$.

In wavelet transformation, the transform domain is represented by the two integer variables k and n. This means that the transform domain is *two dimensional* (the time-frequency domain), and is *discretized.* We say that c_{kn} is a *time-frequency representation of* $x(t)$. We will see in Sec. 3 that this is an improvement over another time-frequency representation called the short time Fourier transform (STFT) introduced earlier in the sinal processing context.

Synthesis Filter bank and reconstruction. The inner sum in (2.14) can be interpreted as follows: for each k, convert the sequence c_{kn} into an impulse train† $\sum_n c_{kn}\delta_a(t - 2^{-k}n)$ and pass it through a bandpass filter $F_k(\omega) = 2^{-k/2}\Psi(2^{-k}\omega)$ with impulse response $f_k(t) = 2^{k/2}\psi(2^k t)$. The outer sum merely adds the outputs of all these filters. Figs. 2.7(a) and 2.10(a) show this interpretation. Therefore, the reconstruction of the signal $x(t)$ from the wavelet coefficients c_{kn} is equivalent to the implementation of a *nonuniform continuous-time synthesis filter bank,* with synthesis filters $f_k(t) = 2^{k/2}f_0(2^k t)$ generated by dilations of a single filter $f_0(t) \triangleq \psi(t)$.

As mentioned in Sec. 2.3, the analyzing wavelet $\eta(t)$ and the synthesis wavelet $\psi(t)$ are related by $\eta(t) = \psi^*(-t)$ in the orthonormal case. So the analysis and synthesis filters are related as $h_k(t) = f_k^*(-t)$, that is, $H_k(\omega) = F_k^*(\omega)$. For the special case of the ideal bandpass wavelet (2.10), $\psi(t)$ is real and symmetric so that $f_k(t) = f_k^*(-t)$, i.e., $h_k(t) = f_k(t)$. Fig. 2.13 summarizes the relations described in the preceding paragraphs.

Design of Wavelet Functions

Since all the filters in the analysis and synthesis banks are derived from the wavelet function $\psi(t)$, the quality of the frequency responses depend directly on $\Psi(\omega)$. In the time domain, the Haar basis has poor smoothness (it is not even continuous) but it is well-localized (compactly supported). Its Fourier transform $\Psi(\omega)$, given in (2.20) decays only as $1/\omega$ for large ω. The ideal bandpass wavelet, on the other hand, is poorly localized in time but has very smooth behavior. In fact since it is bandlimited, $\psi(t)$ is infinitely differentiable. But it decays only as $1/t$ for large t. Thus the Haar wavelet and the ideal bandpass wavelet

† $\delta_a(t)$ is the Dirac delta function [Oppenheim, et. al., 1983]. Here it is used only as a schematic. The true meaning is just that the output of $f_k(t)$ is $\sum_n c_{kn} f_k(t - 2^{-k}n)$.

represent two opposite extremes of the possible choices we have.

We could carefully design the wavelet $\psi(t)$ such that it is reasonably well localized in time domain, while at the same time sufficiently smooth or "regular". The term *regularity* is often used to quantify the degree of smoothness. For example the number of times we can differentiate the wavelet $\psi(t)$, and the degree of continuity (so-called Hölder index) of the last derivative are taken as measures of regularity. We will return to this in Sec. 11–13 where we also present systematic procedures for design of the function $\psi(t)$. This can be designed in such a way that $\{2^{k/2}\psi(2^k t - n)\}$ forms an orthonormal basis with prescribed decay and regularity properties. It is also possible to design $\psi(t)$ such that we obtain other kinds of structures rather than an orthonormal basis, e.g., a Riesz basis or a frame (Sec. 7,8).

2.7. Wavelet Basis and Fourier Basis

Returning to the Fourier basis $g_k(t) = \{e^{j2\pi kt}\}$ for functions supported on $[0,1]$, we see that $g_k(t) = g_1(kt)$ so that all the functions are dilated versions (dilations being integers rather than powers of integers) of $g_1(t)$! However *these do not have the localization property of wavelets.* To understand this, note that $e^{j2\pi kt}$ has unit magnitude everywhere, and sines and cosines are nonzero almost everywhere. Thus if we have a function $x(t)$ that is identically zero in a certain time slot (e.g., Fig. 2.14), then in order for the infinite series $\sum_n \alpha_n e^{j2\pi nt}$ to represent $x(t)$, there has to be extreme cancellation of terms in that time slot.

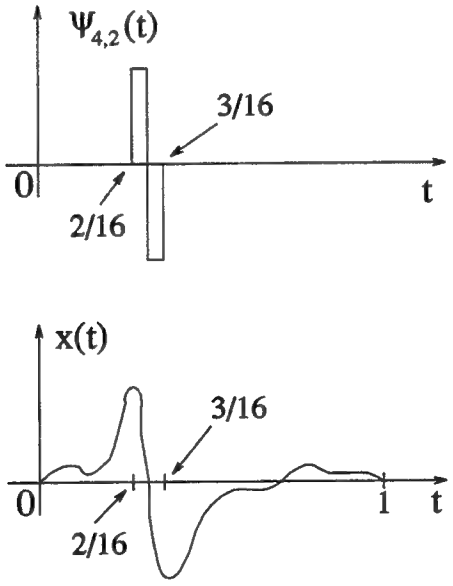

Fig. 2.14. Example of an $L^2[0,1]$ signal $x(t)$ for which the Haar component $\psi_{4,2}(t)$ dominates.

In contrast, if we use a compactly supported wavelet basis, it provides us localization information, as well as information about "frequency contents" in the form of "scales" (Sec. 2.5). The "transform domain"

in traditional Fourier transform is represented by a single continuous variable ω. In the wavelet transform, where the transform coefficients are c_{kn}, the transform domain is represented by two integers k and n.

It is also clear that wavelet transforms provide a great deal of flexibility because we can choose $\psi(t)$. With Fourier transforms on the other hand, the basis functions (sines and cosines) are pretty much fixed (see, however, Sec. 3 on short-time Fourier transform).

2.8. More General Form of Wavelet Transformation

The most general form of the wavelet transform is given by

$$X(a,b) = \frac{1}{\sqrt{|a|}} \int_{-\infty}^{\infty} x(t)\psi\Big(\frac{t-b}{a}\Big)dt \tag{2.21}$$

where a and b are real. This is called the continuous wavelet transform (CWT) because a and b are continuous variables. The transform domain is a two dimensional domain (a,b). The restricted version of this where a and b take a discrete set of values $a = c^{-k}$ and $b = c^{-k}n$ where k and n vary over the set of all integers, is called the Discrete Wavelet Transform (DWT). The further special case where $c = 2$, that is, $a = 2^{-k}$ and $b = 2^{-k}n$ is the wavelet transform discussed so far (see eq. (2.16)) and is called the *dyadic DWT*. Expansions of the form (2.14) are also called *wavelet series expansions* by analogy with the Fourier series expansion (a summation rather than an integral).

For fixed a, Eq. (2.21) is a convolution. Thus, if we apply the input signal $x(t)$ to a filter with impulse response $\psi(-t/a)/\sqrt{|a|}$, then its output, evaluated at time b, will be $X(a,b)$. The filter has frequency response $\sqrt{|a|}\Psi(-a\omega)$. If we imagine that $\Psi(\omega)$ has a good bandpass response with center frequency ω_0, then the above filter is bandpass with center frequency $-a^{-1}\omega_0$. That is, the wavelet transform $X(a,b)$, which is the output of the filter at time b, represents the "frequency content" of $x(t)$ around the frequency $-a^{-1}\omega_0$, "around" time b. Ignoring the minus sign (because $\psi(t)$ and $x(t)$ are typically real anyway), we therefore see that the variable a^{-1} is analogous to frequency. In wavelet literature, the quantity $|a|$ is usually referred to as the " scale" rather than "inverse frequency".

For reasons which cannot be explained with our limited exposure so far, the wavelet function $\psi(t)$ is restricted to be such that $\int \psi(t)dt = 0$. For the moment notice that this is equivalent to $\Psi(0) = 0$, which is consistent with the bandpass property of $\psi(t)$. In Sec. 10.4 where we generate wavelets systematically using multiresolution analysis, we will see that this condition follows naturally from theoretical considerations.

3. THE SHORT TIME FOURIER TRANSFORM (STFT)

In many applications, we have to accomodate the notion of frequency that evolves or changes with time. For example, audio signals are often regarded as signals with a time varying spectrum, e.g., a sequence of

short lived pitch frequencies. This idea cannot be expressed with the traditional FT since $X(\omega)$ for each ω depends on $x(t)$ for all t.

The short time Fourier transform (STFT) was introduced to provide such a time-frequency picture of the signal [Gabor, 1946], [Flanagan and Golden, 1966], [Schafer and Rabiner, 1973], [Allen and Rabiner, 1977], and [Portnoff, 1980]. Here the signal $x(t)$ is multiplied with a window $v(t-\tau)$ centered or localized around time τ (Fig. 3.1) and the FT of $x(t)v(t-\tau)$ computed:

$$X(\omega,\tau) = \int_{-\infty}^{\infty} x(t)v(t-\tau)e^{-j\omega t}dt. \tag{3.1}$$

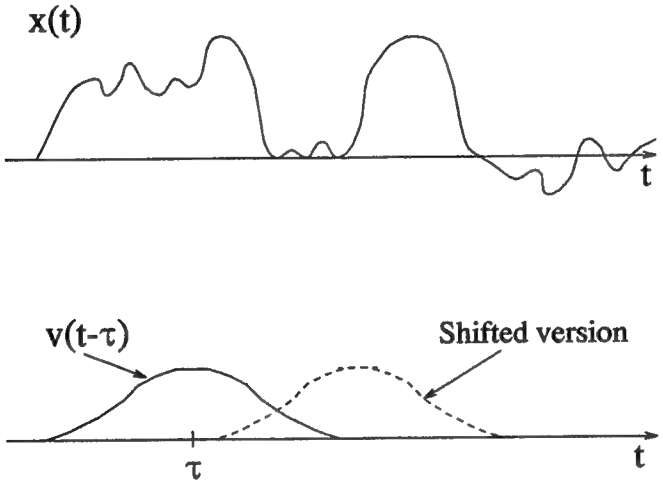

Fig. 3.1. A signal $x(t)$, and the sliding window $v(t-\tau)$.

This is then repeated for shifted locations of the window, i.e., for various values of τ. That is, we compute not just one FT, but infinitely many. The result is a function of both time τ and frequency ω. If this has to be practical we have to make two changes: compute the STFT only for discrete values of ω, and second use only a discrete number of window positions τ. In the traditional STFT both ω and τ are discretized on uniform grids:

$$\omega = k\omega_s, \quad \tau = nT_s. \tag{3.2}$$

The STFT is thus defined as

$$X_{stft}(k\omega_s, nT_s) = \int_{-\infty}^{\infty} x(t)v(t-nT_s)e^{-jk\omega_s t}dt, \tag{3.3}$$

which we abbreviate as $X_{stft}(k,n)$ when there is no confusion. Thus the time domain is mapped into the time-frequency domain. The quantity $X_{stft}(k\omega_s, nT_s)$ represents the FT of $x(t)$ "around time nT_s" and "around frequency $k\omega_s$". This in essence is similar to the wavelet transform: in both cases the transform domain is a two dimensional discrete domain.

We will compare wavelets and STFT on several grounds. We will give a filter-bank view, and compare time-frequency resolution and localization properties. In Sec. 9 we will compare them on deeper grounds. For example, when can we reconstruct a signal $x(t)$ from the STFT coefficients $X_{stft}(k,n)$? Can we construct an orthonormal basis for L^2 signals based on the STFT? And so forth. The advantage of wavelet transforms over the STFT will be clear after these discussions.

3.1. Filter Bank Interpretation

The STFT evaluated for some frequency ω_k can be rewritten as

$$X_{stft}(\omega_k,\tau) = e^{-j\omega_k\tau}\int_{-\infty}^{\infty} x(t)v(t-\tau)e^{-j\omega_k(t-\tau)}dt. \tag{3.4}$$

The integral looks like a convolution of $x(t)$ with the filter impulse response

$$h_k(t)\triangleq v(-t)e^{j\omega_k t}. \tag{3.5}$$

If $v(-t)$ has a Fourier transform looking like a lowpass filter then $h_k(t)$ looks like a bandpass filter with center frequency ω_k (Fig. 3.2). Thus, $X_{stft}(\omega_k,\tau)$ is the output of this bandpass filter at time τ, downshifted in frequency by ω_k.

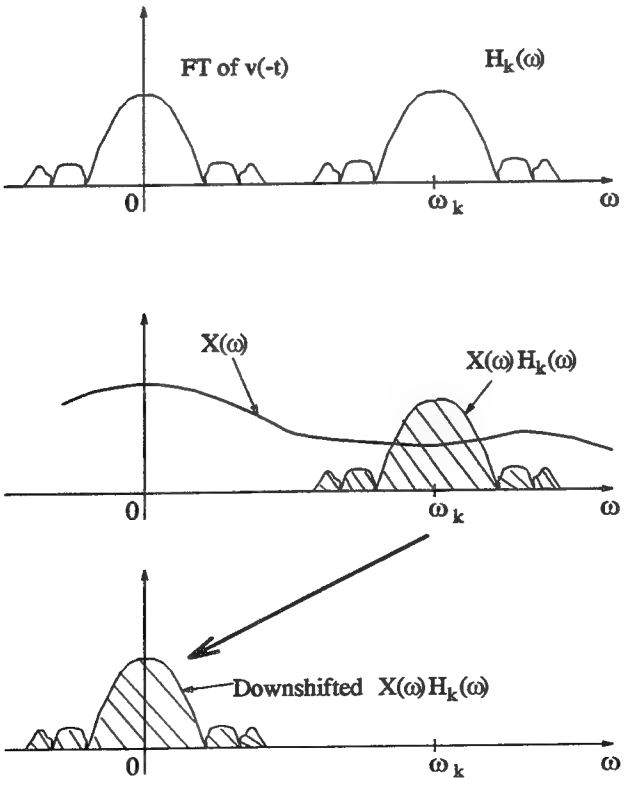

Fig. 3.2. The STFT viewed as a bandpass filter followed by a downshifter.

The result is a lowpass signal $y_k(t)$ whose output is sampled uniformly at time $\tau = nT_s$. For every frequency ω_k so analyzed, there is one such filter channel. With the frequencies uniformly located at $\omega_k = k\omega_s$, we get the analysis filter bank followed by downshifters and samplers as shown in Fig. 3.3.

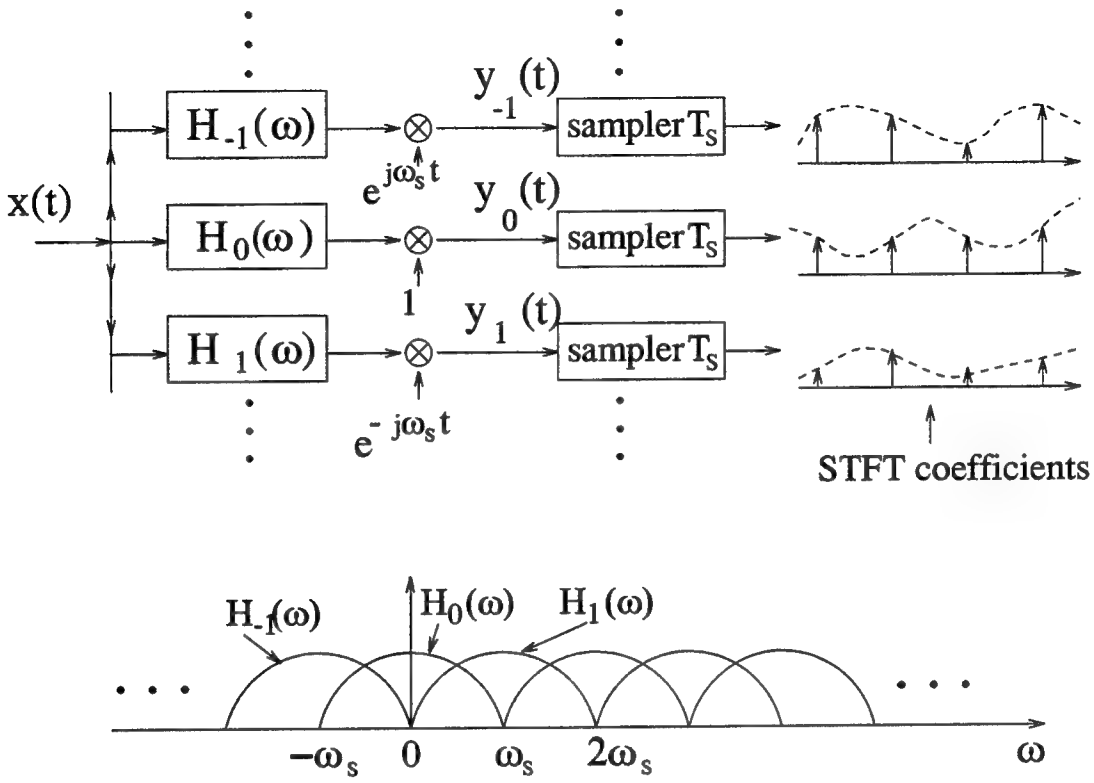

Fig. 3.3. The STFT viewed as an analysis bank of uniformly shifted filters.

The STFT coefficients $X_{stft}(k\omega_s, nT_s)$ can therefore be regarded as the uniformly spaced samples of the outputs of a bank of bandpass filters $H_k(\omega)$, all derived from one filter $h_k(t)$ by modulation: $h_k(t) = e^{jk\omega_s t}h_0(t)$, i.e., $H_k(\omega) = H_0(\omega - k\omega_s)$. (The filters are one-sided in frequency so they have complex coefficients in the time domain, but ignore these details for now). The output of $H_k(\omega)$ represents a portion of the FT $X(\omega)$ around the frequency $k\omega_s$. The downshifted version $y_k(t)$ is therefore a lowpass signal. That is, it is a slowly varying signal, whose evolution as a function of t represents the evolution of the FT $X(\omega)$ around frequency $k\omega_s$. By sampling this slowly varying signal we can therefore compress the transform domain information.

If the window is narrow in the time domain, then $H_k(\omega)$ has large bandwidth. That is, we have good time resolution and poor frequency resolution. If the window is wide the opposite is true. Thus if we try to capture the local information in time by making a narrow window, then we get a fuzzy picture in frequency. Conversely in the limit as the filter becomes extremely localized in frequency the window is very broad, and

STFT approaches the ordinary FT. That is, the time-frequency information collapses to the all-frequency information of ordinary FT. We see that time-frequency representation is inherently a compromise between time and frequency resolutions (or localizations). This is related to the uncertainty principle: as windows get narrow in time they have to get broad in frequency, and vice versa.

Optimal time-frequency resolution: the Gabor window

What is the best frequency resolution one can obtain for a given time resolution? That is, for a given duration of the window $v(t)$ how small can the duration of $V(\omega)$ be? If we define duration according to common sense we are already in trouble because if $v(t)$ has finite duration then $V(\omega)$ has infinite duration. There is a more useful definition of duration called the *root mean square* (rms) duration. The rms time duration D_t and the rms frequency duration D_f for the window $v(t)$ are defined such that

$$D_t^2 = \frac{\int t^2 |v(t)|^2 dt}{\int |v(t)|^2 dt}, \qquad D_f^2 = \frac{\int \omega^2 |V(\omega)|^2 d\omega}{\int |V(\omega)|^2 d\omega} \tag{3.6}$$

Intuitively we can see that D_t cannot be arbitrarily small for a specified D_f. The uncertainty principle says that $D_t D_f \geq 0.5$. Equality holds if and only if $v(t)$ has the shape of a Gaussian, i.e., $v(t) = Ae^{-\alpha t^2}, \alpha > 0$. Thus the best joint time-frequency resolution is obtained by using the Gaussian window. This is also intuitively acceptable for the reason that the Gaussian is its own FT (except for scaling of variables and so forth). Gabor used the Gaussian window as early as 1946! Since it is of infinite duration, a truncated approximation is used in practice. The STFT based on the Gaussian is called the Gabor transform. A limitation of the Gabor transform is that it does not give rise to an orthonormal signal representation; in fact it cannot even provide a "stable basis" (in Sec. 7 and 9 we explain the meaning of this).

3.2. Wavelet Transform Versus STFT

The STFT works with a fixed window $v(t)$. If a high frequency signal is being analyzed, many cycles are captured by the window, and a good estimate of the FT is obtained. But if a signal varies very slowly with respect to the window then the window is not long enough to capture it fully. From a filter bank viewpoint, notice that all the filters have identical bandwidths (Fig. 3.3). This means that the frequency resolution is uniform at all frequencies. That is, the "percentage resolution" or accuracy is poor for low frequencies and becomes better and better at high frequencies. The STFT therefore does not provide uniform percentage accuracy for all frequencies — the computational resources are somehow poorly distributed.

Compare this with the wavelet transform which is represented by a nonuniform filter bank Fig. 2.8(b). Here the frequency resolution gets poorer as the frequency increases but the fractional resolution (i.e., the filter bandwidth $\Delta\omega_k$ divided by the center frequency ω_k) is constant for all k. That is, the percentage

accuracy is uniformly distributed in frequency. In the time domain this is roughly analogous to having a large library of windows; the narrow window is used to analyze high frequency components and very broad windows are used to analyze low frequency components. In electrical engineering language the filter bank representing wavelet transforms is a *constant Q filter bank*, or an *octave band filter bank*.

Consider, for example, the Haar wavelet basis. Here the narrow basis functions $\psi_{2,n}(t)$ in Fig. 2.12 are useful to represent the highly varying components of the input, and are correspondignly narrower (have shorter support than the functions $\psi_{1,n}(t)$.

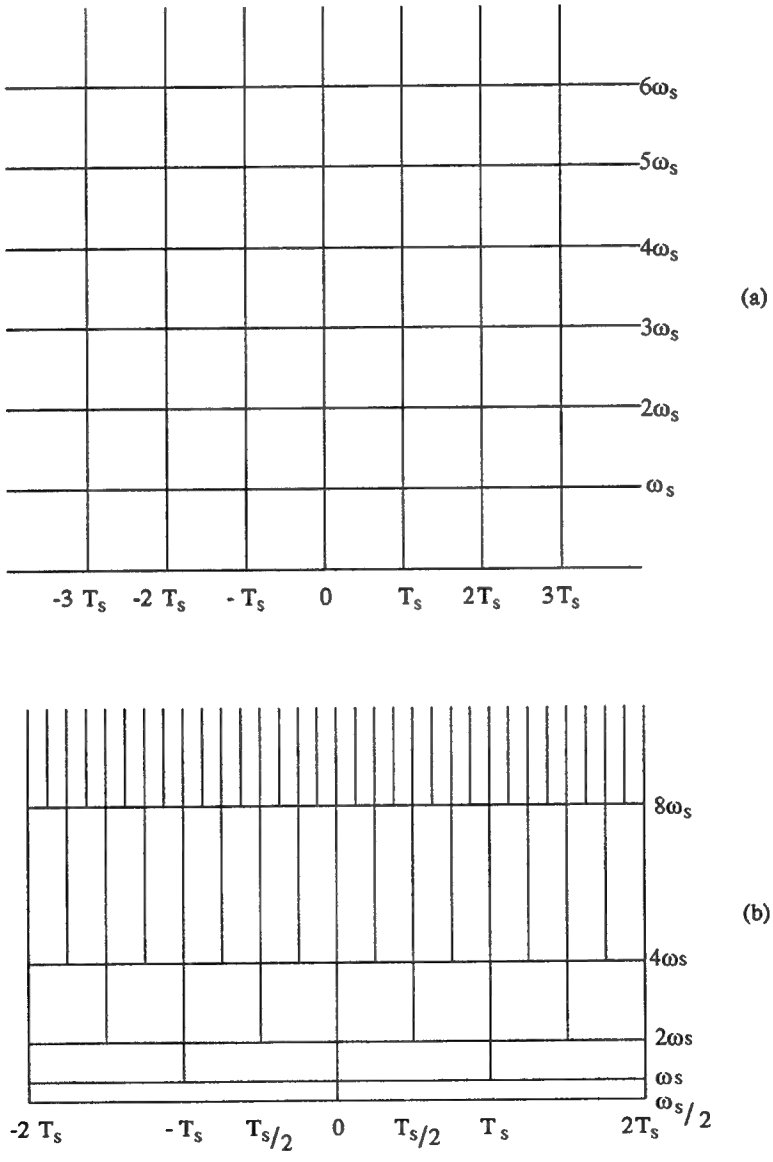

Fig. 3.4. Time-frequency tiling schemes for (a) STFT and (b) the wavelet transform.

A second difference between the STFT and wavelet transforms is the sampling rates at the outputs of

the bandpass filters. These are identical for the STFT filters (all filters have the same bandwidth). For the wavelet filters, these are proportional to the filter bandwidths, hence nonuniform (Fig. 2.10(a)). This is roughly analogous to the situation that the narrower windows move in smaller steps compared to the wider windows. Compare again with Fig. 2.12 where $\psi_{2,n}(t)$ are moved in smaller steps compared to $\psi_{1,n}(t)$, in the process of constructing the complete set of basis functions.

The nonuniform (constant Q) filter stacking (Fig. 2.8(b)) provided by wavelet filters is also naturally suited for analyzing audio signals and sometimes even as components in the modeling of the human hearing system.

The Time-Frequency Tiling

The fact that the STFT performs uniform sampling of time and frequency whereas the wavelet transform performs non uniform sampling is represented by the diagram shown in Fig. 3.4. Here the vertical lines represent time locations where the analysis filter-bank output is sampled and the horizontal lines represent the center frequencies of the bandpass filters. The time frequency tiling for the STFT is a simple rectangular grid, whereas for the wavelet transform it has a more complicated appearance.

Example 3.1. Wavelet Transform Versus STFT

Consider the signal $x(t) = \cos(10\pi t) + 0.5\cos(5\pi t) + 1.2\delta_a(t-0.07) + 1.2\delta_a(t+0.07)$. It has impulses at $t = \pm 0.07$, in the time domain. There are two impulses (or "lines") in the frequency domain, at $\omega_1 = 5\pi$ and $\omega_2 = 10\pi$. The function is shown in Fig. 3.5 (with impulses replaced by narrow pulses). The aim is to try to compute the STFT or WT such that the impulses in time as well as those in frequency are resolved. Figure 3.6 (a)-(c) shows the STFT plot for three widths of the window $v(t)$ and Fig. 3.6(d) shows the wavelet plot. The details of the window $v(t)$ and the wavelet $\psi(t)$ used for this example will be described below, but first let us concentrate on the features of these plots.

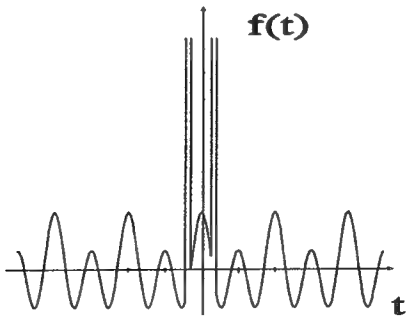

Fig. 3.5. Example 3.1. The signal to be analyzed by STFT and Wavelet transform.

The STFT plots are time-frequency plots, whereas the wavelet plots are (a^{-1}, b) plots where a and b are

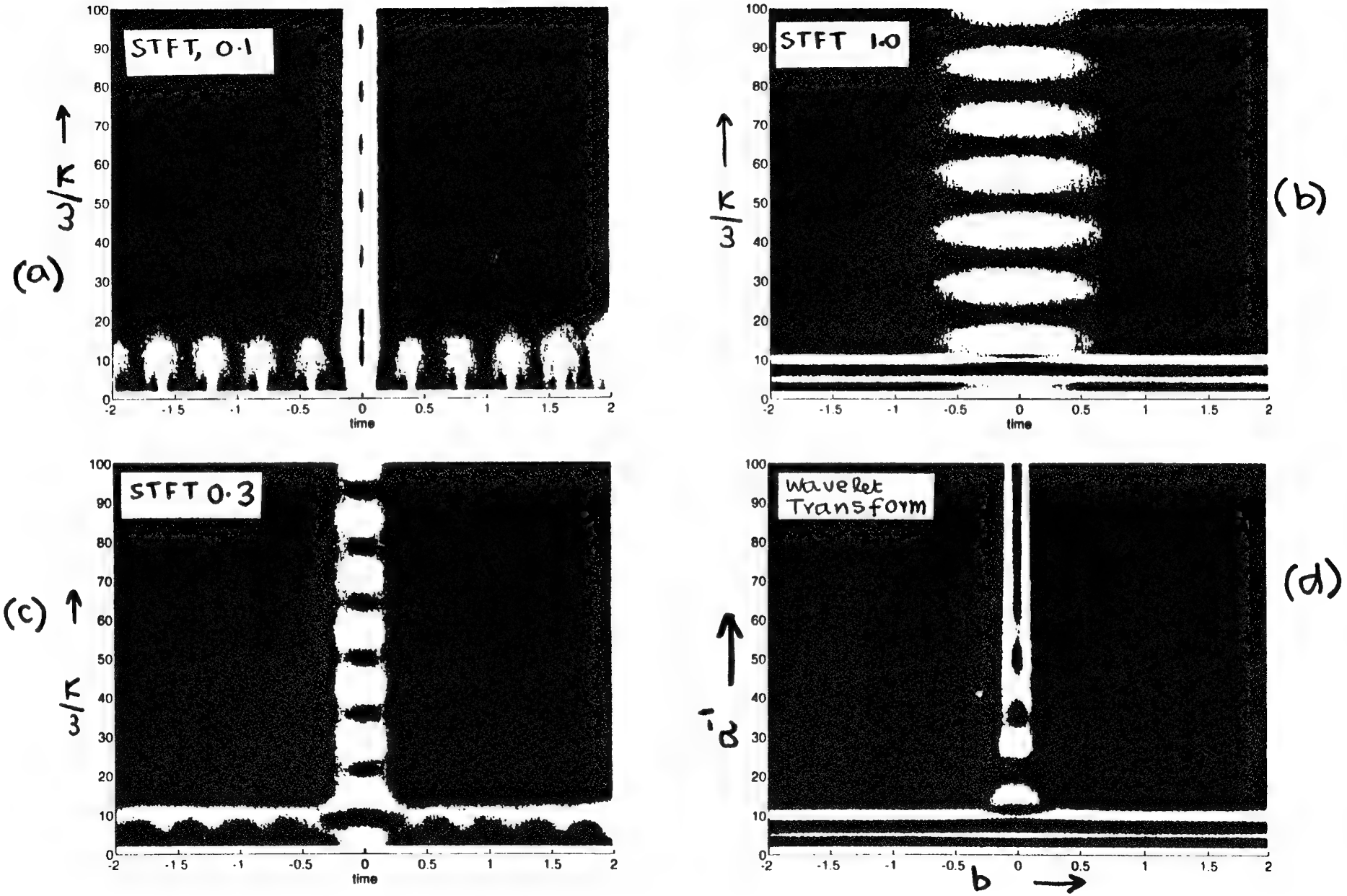

Fig. 3.6. Example 3.1 (a)-(c) STFT plots with window widths of 0.1, 1.0, and 0.3 respectively and (d) Wavelet transform plot.

defined by (2.21). As explained in Sec. 2.8, the quantity a^{-1} is analogous to "frequency" in the STFT, and b is analogous to "time" in the STFT. The brightness of the plots in Fig. 3.6 is proportional to the magnitude of the STFT or WT, so the transform is close to zero in the dark regions. We see that for a narrow window with width = 0.1, the STFT resolves the two impulses in time reasonably well, but the impulses in frequency are not resolved. For a wide window with width = 1.0, the STFT resolves the "lines" in frequency very well, but not the time domain impulses. For an intermediate window width = 0.3, the resolution is poor in both time and frequency. The wavelet transform plot (Fig. 3.6 (d)), on the other hand, simultaneously resolves both time and frequency very well. We can clearly see the locations of the two impulses in time, as well as the two lines in frequency.

Now for the details. The STFT for this example was computed using the Hamming window [Oppenheim and Schafer, 1989] defined as $v(t) = c[0.54+0.46\cos(\pi t/D)]$ for $-D \le t \le D$ and zero outside. The "widths" indicated in the figure correspond to $D = 0.1, 1.0$, and 0.3 (though the two-sided width is twice this). The wavelet transform was computed by using an example of the Morlet wavelet [Daubechies, 1992]. Specifically,

$$\psi(t) = e^{-t^2/16}(e^{j\pi t} - \alpha).$$

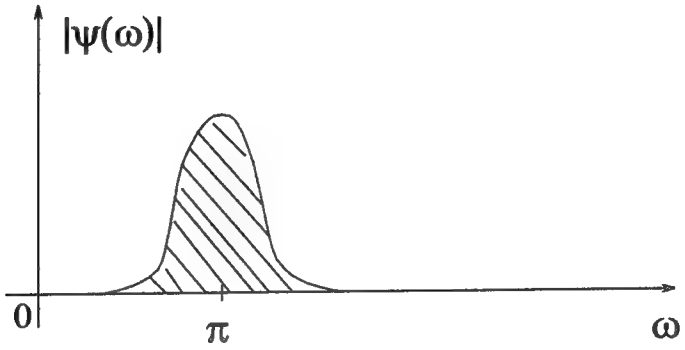

Fig. 3.7. Example 3.1. Fourier transform magnitude for the Morlet wavelet.

First let us understand what this wavelet function is doing. The quantity $e^{-t^2/16}$ is the Gaussain (except for a constant scaler factor) with Fourier transform $4\sqrt{\pi}e^{-4\omega^2}$, which is again Gaussian, concentrated near $\omega = 0$. Thus $e^{-t^2/16}e^{j\pi t}$ has an FT concentrated around $\omega = \pi$. Ignoring† the second term α in the expression for $\psi(t)$, we see that the wavelet is a narrowband bandpass filter concentrated around π (Fig. 3.7). If we set $a = 1$ in (2.21), then $X(1, b)$ represents the frequency contents around π. Thus, the frequencies $\omega_1 = 5\pi$ and $\omega_2 = 10\pi$ in the given signal $x(t)$ show up around points $a^{-1} = 5$ and $a^{-1} = 10$ in the wavelet transform plot, as seen from Fig. 3.6(d). In the STFT plots, we have shown the frequency axis as ω/π so that the

† The quantity α in the expression of $\psi(t)$ is there to ensure that $\int \psi(t)dt = 0$ (Sec. 2.8). Since α is very small, it does not significantly affect the plots in Fig. 3.6.

frequencies ω_1 and ω_2 show up at 5 and 10, making it easy to compare the STFT plots with the wavelet plot.

Mathematical Issues to be Addressed

While the filter bank view point places wavelets and STFT on a unified ground, several mathematical issues still remain to be addressed. It is this deeper study that brings forth further subtle differences, giving wavelets a definite advantage over the STFT.

Returning to the STFT, let us say that we start from a signal $x(t) \in L^2$ and compute the STFT coefficients $X(k\omega_s, nT_s)$. How should we choose the sampling periods T_s and ω_s of the time and frequency grids so that we can reconstruct $x(t)$ from the STFT coefficients? (Remember that we are not talking about bandlimited signals, and there is no sampling theorem at work). If the filters $H_k(\omega)$ are ideal one-sided bandpass filters with bandwidth ω_s, the downshifted lowpass outputs $y_k(t)$ (Fig. 3.2) can be sampled separately at the Nyquist rate ω_s or higher. This then tells us that $T_s \leq 2\pi/\omega_s$, that is

$$\omega_s T_s \leq 2\pi. \tag{3.7}$$

However the use of ideal filters implies an impractical window $v(n)$.

If we use a practical window (e.g., one of finite duration) then how should we choose T_s in relation to ω_s so that we can reconstruct $x(t)$ from the STFT coefficients $X(k\omega_s, nT_s)$? Is this a stable reconstruction, that is if we make a small error in some STFT coefficient does it affect the reconstructed signal in an unbounded manner? Finally, does the STFT provide an orthonormal basis for L^2? These questions are deep and interesting, and require more careful treatment. We will do this in Sec. 9.

4. DIGITAL FILTER BANKS AND SUBBAND CODERS

We will now discuss a totally different set up, namely a discrete-time filter bank or a digital filter bank. This has some qualitative resemblance to the continuous time filter banks which were used to represent the STFT and wavelet transform earlier. An example of a digital filter bank is shown in Fig. 4.1(a) where $x(n)$ is a discrete time signal (sequence). Here $G_a(z)$ and $H_a(z)$ are two digital filters, typically lowpass and highpass which split $x(n)$ into two subbands. The subband signals $x_0(n)$ and $x_1(n)$ are downsampled or decimated (see below for definitions). The total subband data rate counting both subbands is then equal to the number of samples per unit time in the original signal $x(n)$. There are extensions of this system for more than two subbands, called M channel maximally decimated filter banks.

There are several reasons for discussing digital filter banks in this chapter. First, they provide a time-frequency representation for discrete time signals, similar to the STFT and wavelet transforms for continuous

time signals. Second, there is a deep mathematical connection between this digital filter bank and the continuous time wavelet transform. This fundamental relation, discovered by Daubechies [1988], is fully elaborated later in Sec. 10–13, and is what makes the wavelet transform so easy to design, and attractive to implement in practice. This relation also opens up a little world of beautiful research problems for engineers as well as mathematicians. Indeed, the recent boom of interest in wavelet transforms can be traced back to the discovery of this relation.

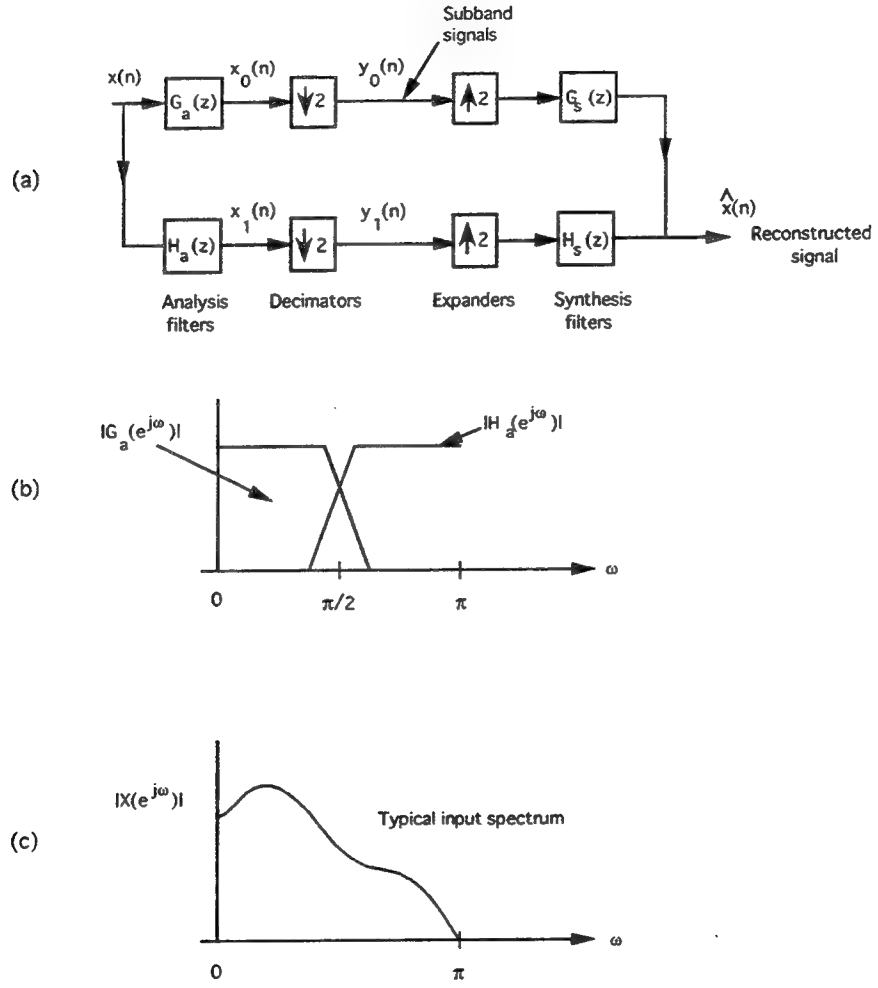

Fig. 4.1. (a) The two channel digital filter bank, (b) Typical filter responses, and (c) Typical input spectrum.

A few words on subband coding.

The most common application of the digital filter bank is in subband coding. The basic idea can be explained using the following simple example: suppose $x(n)$ has its energy mostly in the lowpass region (e.g., as in speech or music). Then we can use lowpass and highpass filters $G_a(z)$ and $H_a(z)$ to split $x(n)$ into subbands. This is demonstrated in Fig. 4.1(b),(c). We then assign more bits to the lower subband $x_0(n)$ as

compared to the higher subband $x_1(n)$. For a fixed bit rate, this allows a judicious utilization of bits. This idea is used in practice in a more elaborate manner; for example $x(n)$ is split into more than two bands, often into unequal bandwidths (using the so-called nonuniform filter banks). Then an optimal subband bit-allocation strategy is adopted. This allocation takes into account not only the energy distribution in the subbands, but also perceptive considerations such as the masking property of the ear as a function of frequency. In this way very significant compression rate can be achieved. For example, digital audio (CD music) has been compressed by more than a factor of four [Veldhuis, et al., 1989]. In image compression applications [Woods, 1991] subband coding is often used in combination with other nonlinear filtering operations. Subband coding has a long history and a rich list of applications, but we will not go into these here.

Detailed studies of filter banks and multirate systems can be found in a number of references, see for example [Vaidyanathan, 1993] and references therein. Our treatment here will be brief, the aim being to lay the foundation that will enable us to explain the connection to wavelet transforms.

4.1. The Multirate Signal Processing Building Blocks

The building blocks in the digital filter bank of Fig. 4.1(a) are digital filters, decimators, and expanders. The M-fold *decimator or downsampler* (denoted $\downarrow M$) is defined by the input-output relation $y(n) = x(Mn)$. For example the two-fold decimator retains even numbered samples, and drops the odd ones. For $M = 2$ the input output relation in the z-domain becomes

$$Y(z) = 0.5\big[X(z^{1/2}) + X(-z^{1/2})\big], \quad \text{that is,} \quad Y(e^{j\omega}) = 0.5\big[X(e^{j\omega/2}) + X(e^{j(\omega-2\pi)/2})\big]. \tag{4.1}$$

whereas for arbitrary M it is $Y(z) = (1/M)\sum_{k=0}^{M-1} X(z^{1/M}e^{-j2\pi k/M})$. This relation is sometimes abbreviated by the notation $Y(z) = X(z)\big|_{\downarrow M}$ or $Y(e^{j\omega}) = X(e^{j\omega})\big|_{\downarrow M}$.

There are two terms in the expression (4.1) for $Y(e^{j\omega})$. The first term $X(e^{j\omega/2})$ represents a stretched version of $X(e^{j\omega})$. The second term $X(e^{j(\omega-2\pi)/2})$ is a shifted version of this stretched version, the shift being by an amount 2π. In general the shifted version may overlap with the stretched version. In this case we cannot recover the input signal from the decimated version. This is exactly the effect of aliasing created by undersampling. If the original spectrum $X(e^{j\omega})$ is bandlimited to $[-\pi/2, \pi/2]$, 2-fold decimation does not cause aliasing.

The M fold *expander or upsampler* (denoted $\uparrow M$) is defined by

$$y(n) = \begin{cases} x(n/M), & n = \text{multiple of } M, \\ 0, & \text{otherwise.} \end{cases} \tag{4.2}$$

Thus the expander simply inserts $M-1$ zero-valued samples between adjacent samples of the input. In the transform domain the relation is $Y(z) = X(z^M)$, that is, $Y(e^{j\omega}) = X(e^{jM\omega})$. Thus the expander squeezes the

Fourier transform by M so that the period becomes $2\pi/M$ rather than 2π. The basic shape of the spectrum is preserved, consistent with the fact that in the time domain there is no loss of information; we can always recover the input to the expander from its output, just by decimating it.

4.2. Reconstruction from Subbands

In many applications it is desirable to reconstruct $x(n)$ from the decimated subband signals $y_k(n)$ (possibly after quantization). For this, we pass $y_k(n)$ through expanders and combine them with synthesis filters $G_s(z)$ and $H_s(z)$ as shown in Fig. 4.1(a). The system is said to have the *perfect reconstruction* (PR) property if $\hat{x}(n) = cx(n - n_0)$ for some $c \neq 0$ and n_0. In general the PR property is not satisfied for several reasons. First, there is subband quantization and bit allocation, which is the key to data compression using subband techniques. But since our interest here is in the connection between filter banks and wavelets, we will not be concerned with subband quantization here.

Second, since the filters $G_a(z)$ and $H_a(z)$ are not ideal there is aliasing due to decimation. Using the above equations for the decimator and expander building blocks, we can obtain the following expression for the reconstructed signal

$$\begin{aligned}\hat{X}(z) =& 0.5\big[G_a(z)G_s(z) + H_a(z)H_s(z)\big]X(z) \\ &+ 0.5\big[G_a(-z)G_s(z) + H_a(-z)H_s(z)\big]X(-z).\end{aligned} \tag{4.3}$$

The second term having $X(-z)$ arises from the term $X(-z^{1/2})$ created by the decimator (see (4.1)) and is therefore the aliasing term. This can be eliminated by designing the filters such that

$$G_a(-z)G_s(z) + H_a(-z)H_s(z) = 0, \qquad \text{(alias cancellation)}. \tag{4.4}$$

Assume that this has been satisfied. By setting

$$G_a(z)G_s(z) + H_a(z)H_s(z) = 1 \tag{4.5}$$

we can then obtain $\hat{X}(z) = 0.5X(z)$, implying perfect reconstruction.

There are many ways to satisfy the perfect reconstruction conditions [Smith and Barnwell, 1984], [Vaidynathan, 1987], [Vetterli, 1987]. For this chapter we are interested in a particular technique to satisfy (4.4) and (4.5). This has been called the conjugate quadrature filter (CQF) method, and was independently reported in [Smith and Barnwell, 1984] and [Mintzer, 1985]. It was shown later [Vaidynathan, 1987] that these constructions are examples of a general class of M channel filter banks called paraunitary filter banks. The two channel CQF solution was later rediscovered in the totally different contexts of multiresolution analysis

[Mallat, 1989] and compactly supported orthonormal wavelet construction [Daubechies, 1988]. These will be discussed in future sections.

The CQF solution. Suppose the analysis filter $G_a(z)$ is chosen such that it satisfies the condition

$$\widetilde{G}_a(z)G_a(z) + \widetilde{G}_a(-z)G_a(-z) = 1 \qquad \text{for all } z. \tag{4.6}$$

If we now choose the analysis filter $H_a(z)$ and the two synthesis filters as

$$H_a(z) = z^{-1}\widetilde{G}_a(-z), \quad G_s(z) = \widetilde{G}_a(z), \quad H_s(z) = \widetilde{H}_a(z), \tag{4.7}$$

then substitution shows that (4.4) and (4.5) are satisfied indeed. There is perfect reconstruction, that is $\hat{x}(n) = 0.5x(n)$. In the time domain the above equations can be written as

$$h_a(n) = -(-1)^n g_a^*(-n+1), \quad g_s(n) = g_a^*(-n), \quad h_s(n) = h_a^*(-n). \tag{4.8}$$

The synthesis filters are *time reversed conjugates* of the analysis filters. If we design a filter $G_a(z)$ satisfying the single condition (4.6) and determine the remaining three filters as above, then the system has the PR property! A filter $G_a(z)$ satisfying (4.6) is said to be *power-symmetric*. Readers familiar with *half-band filters* will notice that the condition (4.6) says simply that $\widetilde{G}_a(z)G_a(z)$ is half-band! We will return to this in Sec. 4.4.

Design procedure. The procedure to design a perfect reconstruction CQF system is very simple. We first design a zero-phase lowpass half-band filter $G(z)$ with $G(e^{j\omega}) \geq 0$ and then extract a spectral factor $G_a(z)$, that is find $G_a(z)$ such that $G(z) = \widetilde{G}_a(z)G_a(z)$. Once the lowpass filter $G_a(z)$ is found like this, the three remaining filters can be found from (4.7).

4.3. The Polyphase Representation

Polyphase representations for transfer functions were introduced first by Bellanger et al. [1976]. The polyphase representation of a filter bank gives a convenient platform for studying theoretical questions and also helps in the design and implementation of PR filter banks. Let $H(z) = \sum_n h(n)z^{-n}$ be any transfer function. We can express it in the form $H(z) = E_0(z^2) + z^{-1}E_1(z^2)$ by splitting the z transform into even powers of z and odd powers of z. This is called a polyphase decomposition and $E_k(z)$ are called the polyphase components.

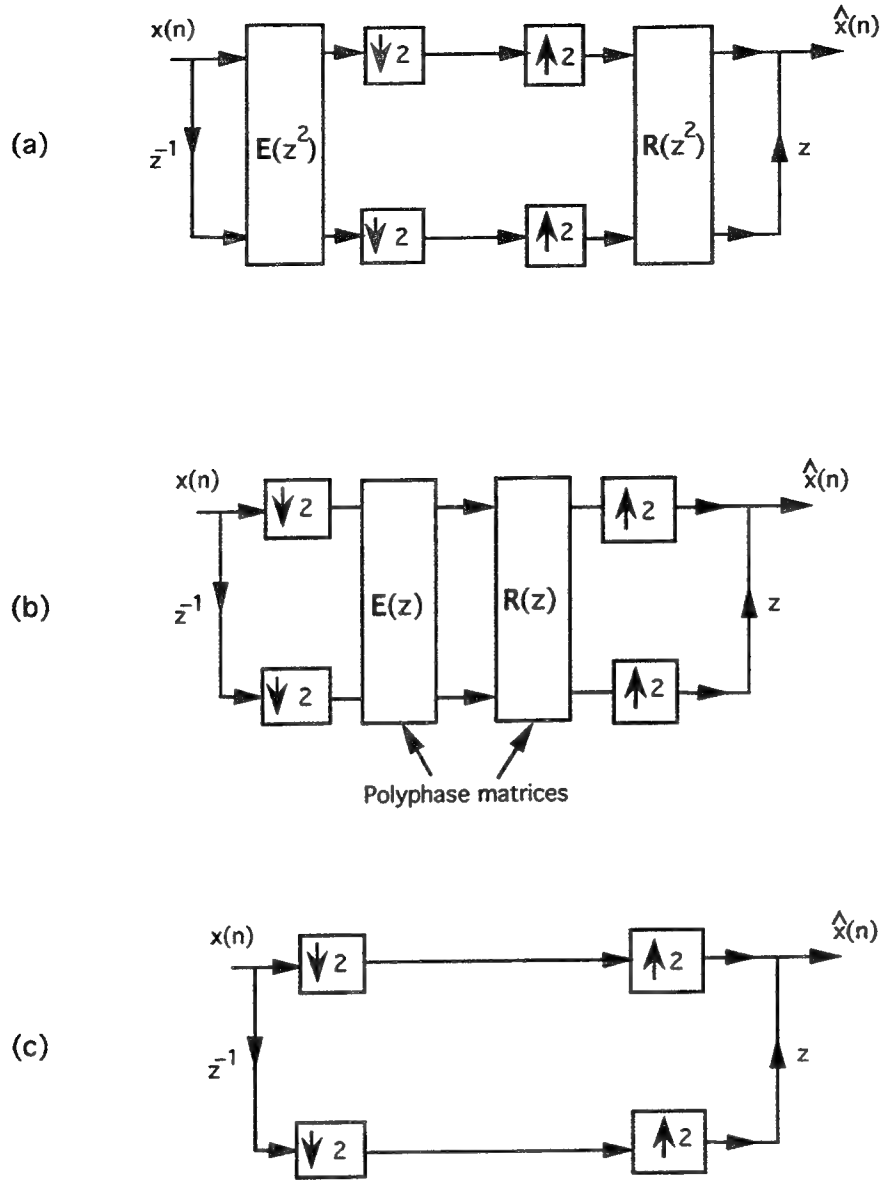

Fig. 4.2. (a) The polyphase form of the filter bank, (b) further simplification, and (c) equivalent structure when $\mathbf{R}(z) = \mathbf{E}^{-1}(z)$.

Similarly we can also write $H(z) = R_0(z^2) + zR_1(z^2)$ where $R_0(z) = E_0(z)$ and $R_1(z) = z^{-1}E_1(z)$. We will express the analysis filters $G_a(z)$ and $H_a(z)$ in the polyphase form

$$\begin{bmatrix} G_a(z) \\ H_a(z) \end{bmatrix} = \underbrace{\begin{bmatrix} E_{00}(z^2) & E_{01}(z^2) \\ E_{10}(z^2) & E_{11}(z^2) \end{bmatrix}}_{\mathbf{E}(z^2)} \begin{bmatrix} 1 \\ z^{-1} \end{bmatrix} \tag{4.9}$$

and the synthesis filters in the polyphase form

$$[G_s(z) \quad H_s(z)] = [1 \quad z] \underbrace{\begin{bmatrix} R_{00}(z^2) & R_{01}(z^2) \\ R_{10}(z^2) & R_{11}(z^2) \end{bmatrix}}_{\mathbf{R}(z^2)} \tag{4.10}$$

The 2×2 matrices $\mathbf{E}(z)$ and $\mathbf{R}(z)$ are called, respectively, the polyphase matrices of the analysis and synthesis banks. Fig. 4.2(a) shows a redrawing of the complete filter bank using the polyphase representation. It can be shown that the decimator and expander can be moved past the even powers of z to obtain the simplified representation shown in Fig. 4.2(b).

If we impose the condition $\mathbf{R}(z)\mathbf{E}(z) = \mathbf{I}$, that is

$$\mathbf{R}(z) = \mathbf{E}^{-1}(z) \tag{4.11}$$

then the system reduces to Fig. 4.2(c) which is a perfect reconstruction (PR) system with $\hat{x}(n) = x(n)$. Eqn. (4.11) will be called the perfect reconstruction condition. Notice that insertion of arbitrary scale factors and delays to obtain $\mathbf{R}(z) = cz^{-K}\mathbf{E}^{-1}(z)$ leads to $\hat{x}(n) = cx(n-2K)$ which is still the PR property.

4.4. The Paraunitary Perfect Reconstruction System

It was pointed out in [Vaidyanathan, 1987] that the CQF solution has a mathematical property called the paraunitary property and this observation makes it possible to generalize the perfect reconstruction solution to M-channel filter banks for arbitrary M. Since then, a class of filter banks called unitary or paraunitary filter banks has been developed. The paraunitary property, specialized to the two channel case, naturally yields all the CQF equations.

Definition 4.1. Paraunitary matrices. A transfer matrix[†] $\mathbf{H}(z)$ is said to be paraunitary if $\mathbf{H}(e^{j\omega})$ is unitary that is, $\mathbf{H}^{\dagger}(e^{j\omega})\mathbf{H}(e^{j\omega}) = \mathbf{I}$, for all ω. In all practical designs the filters are rational transfer functions so that the paraunitary condition implies $\widetilde{\mathbf{H}}(z)\mathbf{H}(z) = \mathbf{I}$ for all z, where the notation $\widetilde{\mathbf{H}}(z)$ is explained in Sec. 1. ◇

We sometimes allow a positive constant $\alpha > 0$, and say that $\mathbf{H}(z)$ is paraunitary if $\widetilde{\mathbf{H}}(z)\mathbf{H}(z) = \alpha\mathbf{I}$. Proper choice of α simplifies notations. Note that $\widetilde{\mathbf{H}}(z)$ reduces to transpose conjugation $\mathbf{H}^{\dagger}(e^{j\omega})$ on the unit circle. The paraunitary property has played a fundamental role in electrical network theory [Brune, 1931], [Belevitch, 1968] and has a rich history (see references in Chap. 6 and 14 of [Vaidyanathan, 1993]). Essentially, the scattering matrices of lossless (LC) multiports are paraunitary, that is unitary on the imaginary axis of the s-plane.

Properties of Paraunitary Filter Banks

A filter bank in which $\mathbf{E}(z)$ is paraunitary and $\mathbf{R}(z) = \widetilde{\mathbf{E}}(z)$ has the perfect reconstruction property $\hat{x}(n) = cx(n), c \neq 0$. We will now study the properties of such systems, which are called *paraunitary filter*

[†] Transfer matrices are essentially transfer functions of multi-input multi-output systems. A review can be found in Chap. 13 of [Vaidyanathan, 1993].

banks. All of these properties derive from a fundamental matrix equation which we first derive. By replacing z with $-z$ in Eqn. (4.9) and rearranging, we obtain

$$\underbrace{\begin{bmatrix} G_a(z) & G_a(-z) \\ H_a(z) & H_a(-z) \end{bmatrix}}_{\mathbf{G}_a(z)} = \mathbf{E}(z^2) \begin{bmatrix} 1 & 0 \\ 0 & z^{-1} \end{bmatrix} \begin{bmatrix} 1 & 1 \\ 1 & -1 \end{bmatrix} \tag{4.12}$$

Similarly for the synthesis filters,

$$\underbrace{\begin{bmatrix} G_s(z) & H_s(z) \\ G_s(-z) & H_s(-z) \end{bmatrix}}_{\mathbf{G}_s(z)} = \begin{bmatrix} 1 & 1 \\ 1 & -1 \end{bmatrix} \begin{bmatrix} 1 & 0 \\ 0 & z \end{bmatrix} \mathbf{R}(z^2) \tag{4.13}$$

Let $\mathbf{E}(z)$ and $\mathbf{R}(z)$ be paraunitary with $\tilde{\mathbf{E}}(z)\mathbf{E}(z) = 0.5\mathbf{I}$ and $\tilde{\mathbf{R}}(z)\mathbf{R}(z) = 0.5\mathbf{I}$. Then the above equations imply

$$\tilde{\mathbf{G}}_a(z)\mathbf{G}_a(z) = \mathbf{I}, \qquad \tilde{\mathbf{G}}_s(z)\mathbf{G}_s(z) = \mathbf{I}. \tag{4.14}$$

That is, the matrices $\mathbf{G}_a(z)$ and $\mathbf{G}_s(z)$ defined above are paraunitary as well. We will next draw a number of conclusions from here.

A word on language. We often say $\{G_a(z), H_a(z)\}$ is paraunitary. By this we mean that the corresponding polyphase matrix is paraunitary.

Half-band Property and Power Symmetry Property.

The paraunitary property $\tilde{\mathbf{G}}_a(z)\mathbf{G}_a(z) = \mathbf{I}$ is also equivalent to $\mathbf{G}_a(z)\tilde{\mathbf{G}}_a(z) = \mathbf{I}$ which implies, in particular, the equation

$$\tilde{G}_a(z)G_a(z) + \tilde{G}_a(-z)G_a(-z) = 1. \tag{4.15}$$

In other words, $G_a(z)$ is a power symmetric filter (Sec. 4.2). Now, a transfer function $G(z)$ satisfying $G(z) + G(-z) = 1$ is called a half-band filter. The impulse response of such $G(z)$ satisfies $g(2n) = 0$ for all $n \neq 0$ and $g(0) = 0.5$. We see that the power symmetry property of $G_a(z)$ says that $\tilde{G}_a(z)G_a(z)$ is a half-band filter. In terms of frequency response, the power symmetry property of $G_a(z)$ is equivalent to

$$|G_a(e^{j\omega})|^2 + |G_a(-e^{j\omega})|^2 = 1. \tag{4.16}$$

Imagine that $G_a(z)$ is a real-coefficient lowpass filter so that $|G_a(e^{j\omega})|^2$ has symmetry with respect to zero frequency. Then $|G_a(-e^{j\omega})|^2$ is as demonstrated in Fig. 4.3, and the power symmetry property means that the two plots in Fig. 4.3 add up to unity. In this figure, ω_p and ω_s are the bandedges, and δ_1 and δ_2 are the peak passband ripples of $G_a(e^{j\omega})$ (for definitions of filter specifications see [Oppenheim and Schafer, 1989] or [Vaidyanathan, 1993]).

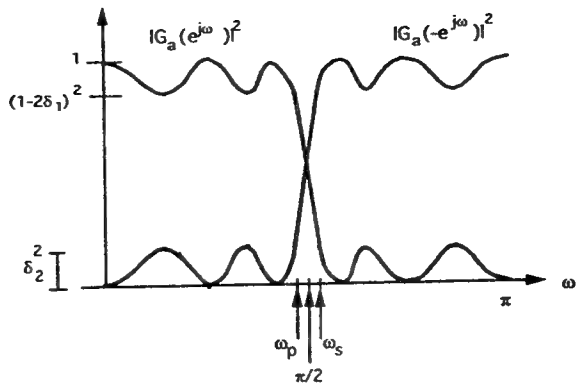

Fig. 4.3. The magnitude response $|G_a(e^{j\omega})|^2$ and $|G_a(-e^{j\omega})|^2$ for a real coefficient power symmetric filter $G_a(z)$.

Notice in particular that power symmetry of $G_a(z)$ implies that there is a symmetry relation between the passband and stopband specifications of $G_a(e^{j\omega})$. This relation is given by

$$\omega_s = \pi - \omega_p, \quad \delta_2^2 = 1 - (1 - 2\delta_1)^2. \tag{4.17}$$

Relation between the two analysis filters. It can be shown that the property $\widetilde{\mathbf{G}}_a(z)\mathbf{G}_a(z) = \mathbf{I}$ implies a relation between the analysis filters $G_a(z)$ and $H_a(z)$, namely $H_a(z) = e^{j\theta}z^N\widetilde{G}_a(-z)$ where θ is arbitrary and N is an arbitrary but odd integer. We will take $N = -1$ and $\theta = 0$ for future simplicity. Then the analysis filters are related as

$$H_a(z) = z^{-1}\widetilde{G}_a(-z). \tag{4.18}$$

In particular we have $|H_a(e^{j\omega})| = |G_a(-e^{j\omega})|$. Combining with the power symmetry property (4.16)) we see that the two analysis filters are *power complementary*, that is,

$$|G_a(e^{j\omega})|^2 + |H_a(e^{j\omega})|^2 = 1 \tag{4.19}$$

for all ω. With $G_a(z) = \sum_n g_a(n)z^{-n}$ and $H_a(z) = \sum_n h_a(n)z^{-n}$ we can rewrite (4.18) in the time domain as

$$h_a(n) = -(-1)^n g_a^*(-n+1). \tag{4.20}$$

Relation between analysis and synthesis filters. If we use the condition $\mathbf{R}(z) = \widetilde{\mathbf{E}}(z)$ in the definitions of $\mathbf{G}_s(z)$ and $\mathbf{G}_a(z)$ we obtain $\mathbf{G}_s(z) = \widetilde{\mathbf{G}}_a(z)$ from which we conclude that the synthesis filters are given by $G_s(z) = \widetilde{G}_a(z)$ and $H_s(z) = \widetilde{H}_a(z)$. We can also rewrite these in the time domain; summarizing all this we have

$$G_s(z) = \widetilde{G}_a(z),\ H_s(z) = \widetilde{H}_a(z), \qquad g_s(n) = g_a^*(-n),\ h_s(n) = h_a^*(-n). \tag{4.21}$$

The synthesis filter cofficients are time-reversed and conjugated versions of the analysis filters. Their frequency response are conjugates of the analysis filter responses. In particular $|G_s(e^{j\omega})| = |G_a(e^{j\omega})|$ and $|H_s(e^{j\omega})| = |H_a(e^{j\omega})|$.

In view of the preceding relations, the synthesis filters have all the properties of the analysis filters. For example, $G_s(e^{j\omega})$ is power symmetric, and the pair $\{G_s(e^{j\omega}), H_s(e^{j\omega})\}$ is power complementary. Finally, $H_s(z) = z\widetilde{G}_s(-z)$, instead of (4.18).

From the preceding discussions we see that in a paraunitary filter bank the filter $G_a(z)$ is power symmetric, and the remaining filters are derived from $G_a(z)$ as in (4.18) and (4.21). This is precisely the CQF solution for perfect reconstruction, stated at the beginning of this section. The observation of the paraunitary condition opens up several advantages. For example it allows us to generalize the perfect reconstruction condition for M channel filter banks. It also allows us to obtain certain cascaded lattice structures which guarantee the perfect reconstruction property in spite of quantization of filter coefficients. These details can be found in [Vaidyanathan, 1993].

Summary of Filter Relations in a Paraunitary Filter Bank

If the filter bank of Fig. 4.1(a) is paraunitary, then the polyphase matrices $\mathbf{E}(z)$ and $\mathbf{R}(z)$ (Fig. 4.2) satisfy $\widetilde{\mathbf{E}}(z)\mathbf{E}(z) = 0.5\mathbf{I}$ and $\widetilde{\mathbf{R}}(z)\mathbf{R}(z) = 0.5\mathbf{I}$. Equivalently the filter matrices $\mathbf{G}_a(z)$ and $\mathbf{G}_s(z)$ satisfy $\widetilde{\mathbf{G}}_a(z)\mathbf{G}_a(z) = \mathbf{I}$ and $\widetilde{\mathbf{G}}_s(z)\mathbf{G}_s(z) = \mathbf{I}$. A number of properties follow from these:

1. All four filters $G_a(z), H_a(z), G_s(z)$ and $H_s(z)$ are power symmetric. This property is defined, for example, by the relation (4.15). This means that the filters are spectral factors of half band filters; for example $\widetilde{G}_s(z)G_s(z)$ is half-band.
2. The analysis filters are related as in (4.18), so the magnitude responses are related as $|H_a(e^{j\omega})| = |G_a(-e^{j\omega})|$. The synthesis filters are time reversed conjugates of the analysis filters as shown by (4.21). In particular $G_s(e^{j\omega}) = G_a^*(e^{j\omega})$ and $H_s(e^{j\omega}) = H_a^*(e^{j\omega})$.
3. The analysis filters form a power complementary pair, that is (4.19) holds. The same is true for the synthesis filters.
4. Any two channel paraunitary system satisfies the CQF equations (4.6),(4.7) (except for delays, constant scale factors, and so forth). Conversely any CQF design is a paraunitary filter bank.
5. The design procedure for two channel paraunitary (i.e., CQF) filter banks is as follows: design a zero-phase lowpass half-band filter $G(z)$ with $G(e^{j\omega}) \geq 0$ and then extract a spectral factor $G_a(z)$, that is find $G_a(z)$ such that $G(z) = \widetilde{G}_a(z)G_a(z)$. Then choose the remaining three filters as in (4.7), or equivalently as in (4.8).

4.5. Parametrization of Paraunitary Filter Banks

There exist factorization theorems for paraunitary matrices which allow us to express the polyphase matrix as a cascade of elementary paraunitary blocks. This is very helpful in the design as well as implementation of these filter banks. In this section we will demonstrate the idea with a simple factorization theorem.

Theorem 4.1. Let $\mathbf{H}(z) = \sum_{n=0}^{L} \mathbf{h}(n) z^{-n}$ be a 2×2 real causal FIR transfer matrix (so $\mathbf{h}(n)$ are 2×2 matrices with real elements). This is paraunitary if and only if it can be expressed as $\mathbf{H}(z) = \mathbf{R}_N \mathbf{\Lambda}(z) \mathbf{R}_{N-1} \ldots \mathbf{R}_1 \mathbf{\Lambda}(z) \mathbf{R}_0 \mathbf{H}_0$ where

$$\mathbf{R}_m = \begin{bmatrix} \cos\theta_m & \sin\theta_m \\ -\sin\theta_m & \cos\theta_m \end{bmatrix}, \quad \mathbf{\Lambda}(z) = \begin{bmatrix} 1 & 0 \\ 0 & z^{-1} \end{bmatrix}, \quad \mathbf{H}_0 = \begin{bmatrix} \alpha & 0 \\ 0 & \pm\alpha \end{bmatrix} \tag{4.22}$$

where α and θ_m are real. ◇

For a proof see [Vaidyanathan, 1993]. The matrix $\mathbf{R}_m$ is unitary. It is called a *rotation operator* or the *Givens rotation.* If $\mathbf{y} = \mathbf{R}_m \mathbf{x}$ then $\mathbf{y}$ is obtained by rotating the vector $\mathbf{x}$ clockwise by θ_m. The matrix $\mathbf{\Lambda}(z)$ is a degree one paraunitary system. Fig. 4.4 shows the cascaded structure that results from this factorization. This is also called a lattice structure. The quantities N and L above are not necessarily equal. For example if $\mathbf{H}(z) = z^{-1}\mathbf{I}$ then $L = 1$ and $N = 2$.

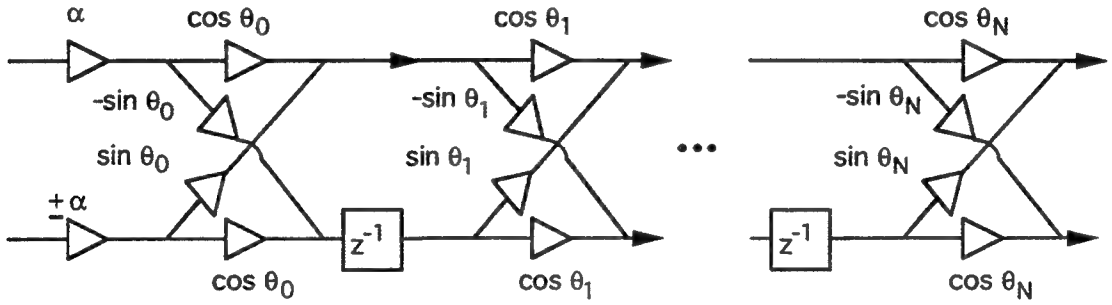

Fig. 4.4. The cascaded lattice structure for FIR paraunitary systems.

We can guarantee the paraunitary property by using the cascaded structure. Thus if the polyphase matrix is computed using the cascaded structure, then $G_a(z)$ is guaranteed to be power symmetric, and the relation $H_a(z) = z^{-1}\widetilde{G}_a(-z)$ between the analysis filters automatically holds (except for a delay). Moreover as the theorem indicates, the cascaded structure covers every paraunitary system with the specified restrictions. That is, all two channel (causal, real) FIR paraunitary filter banks have polyphase matrix of the form shown in the figure. In particular, the real coefficient CQF can be realized in this manner.

4.6. Maximally Flat Solutions

The half band filter $G(z) \triangleq \widetilde{G}_a(z) G_a(z)$ can be designed in many ways. One can get equiripple designs or maximally flat designs [Oppenheim and Schafer, 1989]. An early technique for designing FIR maximally flat

filters was proposed in [Herrmann, 1971]. This method gives closed form expressions for the filter coefficients and can be easily adapted for the special case of half band filters. Moreover, the design automatically guarantees the condition $G(e^{j\omega}) \geq 0$ (which in particular implies zero phase).

The family of maximally flat half band filters designed by Herrmann is demonstrated in Fig. 4.5.

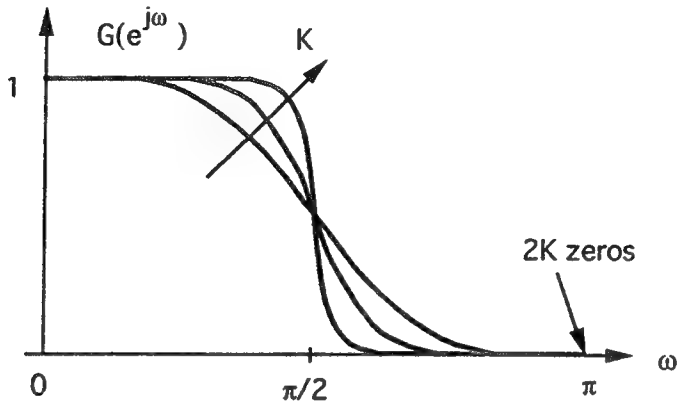

Fig. 4.5. Maximally flat half-band filter responses with $2K$ zeros at π.

The transfer function has the form

$$G(z) = z^K \left(\frac{1+z^{-1}}{2}\right)^{2K} \sum_{n=0}^{K-1} (-z)^n \binom{K+n-1}{n} \left(\frac{1-z^{-1}}{2}\right)^{2n} \tag{4.23}$$

The filter has order $4K-2$. There are $2K$ zeros on the unit circle and all of these zeros are concentrated at the point $z=-1$ (i.e., at $\omega=\pi$). The remaining $2K-2$ zeros are located in the z-plane such that $G(z)$ has the half-band property described earlier (i.e., $G(z)+G(-z)=1$).

We will see later (Sec. 13) that if the CQF bank is designed by starting from Herrmann's maximally flat half-band filter, then it can be used to design continuous time wavelets with excellent regularity (i.e., smoothness) properties.

4.7. Tree Structured Filter Banks

The idea of splitting a signal $x(n)$ into two subbands can be extended by splitting a subband signal further, as demonstrated in Fig. 4.6(a). In this example the lowpass subband is split over and over again. This is called a tree structured filter bank. Each node of the tree is a two-channel analysis filter bank. There are several variations of this scheme; for example we can choose to have differnt filter pairs at different levels of the tree. We can also choose to split the high pass subband; and we can replace the two channel system with a more general (M channel) system at each node of the tree.

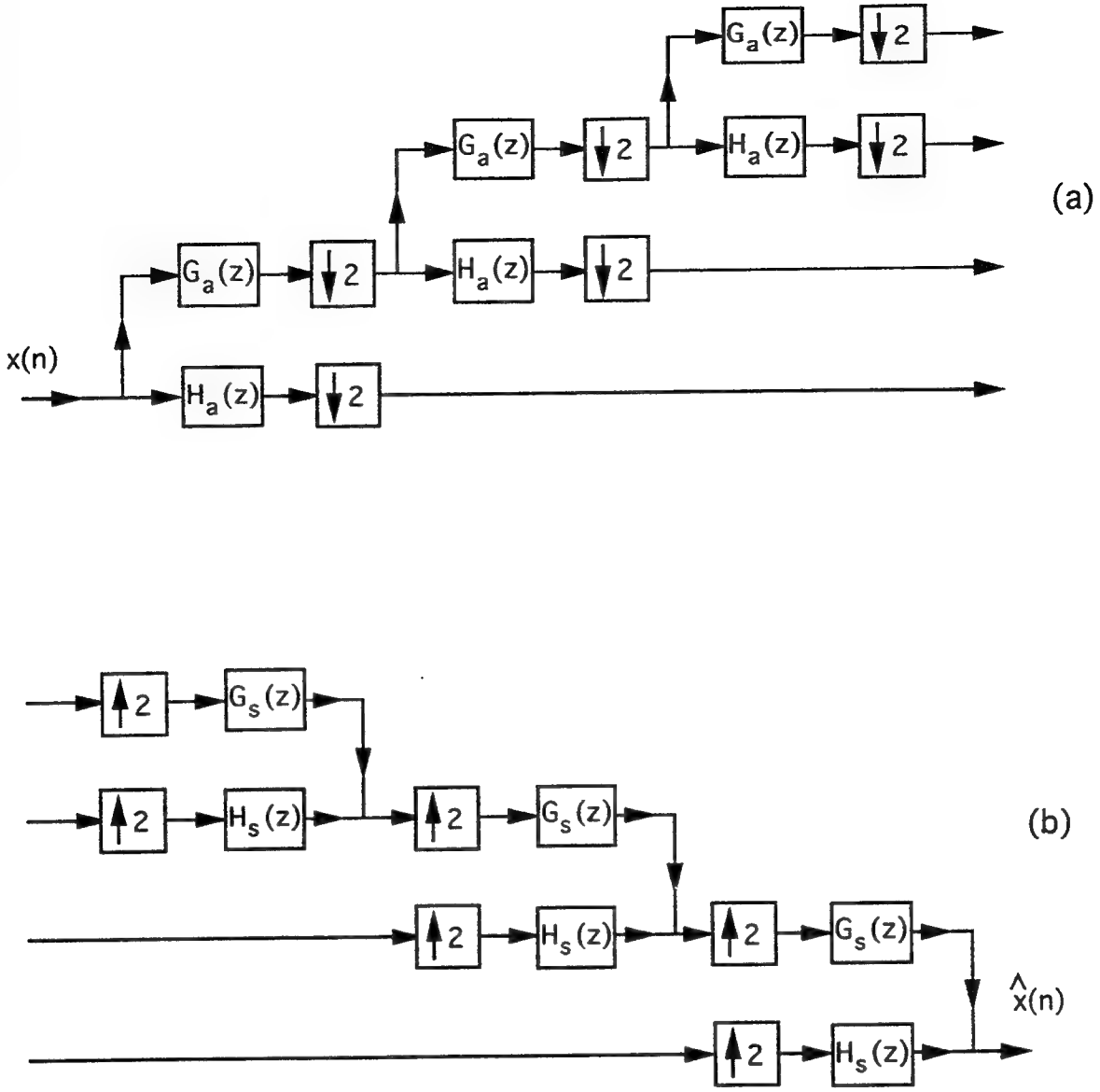

Fig. 4.6. Tree-structured filter banks (a) analysis bank, and (b) synthesis bank.

The synthesis bank corresponding to Fig. 4.6(a) is shown in Fig. 4.6(b). We combine the signals in pairs, in the same manner that we split them. It can be shown that if $\{G_a(z), H_a(z), G_s(z), H_s(z)\}$ is a perfect reconstruction system [i.e., satisfies $\hat{x}(n) = x(n)$ when connected in the form Fig. 4.1(a)] then the tree structured analysis/synthesis system of Fig. 4.6 has perfect reconstruction $\hat{x}(n) = x(n)$.

The tree structured system can be redrawn in the form shown in Fig. 4.7. For example if we have a tree structure like Fig. 4.6 with three levels, we have $M = 4$, $n_0 = 2, n_1 = 4, n_2 = 8$ and $n_3 = 8$. If we assume that the responses of the analysis filters $G_a(e^{j\omega})$ and $H_a(e^{j\omega})$ are as in Fig. 4.8(a) then the responses of the analysis filters $H_k(e^{j\omega})$ are as shown in Fig. 4.8(b). Note that this resembles the wavelet transform

[Fig. 2.8(b)]. The outputs of different filters are subsampled at different rates exactly as for wavelets. Thus the tree structured filter bank has close relation to the wavelet transform. In Sec. 10–13 we will present the precise mathematical connection between the two. We will also see that tree structured filter banks are closely related to multiresolution analysis (Sec. 10).

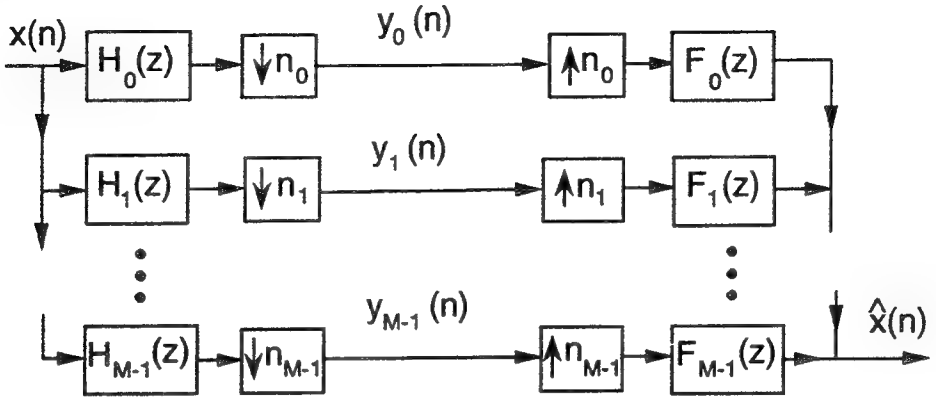

Fig. 4.7. A general nonuniform digital filter bank.

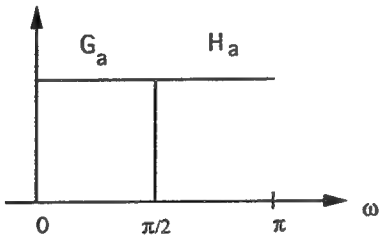

(a)

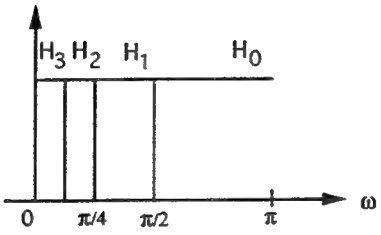

(b)

Fig. 4.8. An example of responses (a) $G_a(z)$ and $H_a(z)$, and
(b) Tree-structured analysis bank.

4.8. Filter Banks and Basis Functions

Consider again Fig. 4.7. Assuming perfect reconstruction we have $\widehat{x}(n) = x(n)$ which means we can express $x(n)$ in terms of the decimated subband signals $y_k(n)$ and the impulse responses $f_k(n)$ of the filters $F_k(z)$.

This expression has the form

$$x(n) = \sum_{k=0}^{M-1} \sum_{m=-\infty}^{\infty} y_k(m) f_k(n - n_k m). \tag{4.24}$$

This system is analogous to the filter bank systems which represented the continuous time STFT and wavelet transforms in Sec. 2 and 3. Thus the collection of subband signals $y_k(m)$ can be regarded as a time-frequency representation for $x(n)$ which, in this section, is a *discrete time signal.* As in Sec. 2.7, k denotes the "frequency index" and m the "time index" in the transform domain. If we have a perfect reconstruction filter bank we can recover $x(n)$ from this time-frequency representation using (4.24). The doubly indexed family of discrete time sequences $\{\eta_{km}(n)\}$ where $\eta_{km}(n) = f_k(n - n_k m)$ can be regarded as "basis functions" for the representation of $x(n)$ in terms of the time-frequency coefficients $\eta_{km}(n)$.

To make things mathematically more accurate let us say that $x(n) \in \ell^2$ (i.e., $\sum_n |x(n)|^2$ is finite). If the two channel filter bank $\{G_a(z), H_a(z), G_s(z), H_s(z)\}$ which makes up the tree structure of Fig. 4.6 is paraunitary, it can be shown that $\eta_{km}(n)$ is an orthonormal basis for ℓ^2. Orthonormality means

$$\sum_{n=-\infty}^{\infty} \eta_{k_1 m_1}(n) \eta^*_{k_2 m_2}(n) = \delta(k_1 - k_2)\delta(m_1 - m_2). \tag{4.25}$$

While (4.24) resembles the STFT and wavelet representations developed in Sec. 2 and 3, there are similarities and differences. First, it is in discrete time, and second the basis functions (sequences) are not derived from a single function. By contrast a wavelet basis $\{2^{k/2}\psi(2^k t - n)\}$ is derived from a *single* wavelet function $\psi(t)$. We say that $\{\eta_{km}(n)\}$ is a *filter-bank* type of basis for the space of ℓ^2 sequences. The basis is a doubly indexed infinite family of sequences, derived from a *finite* number of filters $\{f_k(n)\}$ by time-shifts of a specific form. The filter-bank type basis is orthonormal if $\{G_s(z), H_s(z)\}$ is paraunitary [Soman and Vaidyanathan, 1993].

5. DEEPER STUDY OF WAVELETS, FILTERBANKS, AND STFT

From Sec. 2 and 3, we already know what the wavelet transform is and how it compares with the short time Fourier transform, at least qualitatively. We are also familiar with time-frequency representations and digital filter banks. It is time now to fill several important details, and generally be more quantitative. For example, we would like to mention some major technical limitations of the STFT which are not obvious from its definition, and explain that wavelets do not have this limitation.

For example, we will see that if the STFT is used to obtain an orthonormal basis for L^2 signals, then the time-frequency rms durations of the window $v(t)$ (defined in Sec. 3.1) will satisfy $D_t D_f = \infty$. That is, either the time or the frequency resolution is very poor (Theorem 9.1). It also turns out that if we have an STFT system where the time-frequency sampling product $\omega_s T_s$ is small enough to admit redundancy (i.e.,

the vectors are not linearly independent as they would be in an orthonormal basis) then the above difficulty can be eliminated (Sec. 9).

The Gabor transform described in Section 3.1, while admittedly a tempting candidate because of the optimal time-frequency resolution property ($D_t D_f$ minimized), has a disadvantage. Namely, if we want to recover the signal $x(t)$ from the STFT coefficients, the reconstruction is *unstable* in the so-called critically sampled case (Sec. 9). That is, a small error in the STFT coefficients can lead to a large error in reconstruction.

The wavelet transform does not suffer from the above limitations of the STFT. We will show how to construct orthonormal wavelet bases with good time and frequency resolutions (Sec. 11–13). We will also show that we can start from a paraunitary digital filter bank and construct orthonormal wavelet bases for $L^2(R)$ in a very systematic way (Theorem 11.5). Moreover this can be done in such a way that many desired properties (e.g., compact support, orthonormality, good time frequency resolution, smoothness, and so forth) can be incorporated during the construction (Sec. 13). Such a construction is placed in evidence by the *theory of multiresolution,* which gives a unified platform for wavelet construction and filter banks (Theorems 10.1,10.2).

At this point in time, the reader may want to preview the above mentioned theorems in the future sections, in order to get a flavor of things to come. However, to explain these results in a quantitative way, it is very convenient to review a number of mathematical tools. The need for advanced tools arises because of the intricacies associated with basis functions for infinite dimensional spaces i.e., spaces where the set of basis functions is an infinite set. (For finite dimensional spaces an understanding of elementary matrix theory would have been sufficient.) For example a representation of the form $x(t) = \sum c_n f_n(t)$ in an infinite dimensional space could be *unstable* in the sense that a small error in the transform domain $\{c_n\}$ could get amplified in an unbounded manner during reconstruction. We will talk about a special type of basis called the *Riesz basis* which does not have this problem (orthonormal bases are special cases of these). We will also talk about *frames* which share many good properties of the Riesz bases but may have redundant vectors (i.e., not a linearly independent set of vectors). For example, the concept of frames will arise in the comparison of wavelets and the STFT. We will see that general STFT frames have an advantage over STFT bases. Frames also come into consideration when we explain the connection between wavelets and paraunitary digital filter banks in Sec. 11.4. When explaining the connection between wavelets and non unitary filter banks, one again encounters Riesz bases and the idea of *biorthogonality.*

Since it is difficult to find all the mathematical background material in one place, we have tried to review a carefully selected set of topics in the next few sections. These are very useful for a deeper understanding

of wavelets and STFT. The material in Sec. 6 is fairly standard (Lebesgue integrals, L^p spaces, L^1 and L^2 Fourier transforms). The material in Sec. 7 and 8 (Riesz bases and frames) are less commonly known among engineers but play a significant role in wavelet theory. The reader may want to go through these review sections 6–8 (admittedly dense), once during first reading and then use them primarily as a reference. After this review we will return to our discussions of wavelets, STFT and filter banks.

6. THE SPACE OF L^1 and L^2 SIGNALS

We developed the wavelet representation in Sec. 2.1 based on the framework of a bank of bandpass filters. To make everything mathematically meaningful it becomes necessary to carefully specify the types of signals, types of Fourier transforms, and so forth. For example, as engineers, the concept of ideal bandpass filtering is appealing to us, but there arises a difficulty. An ideal bandpass filter $H(\omega)$ is not stable, that is $\int |h(t)|dt$ does not exist [Oppenheim and Schafer, 1989]. In other words $h(t)$ does not belong to the space L^1 (see below).

Why should this bother us if we are only discussing theory? Take an example. The frequency domain developments based on Fig. 2.7, which finally give rise to the time domain expression (2.8) implicitly rely on the convolution theorem (which says that convolution in time implies multiplication in frequency). However, the convolution theorem is typically proved only for L^1 signals and bounded L^2 signals. It is not valid for arbitrary signals. We therefore need to be careful when using these familiar engineering notions in a mathematical discussion.

6.1. Lebesgue integrals

In most engineering discussions we think of the integrals as Riemann integrals. But in order to handle several convergence questions in the development of Fourier series, convolution theorems, wavelet transforms and so forth, it is necessary to use Lebesgue integration. There are many beautiful results for Lebesgue integration which are not true for the Riemann integral under comparable assumptions about signals. This includes theorems that allow us to interchange limits, integrals, and infinite sums freely.

In this chapter all integrals are Lebesgue integrals. A review of Lebesgue integration is beyond the scope of this chapter. There are many excellent references, for example [Kolmogorov and Fomin, 1970], [Haaser and Sullivan, 1971], and [Apostol, 1974]. A few elementary comparisons between Riemann and Lebesgue integrals are pointed out below.

1. If $x(t)$ is Riemann integrable on a bounded interval $[a, b]$ then it is also Lebesgue integrable on $[a, b]$. But the converse is not true. For example if we define $x(t) = -1$ for all rationals and $x(t) = 1$ for

all irrationals in $[0,1]$ then $x(t)$ is not Riemann integrable in $[0,1]$. But it is Lebesgue integrable, and $\int_0^1 x(t)dt = 1$.

2. A similar statement is not true for the unbounded interval $(-\infty, \infty)$. For the unbounded interval $(-\infty, \infty)$ the Riemann integral is defined only as a limit called the *improper integral.*† Consider the sinc function defined as: $s(t) = \sin t/t$ for $t \neq 0$, and $s(0) = 1$. This has improper Riemann integral $= \pi$ but is not Lebesgue integrable.
3. If $x(t)$ is Lebesgue integrable then so is $|x(t)|$. The same is not true for Riemann integrals, as demonstrated by the sinc function $s(t)$ of the preceding paragraph.
4. If $|x(t)|$ is Lebesgue integrable then so is $x(t)$ as long as it is measurable.‡ This however, is not true for Riemann integrals. For example if we define $x(t) = -1$ for all rationals and 1 for all irrationals in $[0,1]$ then it is not Riemann integrable in $[0,1]$ though $|x(t)|$ is.
5. If $x(t)$ is (measurable and) bounded by a nonnegative Lebesgue integrable function $g(t)$ [i.e., $|x(t)| \leq g(t)$] then $x(t)$ is Lebesgue integrable.

Sets of Measure Zero

A subset $\mathcal{S}$ of real numbers is said to have measure zero if, given $\epsilon > 0$ we can find a countable union $\cup_i I_i$ of open intervals I_i [intervals of the form (a_i, b_i), i.e., $a_i < x < b_i$] such that (i) $\mathcal{S} \subset \cup_i I_i$ and (ii) the total length of the intervals $< \epsilon$. For example the set of all integers (in fact any countable set of real numbers, e.g., rationals) has measure zero. There exist uncountable sets of real numbers which have measure zero, a famous example being the Cantor set [Apostol, 1974].

When we say that something is true "almost everwhere" (abbreviated a.e.), or "for almost all t" it means that the statement holds everywhere except possibly on a set of measure zero. For example if $x(t) = y(t)$ everywhere except for integer values of t, then $x(t) = y(t)$ a.e. An important fact in Lebesgue integration theory is that if two Lebesgue integrable functions are equal a.e., then their integrals are equal. In particular if $x(t) = 0$ a.e., then the Lebesgue integral $\int x(t)dt$ exists and is equal to zero.

---

† Essentially we consider $\int_{-a}^{b} x(t)dt$ and let a and b go to ∞ *separately.* This limit, the improper Riemann integral, should not be confused with the *Cauchy principal value* which is the limit of $\int_{-a}^{a} x(t)dt$ as $a \to \infty$. The function $x(t) = t$ has Cauchy principal value $= 0$, but the improper Riemann integral does not exist.

‡ The notion of a measurable function is very subtle. Any continuous function is measurable, and any Lebesgue integrable function is measurable. In fact, examples of non measureable functions are so rare and so hard to construct, that there is practically no danger we will run into one. We take measurability for granted and never mention it.

Convergence Theorems

What makes the Lebesgue integral so convenient is the existence of some powerful theorems, which allow us to interchange limits with integrals and summations, under very mild conditions. These theorems have been at the center of many beautiful results in Fourier and wavelet transform theory.

Let $\{g_k(t)\}, 1 \leq k \leq \infty$ be a sequence of Lebesgue integrable functions. In general this sequence may not have a limit, and even if it did, the limit may not be integrable. Under some further mild postulates, we can talk about limits and their integrals. In what follows we often say "$g(t)$ is a pointwise limit a.e. of the sequence $\{g_k(t)\}$", or "$g_k(t)$ converges to $g(t)$ a.e." This means that for any chosen value of t (except possibly in a set of measure zero), we have $g_k(t) \rightarrow g(t)$ as $k \rightarrow \infty$.

Monotone convergence theorem. Suppose (a) $\{g_k(t)\}$ is *non decreasing a.e.* (i.e., for almost all values of t, $g_k(t)$ is non decreasing in k) and (b) $\int g_k(t)dt$ is a *bounded sequence.* Then $\{g_k(t)\}$ converges a.e. to a Lebesgue integrable function $g(t)$ and $\lim_k \int g_k(t)dt = \int \lim_k g_k(t)dt$, i.e., $\lim_k \int g_k(t)dt = \int g(t)dt$. That is, we can *interchange the limit with the integral.*

Dominated convergence theorem. Suppose (a) $\{g_k(t)\}$ is dominated by a nonnegative Lebesgue integrable function $f(t)$ i.e., $|g_k(t)| \leq f(t)$ a.e., and (b) $\{g_k(t)\}$ converges to a limit $g(t)$ a.e. Then the limit $g(t)$ is Lebesgue integrable and $\lim_k \int g_k(t)dt = \int \lim_k g_k(t)dt$, i.e., $\lim_k \int g_k(t)dt = \int g(t)dt$. That is, we can interchange the limit with the integral.

Levi's theorem. Suppose $\int \sum_{k=1}^{m} |g_k(t)|dt$ is a bounded sequence in m. Then $\int \sum_{k=1}^{\infty} g_k(t)dt = \sum_{k=1}^{\infty} \int g_k(t)dt$. In particular this means that $\sum_{k=1}^{\infty} g_k(t)$ converges a.e. to a Lebesgue integrable function. This theorem permits us to *interchange infinite sums with the integrals.*

Fatou's Lemma. Let (a) $g_k(t) \geq 0$ a.e., (b) $g_k(t) \rightarrow g(t)$ a.e., and (c) $\int g_k(t)dt \leq A$ for some $0 < A < \infty$. Then the limit $g(t)$ is Lebesgue integrable and $\int g(t) \leq A$. (There exist stronger versions of this result [Rudin, 1966], but we shall not require them here.)

6.2. L^p signals

Let p be an integer such that $1 \leq p < \infty$. A signal $x(t)$ is said to be an L^p signal if (it is measurable, and) $\int |x(t)|^p dt$ exists. We define the L^p norm of $x(t)$ as $\|x(t)\|_p = [\int |x(t)|^p dt]^{1/p}$. For fixed p the set of L^p signals forms a vector space. It is a normed linear vector space, with norm defined as above. The term "linear" means that if $x(t)$ and $y(t)$ are in L^p, then $\alpha x(t) + \beta y(t)$ is also in L^p for any complex α and β.

Since any two signals $x(t)$ and $y(t)$ that are equal a.e. cannot be distinguished (i.e., $\|x(t) - y(t)\| = 0$), each element in L^p is in reality "a set of functions that are equal a.e". Each such set becomes an "equivalence class" in mathematical language.

For $p = 2$ the quantity $\|x(t)\|_p^2$ is equal to the *energy* of $x(t)$, as defined in signal processing texts. Thus an L^2 signal is a finite-energy (or square-integrable) signal. For $p = \infty$ the above definitions do not make sense, and we simply define L^∞ to be the space of *essentially bounded signals*. A signal $x(t)$ is said to be essentially bounded if there is a number $B < \infty$ such that $|x(t)| \leq B$ a.e. We often omit the term "essential" for simplicity; it arises because of the "a.e." in the inequality. The norm $\|x(t)\|_\infty$ is taken as essential supremum of $|x(t)|$ over all t. That is, $\|x(t)\|_\infty$ is the smallest number such that $|x(t)| \leq \|x(t)\|_\infty$ a.e.

For us L^1, L^2 and L^∞ functions are particularly interesting. Note that neither L^1 nor L^2 contains the other. However bounded L^1 functions are in L^2, and L^2 functions on bounded intervals are in L^1. That is,

$$L^1 \cap L^\infty \subset L^2, \qquad \text{and} \qquad L^2[a,b] \subset L^1[a,b]. \tag{6.1}$$

Thus L^2 is already bigger than bounded L^1 functions. Moreover,

$$x(t) \in L^1 \cap L^\infty \qquad \Rightarrow \qquad x(t) \in L^p \text{ for all } p > 1.$$

This follows because $|x(t)|^p \leq |x(t)|\ \|x(t)\|_\infty^{p-1}$. Thus, $|x(t)|^p$ is (measurable and) bounded by a Lebesgue integrable function (since $|x(t)|$ is integrable), and is therefore integrable.

Orthonormal signals in L^2

The inner product $\langle x(t), y(t)\rangle = \int x(t)y^*(t)dt$ always exists for any $x(t)$ and $y(t)$ in L^2. Thus the product of two L^2 functions is an L^1 function. If $\langle x(t), y(t)\rangle = 0$ we say that $x(t)$ and $y(t)$ are orthogonal. Clearly $\|x(t)\|_2^2 = \langle x(t), x(t)\rangle$. Consider a sequence $\{g_n(t)\}$ of signals such that any pair of these are orthogonal, and $\|g_n(t)\|_2 = 1$ for all n. This is said to be an orthonormal sequence. The following two results are fundamental.

Theorem 6.1. Let $\{g_n(t)\}, 1 \leq n \leq \infty$ be an orthonormal sequence in L^2. Define $c_n = \langle x(t), g_n(t)\rangle$ for some $x(t) \in L^2$. Then the sum $\sum_n |c_n|^2$ converges, and $\sum_n |c_n|^2 \leq \|x(t)\|^2$. ◇

Theorem 6.2. (Riesz-Fischer theorem). Let $\{g_n(t)\}, 1 \leq n \leq \infty$ be an orthonormal sequence in L^2 and let $\{c_n\}$ be a sequence of complex numbers such that $\sum_n |c_n|^2$ converges. Then there exists $x(t) \in L^2$ such that $c_n = \langle x(t), g_n(t)\rangle$, and $x(t) = \sum_n c_n g_n(t)$ (with equality interpreted in the L^2 sense, see below). ◇

The space L^2 is more convenient to work with, than L^1. For example the inner product and the concept of orthonormality are undefined in L^1. Moreover, as we shall see Sec. 6.3, the Fourier transform in L^2 has more time-frequency symmetry than in L^1. In Sec. 7.3 we will define *unconditional bases*, which have the property that any rearrangement continues to be a basis. It turns out that any orthonormal basis in L^2 is unconditional, whereas the L^1 space does not even have an unconditional basis!

Equality and Convergence in L^p Sense

Let $x(t)$ and $y(t)$ be L_p functions ($p < \infty$). Then $\|x(t) - y(t)\|_p = 0$ if and only if $x(t) = y(t)$ a.e. Thus if $x(t)$ and $y(t)$ differ only for every rational t we still have $\|x(t) - y(t)\|_p = 0$. Whenever $\|x(t) - y(t)\|_p = 0$, we say that $x(t) = y(t)$ in L^p sense. Now consider a statement of the form

$$x(t) = \sum_{n=1}^{\infty} c_n g_n(t) \tag{6.2}$$

for $p < \infty$, where $g_n(t)$ and $x(t)$ are in L^p. This means that the sum converges to $x(t)$ in the L^p sense, that is $\|x(t) - \sum_{n=1}^{N} c_n g_n(t)\|_p$ goes to zero as $N \to \infty$. If we modify the limit $x(t)$ by adding some number to $x(t)$ for all rational t, the result is still a limit of $\sum_{n=1}^{N} c_n g_n(t)$ in the L^p sense! L^p limits are unique only in the a.e. sense. We omit the phrase "in the L^p sense" whenever it is clear from the context.

The ℓ^p Spaces

Let p be an integer with $1 \leq p \leq \infty$. The collection of all sequences $x(n)$ such that $\sum_n |x(n)|^p$ converges to a finite value is denoted ℓ^p. This is a linear space with norm $\|x(n)\|$ defined such that $\|x(n)\| = \left(\sum_n |x(n)|^p\right)^{1/p}$. Unlike L^p spaces, the ℓ^p spaces satisfy the following inclusion rule:

$$\ell^1 \subset \ell^2 \subset \ell^3 \subset \ldots \ell^\infty \tag{6.3}$$

The spaces ℓ^1 and ℓ^2 are especially interesting in circuits and signal processing. If $h(n) \in \ell^1$ then $\sum_n |h(n)| < \infty$. This is precisely the condition for the BIBO (bounded-input bounded-output) stability of a linear time invariant system with impulse response $h(n)$ [Oppenheim, et al., 1983].

Continuity of Inner Products

If $\{x_n(t)\}$ is a sequence in L^2 and has an L^2 limit $x(t)$, then for any $y(t) \in L^2$,

$$\lim_{n\to\infty} \Big\langle x_n(t), y(t) \Big\rangle = \Big\langle \lim_{n\to\infty} x_n(t), y(t) \Big\rangle = \Big\langle x(t), y(t) \Big\rangle \tag{6.4}$$

with the second limit interpreted in the L^2 sense. Thus, limits can be interchanged with inner product signs. Similarly infinite summation signs can be interchanged with the inner product sign, that is, $\sum_{n=1}^{\infty} \langle \alpha_n x_n(t), y(t) \rangle = \Big\langle \sum_{n=1}^{\infty} \alpha_n x_n(t),\ y(t) \Big\rangle$, provided the second summation is regarded as an L^2 limit. These follow from the fundamental property that *inner products are continuous* [Rudin, 1966].

Next suppose $\{x_n(t)\}$ is a sequence of functions in L^p for some integer $p \geq 1$ and suppose $x_n(t) \to x(t)$ in the L^p sense. Then $\|x_n(t)\|_p \to \|x(t)\|_p$ as well. We can rephrase this as

$$\lim_{n\to\infty} \|x_n(t)\|_p = \| \lim_{n\to\infty} x_n(t)\|_p = \|x(t)\|_p \tag{6.5}$$

Thus the limit sign can be interchanged with the norm sign, where the limit in the second expression is in the L^p sense. This follows because $\left| \|x_n(t)\|_p - \|x(t)\|_p \right| \leq \|x_n(t) - x(t)\|_p \to 0$ as $n \to \infty$.

6.3. Fourier transforms

The Fourier transform (FT) is defined for L^1 signals and L^2 signals in different ways. † The properties of these two types of FT are significantly different. In the signal processing literature, where we ultimately seek engineering solutions (such as filter approximation with rational transfer functions), this distinction often is not necessary. But when we try to establish that a certain set of signals is a basis for a certain class, we have to be careful, especially if we use tools such as the FT, convolution theorem, and so forth (as we implicitly did in Sec. 2). Detailed references for this section include Rudin [1966], Apostol [1974], and Chui [1992a].

The L^1 Fourier Transform.

Given a signal $x(t) \in L^1$, its Fourier transform $X(\omega)$ (the L^1 FT) is defined in the way familiar to engineers:

$$X(\omega) = \int_{-\infty}^{\infty} x(t) e^{-j\omega t} dt \tag{6.6}$$

The existence of this integral is assured by the fact that $x(t)$ is in L^1.‡ In fact the above integral exists if and only if $x(t) \in L^1$. The L^1 Fourier transform has the following properties:

1. $X(\omega)$ is a continuous function of ω.
2. $X(\omega) \to 0$ as $|\omega| \to \infty$. This is called the *Riemann-Lebesgue Lemma.*
3. $X(\omega)$ is bounded, and $|X(\omega)| \leq \|x(t)\|_1$.

In engineering applications we often draw the ideal lowpass filter response ($F(\omega)$ in Fig. 2.3) and consider it as the Fourier transform of the impulse response $f(t)$. But this frequency response is discontinuous and already violates Property 1. This is because $f(t)$ is not in L^1 and $F(\omega)$ is not the L^1-FT of $f(t)$. That $f(t)$ is not in L^1 is consistent with the fact that the ideal filter is not BIBO stable (i.e., a bounded input may not produce bounded output, since $\int |f(t)| dt$ is not finite).

The inverse Fourier transform. In general the FT $X(\omega)$ of an L^1 signal is not in L^1. Example: if $x(t)$ is the rectangular pulse, then $X(\omega)$ is the sinc function which is not absolutely integrable. Thus the familiar inverse transform formula

$$x(t) = \frac{1}{2\pi} \int_{-\infty}^{\infty} X(\omega) e^{j\omega t} d\omega \tag{6.7}$$

---

† For more general signals the FT can sometimes be defined in the "distribution sense"; see Appendix A.

‡ Since $x(t)$ is Lebesgue integrable (hence measurable) the product $x(t)e^{-j\omega t}$ is measurable, and it is bounded by the integrable function $|x(t)|$. So $x(t)e^{-j\omega t}$ is integrable.

does not make sense in general. However since $X(\omega)$ is continuous and bounded, it is integrable on any bounded interval, so $\int_{-c}^{c} X(\omega)e^{j\omega t}d\omega/2\pi$ exists for any finite c. This quantity may even have a limit as $c \to \infty$, even if the Lebesgue integral or improper Rieman integral, does not exist. Such a limit (the Cauchy principal value) does represent the original function $x(t)$ under some conditions.

Case 1. Thus, suppose $x(t) \in L^1$ and suppose that it is of *bounded variation* in an interval $[a, b]$, that is, it can be expressed as the difference of two nondecreasing functions [Apostol, 1974]. Then we can show that the above Cauchy principal value exists, and

$$\frac{x(t^+) + x(t^-)}{2} = \lim_{c\to\infty} \frac{1}{2\pi} \int_{-c}^{c} X(\omega)e^{j\omega t}d\omega \tag{6.8}$$

for every $t \in (a, b)$. The notations $x(t^-)$ and $x(t^+)$ are the left hand limit and right hand limit, respectively, of $x(\cdot)$ at t; for functions of bounded variation, these limits can be shown to exist. If $x(\cdot)$ is continuous at t, then $x(t^-) = x(t^+) = x(t)$ and the above reduces to the familiar inversion formula.

Case 2. Suppose now that $x(t) \in L^1$ and $X(\omega) \in L^1$ as well. Then the integral $y(t) \triangleq \int_{\infty}^{\infty} X(\omega)e^{j\omega t}d\omega/2\pi$ exists as a Lebesgue integral, and $y(t) = x(t)$ almost everywhere [Rudin, 1966]. In particular, if $x(\cdot)$ is continuous at t then $x(t) = \int_{\infty}^{\infty} X(\omega)e^{j\omega t}d\omega/2\pi$.

It turns out that if $x(t)$ and $X(\omega)$ are both in L^1 then they are both in L^2 as well. This is shown as follows: since $x(t) \in L^1$ implies that $X(\omega)$ is bounded, we see that $X(\omega) \in L^1 \cap L^\infty$. So $X(\omega) \in L^p$ for all integer p (Sec. 6.2). In particular $X(\omega) \in L^2$, so $x(t) \in L^2$ as well (by Parseval's relation, see below).

The L^2 Fourier Transform

The L^1 Fourier transform lacks the convenient property of time-frequency symmtery. For example, even though $x(t)$ is in L^1, $X(\omega)$ may not be in L^1. Also even though $x(t)$ may not be contiuous, $X(\omega)$ is necessarily continuous. The space L^2 is much easier to work with. Not only can we talk about inner products and orthonormal bases, there is also perfect symmetry between time and frequency domains, as we shall see. We need to define the L^2-FT differently because the ususal definition (6.6) is meaningful only for L^1 signals. Suppose $x(t) \in L^2$ and we truncate it to the interval $[-n, n]$. This truncated version is in L^1 because of (6.1), and its L^1 Fourier transform exists:

$$X_n(\omega) = \int_{-n}^{n} x(t)e^{-j\omega t}dt \tag{6.9}$$

It can be shown that $X_n(\omega)$ is in L^2 and that the sequence $\{X_n(\omega)\}$ has a limit in L^2. That is, there exists an L^2 function $X(\omega)$ such that

$$\lim_{n\to\infty} \|X_n(\omega) - X(\omega)\|_2 = 0 \tag{6.10}$$

This limit $X(\omega)$ is defined to be the L^2 Fourier transform of $x(t)$. Some of the properties are listed next.

1. $X(\omega)$ is in L^2 and we can compute $x(t)$ from $X(\omega)$ in an entirely analogous manner, namely the L^2 limit of $\int_{-n}^{n} X(\omega)e^{j\omega t}d\omega/2\pi$.
2. If $x(t)$ is in L^1 and L^2, then the above computation gives the same answer as the L^1 FT (6.6) a.e. For example consider the rectangular pulse $x(t) = 1$ in $[-1, 1]$ and zero otherwise. This is in L^1 and L^2 and the Fourier transform using either definition is is $X(\omega) = 2\sin\omega/\omega$. This answer is in L^2 but not in L^1. The inverse L^2-FT of $X(\omega)$ is the original $x(t)$.
3. If $x(t) \in L^2$ and $X(\omega) \in L^1$ then the Lebesgue integral $\int_{-\infty}^{\infty} X(\omega)e^{j\omega t}d\omega/2\pi$ exists, and equals $x(t)$ a.e.
4. Parseval's relation holds, i.e., $\sqrt{2\pi}\|x(t)\|_2 = \|X(\omega)\|_2$. Thus the FT is a linear transformation from L^2 to L^2 which preserves norms except the scale factor $\sqrt{2\pi}$. (Note that this would not make sense if $x(t)$ were only in L^1.) In particular it is a bounded transformation because the norm $\|X(\omega)\|_2$ in the transform domain is bounded by the norm $\|x(t)\|_2$ in the original domain.
5. Unlike the L^1 FT, the L^2 FT $X(\omega)$ need not be continuous. For example, the impulse response of an ideal lowpass filter (sinc function) is in L^2 and its Fourier transform is not continuous.
6. Let $\{f_n(t)\}$ be a sequence in L^2 and let $x(t) = \sum_n c_n f_n(t)$ be a convergent summation (in the L^2 sense). With upper case letters denoting the L^2-FTs, we then have $X(\omega) = \sum_n c_n F_n(\omega)$. This result is obvious for finite summations because of linearity of the FT. For infinite summations this follows from the property that the L^2-FT is a continuous mapping from L^2 to L^2. (This in turn follows from the result that it is a bounded linear transformation [Naylor and Sell, 1982]). The continuity allows us to move the FT operation inside the infinite summation.

Thus there is complete symmetry between the time and frequency domains. The L^2-FT is a one-to-one mapping from L^2 onto L^2. Moreover since $\sqrt{2\pi}\|x(t)\|_2 = \|X(\omega)\|_2$, it is a norm preserving mapping – one says that the L^2-FT is an isometry from L^2 to L^2.

The ℓ^1 Fourier Transform.

If a sequence $x(n) \in \ell^1$ then its discrete-time FT $X(e^{j\omega}) = \sum_n x(n)e^{-j\omega n}$ exists, and is the ℓ^1 FT of $x(n)$. It can be shown that $X(e^{j\omega})$ is a continuous function of ω and that $|X(e^{j\omega})|$ is bounded.

6.4. Convolutions

Suppose $h(t) \in L^1$ and $x(t) \in L^p$ for some p in $1 \le p \le \infty$. Then the familar convolution integral defined by $(x * h)(t) = \int x(\tau)h(t-\tau)d\tau$ exists for almost all t [Rudin, 1966]. If we define a function $y(t)$ to be $x * h$ where it exists and to be zero elsewhere, the result is in fact an L^p function. We simply say that the convolution of an L^1 function with an L^p function gives an L^p function. By recalling that an LTI system is stable (i.e., BIBO stable, Sec. 1), if and only its impulse response is in L^1, we therefore have the following

examples:

1. If an L^1 signal is input to a stable LTI system, the output is in L^1. Since the convolution of two L^1 signals is in L^1, the cascade of two stable LTI systems is stable, a readily accepted fact in engineering.
2. If an L^2 signal (finite energy input) is input to a stable LTI system, the output is in L^2.
3. If an L^∞ signal is input to a stable LTI system, the output is in L^∞ (i.e., bounded inputs produce bounded outputs).

If $x(t)$ and $h(t)$ are both in L^1, their convolution $y(t)$ is in L^1, and all three signals have L^1 Fourier transform. The *convolution theorem* [Rudin, 1966] says that these three are related as $Y(\omega) = H(\omega)X(\omega)$. When signals are not necessarily in L^1 we cannot in general write this, even if convolution might itself be well defined!

Convolution Theorems for L^2 Signals

For all our discussions in the preceding sections, the signals have been restricted to be in L^2 but not necessarily in L^1. In fact, even the filters are often only in L^2. For example, ideal bandpass filters (Fig 2.8) are unstable, and therefore only in L^2. For arbitary L^2 signals $x(t)$ and $h(t)$, the convolution theorem does not hold. We therefore need to understand L^2 convolution more carefully.

Assume that $x(t)$ and $h(t)$ are both in L^2. Their convolution $y(t) = \int x(\tau)h(t-\tau)d\tau$ exists for all t, since the integral is just an inner product in L^2. Using Schwartz inequality [Rudin, 1966], we also have $|y(t)| \leq \|x(t)\|_2\|h(t)\|_2$, that is $y(t) \in L^\infty$. Suppose the filter $h(t)$ has the further property that the frequency response $H(\omega)$ is bounded, that is, $|H(\omega)| \leq B$ a.e., for some $B < \infty$. Then we can show that $y(t) \in L^2$, and that the convolution theorem holds, that is $Y(\omega) = H(\omega)X(\omega)$. To prove this, note that

$$y(t) = \int x(\tau)h(t-\tau)d\tau = \frac{1}{2\pi}\int X(\omega)H(\omega)e^{j\omega t}d\omega \tag{6.11}$$

from Parseval's relation which holds for L^2 signals [Rudin, 1966]. If $|H(\omega)| \leq B$, then $|X(\omega)H(\omega)|^2 \leq B^2|X(\omega)|^2$. So $|X(\omega)H(\omega)|^2$ is bounded by the integrable function $|X(\omega)|^2$, and is therefore integrable (Sec. 6.1). Thus $X(\omega)H(\omega) \in L^2$, and the preceding equation establishes that $y(t) \in L^2$. The equation also shows that $y(t)$ and $H(\omega)X(\omega)$ form an L^2 FT pair, so $Y(\omega) = H(\omega)X(\omega)$ indeed.

Bounded L^2 filters. Filters for which $h(t) \in L^2$ and $H(\omega)$ bounded will be called *bounded L^2 filters*. The preceding discussion shows that bounded L^2 filters admit the convolution theorem though arbitrary L^2 filters do not. Another advantage of bounded L^2 filters is that a cascade of two bounded L^2 filters $h_1(t)$ and $h_2(t)$ is a bounded L^2 filter, just as a cascade of two stable filters would be stable. To see this note that the cascaded impulse response is the convolution $h(t) = (h_1 * h_2)(t)$. By the preceding discussion, $h(t) \in L^2$, and moreover $H(\omega) = H_1(\omega)H_2(\omega)$. Clearly $H(\omega)$ is still bounded. Bounded L^2 filters are therefore very

convenient to work with. Fortunately, all filters in the discussion of wavelets and filter banks are bounded L^2 filters, even though they may not be BIBO stable (like the ideal bandpass filters in Fig. 2.8). We summarize the preceding discussions as follows:

Theorem 6.3. Convolution of L^2 functions. We say that $h(t)$ is a bounded L^2 filter if $h(t) \in L^2$ and $|H(\omega)| \leq B < \infty$ a.e.

1. Let $x(t) \in L^2$, and let $h(t)$ be a bounded L^2 filter. Then $y(t) = (x * h)(t)$ exists for all t and $y(t) \in L^2$. Moreover $Y(\omega) = H(\omega)X(\omega)$.
2. If $h_1(t)$ and $h_2(t)$ are bounded L^2 filters, then their cascade $h(t) = (h_1 * h_2)(t)$ is a bounded L^2 filter, and $H(\omega) = H_1(\omega)H_2(\omega)$. ◇

7. RIESZ BASIS, BIORTHOGONALITY, AND OTHER FINE POINTS

In a finite dimensional space such as the space of all N-component Euclidean vectors, the ideas of basis and orthonormal basis are easy to appreciate. When we extend these ideas to infinite dimensional spaces (i.e., where the basis $\{g_n(t)\}$ has infinite number of functions), a number of complications and subtleties arise. Our aim is to point these out here. References for this section include [Riesz and Nagy, 1955], and [Haaser and Sullivan, 1971], [Young, 1980], [Chui, 1992a], and [Daubechies, 1992].

Readers familiar with *Hilbert spaces* will note that the L^2 space is a Hilbert space; all our developments here are valid for any Hilbert space $\mathcal{H}$. Elements in $\mathcal{H}$ (vectors) are typically denoted x, y and so forth. When we deal with the Hilbert space L^2, the vectors are functions and are denoted as $x(t)$, $y(t)$ and so forth for clarity. Similarly for the special case of Euclidean vectors we use bold face, e.g., $\mathbf{x}$, $\mathbf{y}$ and so forth. The reader not familiar with Hilbert spaces can assume that all discussions are in L^2 and that x is merely a simplification of the notation $x(t)$.

7.1. Finite dimensional vector spaces

We will first look at the finite dimensional case and then proceed to the infinite dimensional case. Consider an $N \times N$ matrix $\mathbf{F} = [\,\mathbf{f}_1 \quad \mathbf{f}_2 \quad \ldots \quad \mathbf{f}_N\,]$. We assume that this is nonsingular, that is, the columns $\mathbf{f}_n$ are linearly independent. These column vectors form a basis for the N-dimensional Euclidean space $\mathcal{C}^N$ of complex N-component vectors. This space is an example of a finite dimensional Hilbert space, with inner product defined as $\langle \mathbf{x}, \mathbf{y} \rangle = \mathbf{y}^\dagger \mathbf{x} = \sum_{n=1}^{N} x_n y_n^*$. The norm $\|\mathbf{x}\|$ induced by this inner product is defined as $\|\mathbf{x}\| = \sqrt{\langle \mathbf{x}, \mathbf{x} \rangle}$. Thus $\|\mathbf{x}\|^2 = \mathbf{x}^\dagger \mathbf{x} = \sum_{n=1}^{N} |x_n|^2$.

Any vector $\mathbf{x} \in \mathcal{C}^N$ can be expressed as $\mathbf{x} = \sum_{n=1}^{N} c_n \mathbf{f}_n$ for some uniquely determined set of scalars c_n. We can abbreviate this as $\mathbf{x} = \mathbf{F}\mathbf{c}$ where $\mathbf{c} = [\,c_1 \quad c_2 \quad \ldots \quad c_N\,]^T$. The matrix $\mathbf{F}$ can be regarded as a linear

transformation from $\mathcal{C}^N$ to $\mathcal{C}^N$. The nonsingularity of $\mathbf{F}$ means that for every $\mathbf{x} \in \mathcal{C}^N$ we can find a unique $\mathbf{c}$ such that $\mathbf{x} = \mathbf{F}\mathbf{c}$.

Boundedness of F and its Inverse.

In practice we have a further requirement, namely that if the norm $\|\mathbf{c}\|$ is "small" then $\|\mathbf{x}\|$ should also be "small", and vice versa. This requirement implies, for example, that if there is a small error in the transmission or estimate of the vector $\mathbf{c}$ then the corresponding error in $\mathbf{x}$ is also small. From the relation $\mathbf{x} = \mathbf{F}\mathbf{c}$ we obtain

$$\|\mathbf{x}\|^2 = \mathbf{x}^\dagger \mathbf{x} = \mathbf{c}^\dagger \mathbf{F}^\dagger \mathbf{F} \mathbf{c} \tag{7.1}$$

Letting λ_M and λ_m denote the maximum and minimum eigenvalues of $\mathbf{F}^\dagger\mathbf{F}$ it then follows that $\|\mathbf{x}\|^2 \geq \lambda_m \|\mathbf{c}\|^2$ and that $\|\mathbf{x}\|^2 \leq \lambda_M \|\mathbf{c}\|^2$. That is,

$$\lambda_m \|\mathbf{c}\|^2 \leq \|\mathbf{x}\|^2 \leq \lambda_M \|\mathbf{c}\|^2 \tag{7.2}$$

with $0 < \lambda_m \leq \lambda_M < \infty$, where $0 < \lambda_m$ follows from nonsingularity of $\mathbf{F}$. Thus the transformation $\mathbf{F}$ which converts $\mathbf{c}$ into $\mathbf{x}$ has an amplification factor bounded by λ_M in the sense that $\|\mathbf{x}\|^2 \leq \lambda_M \|\mathbf{c}\|^2$. Similarly the inverse transformation $\mathbf{G} = \mathbf{F}^{-1}$ which converts $\mathbf{x}$ into $\mathbf{c}$ has amplification bounded by $1/\lambda_m$. Since λ_M is finite, we say that $\mathbf{F}$ is a bounded linear transformation. And since $\lambda_m \neq 0$ we see that the inverse transformation is also bounded.

Using $\mathbf{x} = \sum_n c_n \mathbf{f}_n$ and $\|\mathbf{c}\|^2 = \sum_n |c_n|^2$ we can rewrite the preceding inequality as

$$A \sum_n |c_n|^2 \leq \left\| \sum_n c_n \mathbf{f}_n \right\|^2 \leq B \sum_n |c_n|^2 \tag{7.3}$$

where $A = \lambda_m > 0$ and $B = \lambda_M < \infty$, and all summations are for $1 \leq n \leq N$. Readers familiar with the idea of a Riesz basis in infinite dimensional Hilbert spaces will notice that the above is in the form that agrees with that definition. We will return to this later.

Biorthogonality

With $\mathbf{F}^{-1}$ denoted as $\mathbf{G}$, let $\mathbf{g}_n^\dagger$ denote the rows of $\mathbf{G}$, that is

$$\mathbf{G} = \begin{bmatrix} \mathbf{g}_1^\dagger \\ \mathbf{g}_2^\dagger \\ \vdots \\ \mathbf{g}_N^\dagger \end{bmatrix}, \quad \mathbf{F} = [\,\mathbf{f}_1 \quad \mathbf{f}_2 \quad \ldots \quad \mathbf{f}_N\,] \tag{7.4}$$

The property $\mathbf{GF} = \mathbf{I}$ implies $\mathbf{g}_k^\dagger \mathbf{f}_n = \delta(k-n)$, that is

$$\langle \mathbf{f}_n, \mathbf{g}_k \rangle = \delta(k-n) \tag{7.5}$$

for $1 \le k, n \le N$. Equivalently, $\langle \mathbf{g}_k, \mathbf{f}_n \rangle = \delta(k-n)$.

Two sets of vectors $\{\mathbf{f}_n\}$ and $\{\mathbf{g}_k\}$ satisfying (7.5) are said to be *biorthogonal.* Since $\mathbf{c} = \mathbf{F}^{-1}\mathbf{x} = \mathbf{G}\mathbf{x}$ we can write the elements of $\mathbf{c}$ as $c_n = \mathbf{g}_n^\dagger \mathbf{x} = \langle \mathbf{x}, \mathbf{g}_n \rangle$. Then $\mathbf{x} = \sum_n c_n \mathbf{f}_n = \sum_n \langle \mathbf{x}, \mathbf{g}_n \rangle \mathbf{f}_n$. Since $\mathbf{G}^\dagger$ is a nonsingular matrix, we can use its columns $\mathbf{g}_n$ (instead of the columns of $\mathbf{F}$) to obtain a similar development, and express the arbitrary vector $\mathbf{x} \in \mathcal{C}^N$ as $\mathbf{x} = \sum_n \langle \mathbf{x}, \mathbf{f}_n \rangle \mathbf{g}_n$. Thus

$$\mathbf{x} = \sum_n \langle \mathbf{x}, \mathbf{g}_n \rangle \mathbf{f}_n = \sum_n \langle \mathbf{x}, \mathbf{f}_n \rangle \mathbf{g}_n, \tag{7.6}$$

where the summations are for $1 \le n \le N$. By using the expressions $c_n = \langle \mathbf{x}, \mathbf{g}_n \rangle$ and $\mathbf{x} = \sum_n c_n \mathbf{f}_n$ we can rearrange the inequality (7.3) into $B^{-1}\|\mathbf{x}\|^2 \le \sum_n |\langle \mathbf{x}, \mathbf{g}_n \rangle|^2 \le A^{-1}\|\mathbf{x}\|^2$. With the columns $\mathbf{g}_n$ of $\mathbf{G}^\dagger$ (rather than the columns of $\mathbf{F}$) used as the basis for $\mathcal{C}^N$ we obtain similarly

$$A\|\mathbf{x}\|^2 \le \sum_n \Big| \langle \mathbf{x}, \mathbf{f}_n \rangle \Big|^2 \le B\|\mathbf{x}\|^2 \tag{7.7}$$

where $1 \le n \le N$, and $A = \lambda_m$, $B = \lambda_M$ again. Readers familiar with the idea of a frame in an infinite dimensional Hilbert space will recognize that the above inequality defines a frame $\{\mathbf{f}_n\}$. We will return to this in Sec. 8.

Orthonormality.

The basis $\mathbf{f}_n$ is said to be orthonormal if $\langle \mathbf{f}_k, \mathbf{f}_n \rangle = \delta(k-n)$ i.e., $\mathbf{f}_n^\dagger \mathbf{f}_k = \delta(k-n)$. Equivalently $\mathbf{F}$ is unitary, that is $\mathbf{F}^\dagger \mathbf{F} = \mathbf{I}$. In this case the rows of the inverse matrix $\mathbf{G}$ are the quantities $\mathbf{f}_n^\dagger$. Since $\mathbf{F}^\dagger \mathbf{F} = \mathbf{I}$ we have $\lambda_m = \lambda_M = 1$, that is, $A = B = 1$. With this, (7.2) becomes $\|\mathbf{c}\| = \|\mathbf{x}\|$, that is, $\sum_n |c_n|^2 = \| \sum_n c_n \mathbf{f}_n \|^2$. Thus (7.3) is a generalization of the orthonormal situation. Similarly biorthogonality (7.5) is a generalization of orthonormality.

7.2. Basis in infinite dimensional spaces

When the simple idea of a basis in a finite dimensional space (e.g., the Euclidean space $\mathcal{C}^N$) is extended to infinite dimensions, several new issues arise which make the problem nontrivial. Thus consider the sequence of functions $\{f_n\}, 1 \le n \le \infty$ in a Hilbert space $\mathcal{H}$. Because of the infinite range of n we now have to consider linear combinations of the form $\sum_{n=1}^{\infty} c_n f_n$. The problem that immediately arises is one of convergence. For arbitrary sequences c_n this sum does not converge, so we have to replace the statement "all linear combinations" with something else.†

† In our review we will use $1 \le n \le \infty$ to be consistent with standard math texts, but all the crucial results hold for doubly infinite sequences and summations, i.e., for the case $-\infty \le n \le \infty$. This is what we need in the case of Fourier and wavelet bases, see for example Eq. (2.3) and (2.4).

Closure of span. Let us first define the set of all *finite* linear combinations of the form $\sum_{n=1}^{N} c_n f_n$, where N varies over all integers ≥ 1. This is called the *span of* $\{f_n\}$. Now suppose $x \in \mathcal{H}$ is a vector not necessarily in the span of $\{f_n\}$ but can be approximated as closely as we wish, by vectors in the span. In other words given an $\epsilon > 0$ we can find N and the sequence of constants c_{nN} such that

$$\|x - \sum_{n=1}^{N} c_{nN} f_n\| < \epsilon, \tag{7.8}$$

where $\|x\|$ is the norm defined as $\|x\| = \sqrt{\langle x, x \rangle}$. If we append all such vectors x to the span of $\{f_n\}$ we get the *closure of the span* of $\{f_n\}$.‡ Note that c_{nN} in general depends on ϵ since N depends on ϵ.

Completeness. We say that a sequence of vectors $\{f_n\}$ is *complete* in $\mathcal{H}$ if the closure of the linear span of $\{f_n\}$ equals $\mathcal{H}$. Thus any $x \in \mathcal{H}$ can be approximated, as closely as we wish, by finite linear combinations of f_n in the sense (7.8). This is also expressed by saying that the linear span of $\{f_n\}$ is *dense* in $\mathcal{H}$. It turns out that completeness of $\{f_n\}$ in a Hilbert space is equivalent to the statement that the only vector orthogonal to all f_n is the zero vector.

Infinite summations. When we write $x = \sum_{n=1}^{\infty} c_n f_n$ we mean that the infinite summation converges to x in the norm of $\mathcal{H}$. In other words, given $\epsilon > 0$ there exists n_0 such that

$$\|x - \sum_{n=1}^{N} c_n f_n\| < \epsilon \qquad \text{for all } N \geq n_0. \tag{7.9}$$

This statement is stronger than saying that x is in the closure of the linear span of $\{f_n\}$. The latter statement only requires (7.8), where N, and hence c_{nN}, depends on ϵ. In the former statement (7.9), $\{c_n\}$ is a fixed sequence.

Linear independence.

Let $\{f_n\}, n = 1, 2, \ldots$ be a sequence of vectors in an infinite dimensional Hilbert space $\mathcal{H}$. Unlike in a finite dimensional space, one has to distinguish between several types of linear independence.

Type 1: $\{f_n\}$ has *finite linear independence* if $\sum_{n=1}^{N} c_n f_n = 0$ for any finite N implies $c_n = 0, 1 \leq n \leq N$.

Type 2: $\{f_n\}$ is *ω-independent* if $\sum_{n=1}^{\infty} c_n f_n = 0$ implies $c_n = 0$ for all n (where the infinite sum is interpreted as explained above).

Type 3. $\{f_n\}$ is *minimal* if none of the f_m is in the closure of the span of the remaining set of f_n.

Type 3 independence implies Type 2, which in turn implies Type 1. Thus, Type 3 is the strongest kind of linear independence. The reason why it is stronger than Type 2 is this: Type 2 implies that we cannot have

‡ The term "closure" has its origin from the theory of metric spaces, more generally topological vector spaces. We will not require the deeper, more general meaning here.

$f_m = \sum_{n \neq m} c_n f_n$. However, for a Type 2 independent sequence $\{f_n\}$, it is possible that we can make

$$\|f_m - \sum_{\substack{n=1 \\ n \neq m}}^{N} c_{nN} f_n\| < \epsilon \tag{7.10}$$

for any given $\epsilon > 0$ by choosing N and c_{nN} properly.§ Type 3 linear independence prohibits even this. Example 7.2 will make this distinction clearer.

Basis or Shcauder basis. A sequence of vectors $\{f_n\}$ in $\mathcal{H}$ is a Schauder basis for $\mathcal{H}$ if (i) any $x \in \mathcal{H}$ can be expressed as $x = \sum_{n=1}^{\infty} c_n f_n$, and (b) the sequence of scalars $\{c_n\}$ is unique for a given x. The second condition can be replaced with the statement that $\{f_n\}$ is ω-independent. A subtle result for Hilbert spaces [Young, 1980] is that a Schauder basis automatically satisfies minimality (i.e., Type 3 independence).

A Schauder basis is ω-independent and complete in the sense defined above. Conversely, ω-independence and completeness do not imply that $\{f_n\}$ is a Schauder basis; completeness only means that we can approximate any vector as closely as we wish in the sense of (7.8) where c_{kN} *depend on* N. In this chapter "independence" (or linear independence) stands for ω-independence. Similarly "basis" stands for Schauder basis unless qualified otherwise.

7.3. Riesz Basis

Any basis $\{\mathbf{f}_n\}$ in a finite dimensional space satisfies (7.3), which in turn ensures that the transformation from $\mathbf{x}$ to $\{c_n\}$ and that from $\{c_n\}$ to $\mathbf{x}$ are stable. For a basis in an infinite dimensional space, Eq. (7.3) is not automatically guaranteed, as shown by the following example.

Example 7.1. Let $\{e_n\}$, $1 \leq n \leq \infty$ be an orthonormal basis in a Hilbert space $\mathcal{H}$ and define the sequence $\{f_n\}$ by $f_n = e_n/n$. Then we can show that f_n is still a basis, i.e., it satisfies the definition of a Schauder basis. Suppose we pick $x = \epsilon e_k$ for some k. Then $x = \sum_n c_n f_n$ with $c_k = \epsilon k$, and $c_n = 0$ for all other n. Thus $\sum_n |c_n|^2 = \epsilon^2 k^2$ and grows as k increases, though $\|x\| = \epsilon$ for all k. That is, a "small" error in x can get amplified in an unbounded manner. Recall that this could never happen in the finite dimensional case (Sec. 7.1) because $A > 0$ in Eq. (7.3). For our basis $\{f_n\}$, we can indeed show that there is no $A > 0$ satisfying (7.3)! To see this let $c_n = 0$ for all n except that $c_k = 1$. Then $\sum_n c_n f_n = f_k = e_k/k$ and has norm $1/k$. So (7.3) reads $A \leq 1/k^2 \leq B$ for all $k \geq 1$. This is not possible with $A > 0$. ◇

If $\{e_n\}$, $1 \leq n \leq \infty$ is an orthonormal basis in an infinite dimensional Hilbert space $\mathcal{H}$, then any vector

§ As we make ϵ smaller and smaller, we may need to change N and *all coefficients* c_{kN}. Therefore, this does not imply $f_m = \sum_{n \neq m} c_n f_n$ for fixed $\{c_n\}$.

$x \in \mathcal{H}$ can be expressed uniquely as $x = \sum_{n=1}^{\infty} c_n e_n$ where

$$\|x\|^2 = \sum_{n=1}^{\infty} |c_n|^2.$$

This property automatically ensures the stability of the transformations from x to $\{c_n\}$ and vice versa. The Riesz basis is defined such that this property is made more general. †

Definition of a Riesz basis. A sequence $\{f_n\}, 1 \leq n \leq \infty$ in a Hilbert space $\mathcal{H}$ is a Riesz basis if it is *complete* (Sec. 7.2.) and there exist constants A and B such that $0 < A \leq B < \infty$ and

$$A \sum_{n=1}^{\infty} |c_n|^2 \leq \left\| \sum_{n=1}^{\infty} c_n f_n \right\|^2 \leq B \sum_{n=1}^{\infty} |c_n|^2 \tag{7.11}$$

for all choice of c_n satisfying $\sum_n |c_n|^2 < \infty$. ◇

In a finite dimensional Hilbert space, A and B come from the extreme eigenvalues of a nonsingular matrix $\mathbf{F}^\dagger\mathbf{F}$, so $A > 0$ and $B < \infty$ automatically (Sec. 7.1). That is, any basis in a finite dimensional space is a Riesz basis. As Example 7.1 shows, this may not be the case in infinite dimensions.

Unconditional basis. It can be shown that a Riesz basis is an *unconditional basis*, that is, any reordering of $\{f_n\}$ is also a basis (and the new c_n are the correspondingly reordered versions). This is a nontrivial statement; an arbitrary (Schauder) basis is not necessarily unconditional; in fact the space of L^1 functions (which is a Banach space, not a Hilbert space) does not have an unconditional basis.

Role of the Constants A and B

1. *Strongest linear-independence.* The condition $A > 0$ means, in particular, that $\sum_n c_n f_n \neq 0$ unless c_n is zero for all n. This is just ω-independence. Actually the condition $A > 0$ means that the vectors $\{f_n\}$ are independent in the strongest sense (Type 3), that is, $\{f_n\}$ is minimal. To see this assume this is not the case. That is, suppose some vector f_m is in the closure of the span of the others. Then, given arbitrary $\epsilon > 0$ we can find N and c_{nN} satisfying (7.8) with $x = f_m$. Defining $c_n = -c_{nN}$ for $n \neq m$ and $c_m = 1$, we see that (7.11) implies $A(1 + \sum_{n \neq m} |c_{nN}|^2) \leq \epsilon^2$. Since ϵ is arbitrary, this is not possible for $A > 0$.
2. *Distance between vectors.* The condition $A > 0$ also implies that no two vectors in $\{f_n\}$ can get "arbitrarily close". To see this, choose $c_k = -c_m = 1$ for some k, m and $c_n = 0$ for all other n. Then

† For readers familiar with bounded linear transformations in Hilbert spaces, we state that a basis is a Riesz basis if and only if it is related to an orthonormal basis via a bounded linear transformation with bounded inverse.

(7.11) gives $2A \leq \|f_k - f_m\|^2 \leq 2B$. That is, the distance between any two vectors is at least $\sqrt{2A}$, at most $\sqrt{2B}$.

3. *Bounded basis.* A Riesz basis is a bounded basis in the sense that $\|f_n\|$ cannot get arbitrarily large. In fact, by choosing $c_n = 0$ for all but one value of n, we can see that $0 < A \leq \|f_n\|^2 \leq B < \infty$. That is, the norms of the vectors in the basis cannot get arbitrarily small or large. Note that the basis in Example 7.1 violates this, since $\|f_n\| = 1/n$. Therefore, Example 7.1 is only a Schauder basis and not a Riesz basis.

4. *Stability of Basis.* The condition $A > 0$ yields $\sum_n |c_n|^2 \leq A^{-1}\|x\|^2$ where $x = \sum_n c_n f_n$. This means that the transformation from the vector x to the sequence $\{c_n\}$, is bounded; so a small error in x is not amplified in an unbounded manner. Similarly the inequality $\|x\|^2 \leq B \sum_n |c_n|^2$ shows that the role of B is to ensure that the inverse transformation from c_n to x is bounded. Summarizing, the transformation from x to $\{c_n\}$ is numerically stable (i.e., small errors not severly amplified) because $A > 0$ and the reconstruction of x from $\{c_n\}$ is numerically stable because $B < \infty$.

5. *Orthonormality.* For a Riesz basis with $A = B = 1$ the condition (7.11) reduces to $\sum_n |c_n|^2 = \|\sum_n c_n f_n\|^2$. It can be shown that such a Riesz basis is just an orthonormal basis. The properties listed above show that the Riesz basis is as good as an orthonormal basis in most applications. It can be shown that any Riesz basis can be obtained from an orthonormal basis by means of a bounded linear transformation with bounded linear inverse.

Example 7.2. Mishaps with system which is not a Riesz basis. Let us modify Example 7.1 to $f_n = (e_n/n) + e_1$, $n \geq 1$, where $\{e_n\}$ is an orthonormal basis. It turns out that as $n \to \infty$ the vectors f_n get arbitrarily closer together (though $\|f_n\|$ approaches unity from above). Formally $f_n - f_m = (e_n/n) - (e_m/m)$, so $\|f_n - f_m\|^2 = (1/n^2) + (1/m^2)$, which goes to zero as $n, m \to \infty$. Thus there is no $A > 0$ satisfying (7.11) (because of comment 2 above). This, then, is not a Riesz basis (in fact this is not even a Schauder basis, see below). This example also has $B = \infty$. To see this let $c_n = 1/n$, then $\sum_n |c_n|^2$ converges but $\|\sum_{n=1}^N c_n f_n\|^2$ does not converge as $N \to \infty$ (as we can verify), so (7.11) is not satisfied for finite B. *Such mishaps cannot occur with a Riesz basis.* ◇

In this example $\{f_n\}$ is not minimal (which is Type 3 indenendence). To see this note that $\|f_1 - f_n\|$ gets arbitrarily small as n increases to infinity. So f_1 is in the closure of the span of $\{f_n\}, n \neq 1$. However $\{f_n\}$ is ω-independent; there is no sequence $\{c_n\}$ such that $\|\sum_{n=1}^N c_n f_n\| \to 0$ as $N \to \infty$. In any case, the fact that $\{f_n\}$ is not minimal (i.e., not independent in the strongest sense) shows that it is not even a Schauder basis (see Sec. 7.2).

7.4. Biorthogonal Systems, Riesz Bases and Inner Products

When discussing finite dimensional Hilbert spaces (Sec. 7.1) we found that given a basis $\mathbf{f}_n$ (columns of a nonsingular matrix) we can express any vector $\mathbf{x}$ as a linear combination $\mathbf{x} = \sum_n \langle \mathbf{x}, \mathbf{g}_n \rangle \mathbf{f}_n$ where $\mathbf{g}_n$ is such that the biorthogonality property $\langle \mathbf{f}_m, \mathbf{g}_n \rangle = \delta(m-n)$ holds. A similar result is true for infinite dimensional Hilbert spaces.

Theorem 7.1. Biorthogonality and Riesz basis. Let $\{f_n\}$ be a basis in a Hilbert space $\mathcal{H}$. Then there is a unique sequence $\{g_n\}$ biorthogonal to $\{f_n\}$, that is,

$$\langle f_m, g_n \rangle = \delta(m-n) \qquad \text{(biorthogonality)}. \tag{7.12}$$

Moreover the unique expansion of any $x \in \mathcal{H}$ in terms of the basis $\{f_n\}$ is given by

$$x = \sum_{n=1}^{\infty} \langle x, g_n \rangle f_n. \tag{7.13}$$

It is also true that the biorthogonal sequence $\{g_n\}$ is a basis and that $x = \sum_{n=1}^{\infty} \langle x, f_n \rangle g_n$. Moreover if $\{f_n\}$ is a Riesz basis, then $\sum_n |\langle x, g_n \rangle|^2$ and $\sum_n |\langle x, f_n \rangle|^2$ are finite, and we have

$$A\|x\|^2 \leq \sum_{n=1}^{\infty} |\langle x, f_n \rangle|^2 \leq B\|x\|^2 \tag{7.14}$$

where A and B are the same constants as in the definition (7.11) of a Riesz basis. ◇

This beautiful result resembles the finite dimensional version (Sec. 7.1) where f_n corresponds to the column of a matrix and g_n corresponds to the rows (conjugated) of the inverse matrix. In this sense we can regard the biorthogonal pair of sequences $\{f_n\}$, $\{g_n\}$ as inverses of each other. Both of these are bases for $\mathcal{H}$. A proof of the above result can be obtained by combining the ideas on p. 28–32 of [Young, 1980]. The theorem implies, in particular, that if $\{f_n\}$ is a Riesz basis, then any vector in the space can be written in the form $\sum_{n=1}^{\infty} c_n f_n$, where $c_n \in \ell^2$.

Summary on Riesz basis. The Riesz basis $\{f_n\}$ in a Hilbert space $\mathcal{H}$ was defined in Sec. 7.3. The set $\{f_n\}$ is a complete set of vectors, linearly independent in the strongest sense (i.e., Type 3 or minimal.) It is a bounded basis with bounded inverse. Any two vectors are separated by at least $\sqrt{2A}$, that is $\|f_n - f_m\|^2 \geq 2A$. The norm of each basis vector is bounded as $\|f_n\| \leq \sqrt{B}$. In the expression $x = \sum_n c_n f_n$ the computation of x from c_n as well as the computation of c_n from x are numerically stable, because $B < \infty$ and $A > 0$ respectively. A Riesz basis with $A = B = 1$ is an orthonormal basis. In fact, any Riesz basis can be obtained from an orthonormal basis, via a bounded linear transformation with a bounded inverse. Given any basis $\{f_n\}$ in a Hilbert space, there exists a unique biorthogonal sequence $\{g_n\}$ such that we can express any $x \in \mathcal{H}$

as $x = \sum_{n=1}^{\infty} \langle x, g_n \rangle f_n$ as well as $x = \sum_{n=1}^{\infty} \langle x, f_n \rangle g_n$; if this basis is also a Riesz basis then $\sum_n |\langle x, f_n \rangle|^2$ and $\sum_n |\langle x, g_n \rangle|^2$ are finite. If $\{f_n\}$ is a Riesz basis, then any vector $x \in \mathcal{H}$ can be written in the form $x = \sum_{n=1}^{\infty} c_n f_n$, where $c_n \in \ell^2$.

8. FRAMES IN HILBERT SPACES

A frame in a Hilbert space $\mathcal{H}$ is a sequence of vectors $\{f_n\}$ with certain special properties. While a frame is not necessarily a basis, it shares some properties of a basis. For example we can express any vector $x \in \mathcal{H}$ as a linear combination of the frame elements, i.e., $x = \sum_n c_n f_n$. But frames in general have redundancy, that is the frame vectors are not necessarily linearly independent, even in the weakest sense defined in Sec. 7.2. We will see that the Riesz basis (hence any orthonormal basis) is a special case of frames. The concept of a frame is useful when discussing the relation between wavelets, short time Fourier transforms and filter banks. The idea of frames was introduced by Duffin and Schaeffer [1952], and used in the context of wavelets and STFT by Daubechies [1992]. Excellent tutorials can be found in Young [1980] and Heil and Walnut [1989].

Definition of a frame. A sequence of vectors $\{f_n\}$ in a (possibly infinite dimensional) Hilbert space $\mathcal{H}$ is a frame if there exist constants A and B with $0 < A \leq B < \infty$ such that for any $x \in \mathcal{H}$ we have

$$A\|x\|^2 \leq \sum_{n=1}^{\infty} \Big| \langle x, f_n \rangle \Big|^2 \leq B\|x\|^2. \tag{8.1}$$

The constants A and B are called frame bounds. ◇

In Sec. 7.4 we saw that a Riesz basis which by definition satisfies (7.11), also satisfies (7.14) which is precisely the frame definition! A Riesz basis is, therefore, also a frame. But it is a special case of a frame where the set of vectors is minimal (see below).

Any frame is complete. That is, if a vector $x \in \mathcal{H}$ is orthogonal to all elements in $\{f_n\}$ then $x = 0$ (otherwise $A > 0$ is violated). Thus, any $x \in \mathcal{H}$ is in the closure of the span of the frame. In fact, we will see that more is true, namely we can express $x = \sum c_n f_n$, though $\{c_n\}$ may not be unique. The frame elements are not necessarily linearly independent, as demonstrated by examples below. A frame, then, is not necessarily a basis. Compare (8.1) with the Riesz basis definition (7.11), where the left inequality forced the vectors f_n to be linearly independent (in fact minimal). The left inequality for a frame only ensures completeness, not linear independence.

8.1. Representing Arbitrary Vectors in Terms of Frame Elements

We will see later that, given a frame $\{f_n\}$ we can associate with it another sequence $\{g_n\}$ called the dual frame, such that any element $x \in \mathcal{H}$ can be represented as $x = \sum_{n=1}^{\infty} \langle x, g_n \rangle f_n$. It turns out that we can also

write $x = \sum_{n=1}^{\infty} \langle x, f_n \rangle g_n$. This representation in terms of $\{f_n\}$ and $\{g_n\}$ resembles the biorthogonal system discussed in Sec. 7.4, but we will point out some differences later.

Stability of computations. To obtain the representation $x = \sum_{n=1}^{\infty} \langle x, f_n \rangle g_n$ we compute (at least conceptually) the coefficients $\langle x, f_n \rangle$ for all n. This computation is a linear transformation from $\mathcal{H}$ to the space of sequences. The inverse transform computes x from this sequence by using the formula $x = \sum_{n=1}^{\infty} \langle x, f_n \rangle g_n$. The condition $B < \infty$ in the frame definition ensures that the transformation from x to $\langle x, f_n \rangle$ is bounded. Similarly the condition $A > 0$ ensures that the inverse transformation from $\langle x, f_n \rangle$ to x is bounded. Thus the conditions $A > 0$ and $B < \infty$ ensure stability; small errors in one domain are not arbitrarily amplified in the other domain. A similar advantage was pointed out in Sec. 7.3 for the Riesz basis – for arbitrary bases in infinite dimensional spaces such an advantage cannot be claimed (Example 8.11).

Instead of $x = \sum_{n=1}^{\infty} \langle x, f_n \rangle g_n$ if we wish to use the dual representation $x = \sum_{n=1}^{\infty} \langle x, g_n \rangle f_n$ then we would have to compute $\langle x, g_n \rangle$ and so forth; then the roles of A and B are taken up by $1/B$ and $1/A$ respectively, and similar discussions hold. This is summarized in Fig. 8.1.

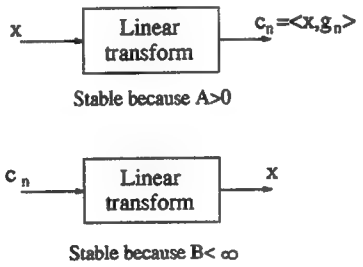

Fig. 8.1. Representation of x using frame elements $\{f_n\}$.
The transformation from x to $\{c_n\}$ and vice versa are stable.

8.2. Exact Frames, Tight Frames, Riesz Bases, and Orthonormal Bases

The resemblance between a Riesz basis and a frame is striking. Compare (7.11) with (8.1). One might wonder what the precise relation is. So far we know that a Riesz basis is a frame. To go deeper, we need a definition: a frame $\{f_n\}$ which ceases to be a frame if any element f_k is deleted is said to be an *exact frame*. Such a frame has no redundancy. A frame with $A = B$ is said to be a *tight frame*. The defining property reduces to $\|x\|^2 = A^{-1} \sum_n |\langle x, f_n \rangle|^2$ resembling Parseval's theorem for an orthonormal basis. A frame is *normalized* if $\|f_n\| = 1$ for all n. The following facts concerning exact frames and tight frames are fundamental.

1. A tight frame with $A = B = 1$ and $\|f_n\| = 1$ for all n (i.e., a normalized tight frame with frame bound $= 1$) is an orthonormal basis [Daubechies, 1992].

2. $\{f_n\}$ is an exact frame if and only if it is a Riesz basis [Young, 1980]. Moreover, if a frame is not exact then it cannot be a basis [Heil and Walnut, 1989]. Thus if a frame is a basis it is certainly a Riesz basis.
3. Since an orthonormal basis is a Riesz basis, a normalized tight frame with frame bound = 1 is automatically an exact frame.

Examples.

We now provide some examples which serve to clarify the preceding concepts and definitions. In these examples the sequence $\{e_n\}, n \geq 1$ is an orthonormal basis for $\mathcal{H}$. Thus, $\{e_n\}$ is a tight frame with $A = B = 1$, and $\|e_n\| = 1$.

Example 8.1. Let $f_n = e_n/n$ as in Example 7.1. Then $\{f_n\}$ is still a (Schauder) basis for $\mathcal{H}$ but it is not a frame. In fact this satisfies (8.1) only with $A = 0$. That is, the inverse transformation (reconstruction) from $\langle x, f_n \rangle$ to x is not bounded. To see why $A = 0$, note that if we let $x = e_k$ for some $k > 0$ then $\|x\| = 1$ whereas $\sum_n |\langle x, f_n \rangle|^2 = 1/k^2$. The first inequality in the frame definition becomes $A \leq 1/k^2$ which cannot be satisfied for all k unless $A = 0$. In this example a finite B works because $|\langle x, f_n \rangle| = |\langle x, e_n \rangle|/n$ for each n. So $\sum |\langle x, f_n \rangle|^2 \leq \sum |\langle x, e_n \rangle|^2 = \|x\|^2$. ◇

Example 8.2. Suppose we modify the above example as follows: define $f_n = \frac{e_n}{n} + e_1$. We know that this is no longer a basis (Example 7.2). We now have $B = \infty$ in the frame definition, so this is not a frame. To verify this, let $x = e_1$ so $\|x\| = 1$. Then $\langle x, f_n \rangle = 1$ for all $n > 1$, so $\sum_n |\langle x, f_n \rangle|^2$ does not converge to a finite value. ◇

Example 8.3. Consider the sequence of vectors $\{e_1, e_1, e_2, e_2, \ldots\}$ This is a tight frame with frame bounds $A = B = 2$. Note that even though the vectors are normalized and the frame is tight this is not a orthonormal basis: This has a redundancy of two in the sense that each vector is repeated twice. This frame is not even a basis, therefore not a Riesz basis. ◇

Example 8.4. Consider the sequence of vectors $\{e_1, \frac{e_2}{\sqrt{2}}, \frac{e_2}{\sqrt{2}}, \frac{e_3}{\sqrt{3}}, \frac{e_3}{\sqrt{3}}, \frac{e_3}{\sqrt{3}}, \ldots\}$ Again there is redundancy so it is not a basis. It is a tight frame with $A = B = 1$, but not an exact frame, and clearly not a basis. It has redundancy (repeated vectors). ◇

Frame bounds and redundancy. For a tight frame with unit norm vectors f_n, the frame bound measures the redundancy. In Example 8.3 the redundancy is two (every vector repeated twice) and indeed $A = B = 2$. In Example 8.4 where we still have redundancy, the frame bound $A = B = 1$ does not indicate it. The frame bound of a tight frame measures redundancy only if the vectors f_n have unit norm as in Example 8.3.

8.3. The Frame Operator, Dual Frame, and Biorthogonality

The frame operator $\mathcal{F}$ associated with a frame $\{f_n\}$ in a Hilbert space $\mathcal{H}$ is a linear operator defined as follows:

$$\mathcal{F}x = \sum_{n=1}^{\infty} \langle x, f_n \rangle f_n \tag{8.2}$$

The summation can be shown to be convergent using the definition of the frame. The frame operator $\mathcal{F}$ takes a vector $x \in \mathcal{H}$ and produces another vector in $\mathcal{H}$. It can be shown that the norm of $\mathcal{F}x$ is bounded as follows:

$$A\|x\| \leq \|\mathcal{F}x\| \leq B\|x\|. \tag{8.3}$$

The frame operator is a *bounded linear operator* (since $B < \infty$), hence a continuous operator [Naylor and Sell, 1982]. Its inverse is also a bounded linear operator (since $A > 0$).

From Eq. (8.2) we have $\langle \mathcal{F}x, x \rangle = \sum_n |\langle x, f_n \rangle|^2$ by interchanging the inner product with the infinite summation. [This is permitted by the continuity of the operator $\mathcal{F}$ and the continuity of inner products (Sec. 6.2).] Since $\{f_n\}$ is complete, the right hand side is positive for $x \neq 0$. Thus $\langle \mathcal{F}x, x \rangle > 0$ unless $x = 0$, that is, $\mathcal{F}$ is a positive definite operator. The realness of $\langle \mathcal{F}x, x \rangle$ also means that $\mathcal{F}$ is self-adjoint, that is, $\langle \mathcal{F}x, y \rangle = \langle x, \mathcal{F}y \rangle$ for any $x, y \in \mathcal{H}$ [Naylor and Sell, 1982].

The importance of the frame operator arises from the fact that if we define $g_n = \mathcal{F}^{-1} f_n$ then any $x \in \mathcal{H}$ can be expressed as

$$x = \sum_{n=1}^{\infty} \langle x, g_n \rangle f_n = \sum_{n=1}^{\infty} \langle x, f_n \rangle g_n. \tag{8.4}$$

The sequence $\{g_n\}$ is itself a frame in $\mathcal{H}$ called the *dual frame*. It has frame bounds B^{-1} and A^{-1}. Among all representations of the form $x = \sum_n c_n f_n$, the representation $x = \sum_n \langle x, g_n \rangle f_n$ has the special property that the energy of the coefficients is minimized, that is, $\sum_n \left| \langle x, g_n \rangle \right|^2 \leq \sum_n |c_n|^2$ with equality if and only if $c_n = \langle x, g_n \rangle$ for all n [Heil and Walnut, 1989]. As argued earlier the computation of $\langle x, f_n \rangle$ from x and the inverse computation of x from $\langle x, f_n \rangle$ are numerically stable operations because $B < \infty$ and $A > 0$ respectively.

For the special case of a tight frame ($A = B$), the frame operator is particularly simple, that is $\mathcal{F}x = Ax$. In this case $g_n = \mathcal{F}^{-1} f_n = f_n / A$. Any vector $x \in \mathcal{H}$ can be expressed as

$$x = \frac{1}{A} \sum_{n=1}^{\infty} \langle x, f_n \rangle f_n \qquad \text{(tight frames)}. \tag{8.5}$$

Notice also that (8.1) gives

$$\sum_{n=1}^{\infty} \left| \langle x, f_n \rangle \right|^2 = A\|x\|^2 \qquad \text{(tight frames)}. \tag{8.6}$$

For a tight frame with $A = 1$, the above equations resemble the representation of x using an orthonormal basis even though such a tight frame is not necessarily a basis, because of possible redundancy (Example 8.4).

Exact frames and biorthogonality. For the special case of an exact frame (i.e., a Riesz basis) the sequence $\{f_n\}$ is minimal, and it is biorthogonal to the dual frame sequence $\{g_n\}$. This is consistent with our observation at the end of Sec. 7.4.

Summary on Frames. A sequence of vectors $\{f_n\}$ in a Hilbert space $\mathcal{H}$ is a frame if there are constants $A > 0$ and $B < \infty$ such that (8.1) holds for every vector $x \in \mathcal{H}$. Frames are complete (since $A > 0$) but not necessarily linearly independent. The constants A and B are called the frame bounds. A frame is *tight* if $A = B$. A tight frame with $A = B = 1$ and with normalized vectors ($\|f_n\| = 1$) is an orthonormal basis. For a tight frame with $\|f_n\| = 1$, the frame bound A measures redundancy. Any vector $x \in \mathcal{H}$ can be expressed in either of the two ways shown in (8.4). Here $g_n = \mathcal{F}^{-1} f_n$ where $\mathcal{F}$ is the *frame operator* defined in (8.2). The frame operator is a bounded linear operator, and is self-adjoint (in fact positive). The sequence $\{g_n\}$ is the *dual frame* and has frame bounds B^{-1} and A^{-1}. For a tight frame the frame representation reduces to (8.5). A frame is *exact* if deletion of any vector f_m destroys the frame property. A sequence $\{f_n\}$ is an exact frame if and only if it is a Riesz basis. An exact frame $\{f_n\}$ is biorthogonal to the dual frame $\{g_n\}$.

Fig. 8.2 is a Venn diagram which shows the classification of frames and bases, and the relationship between these. There are five classes, each shown by a rectangle.

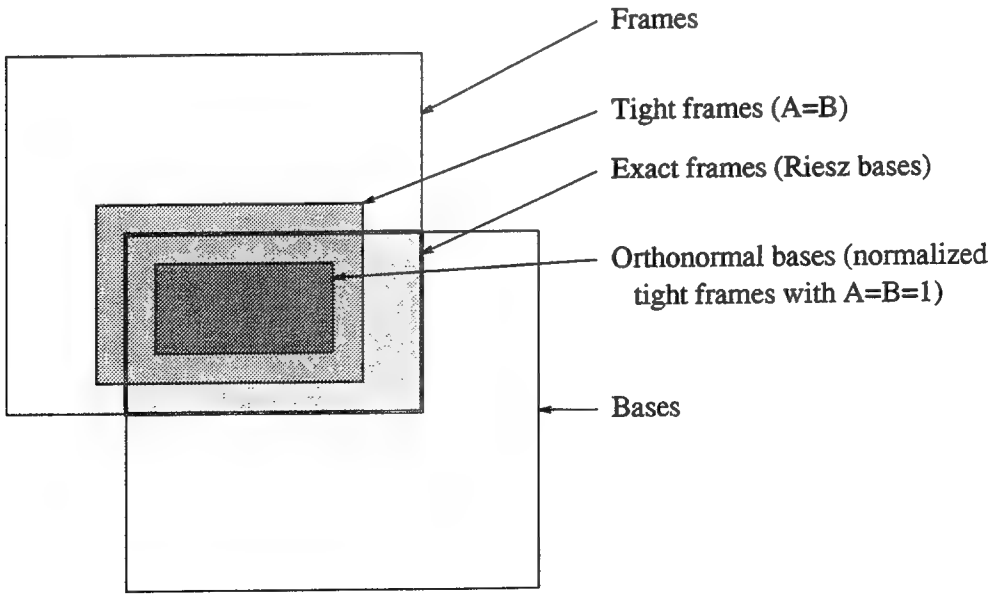

Fig. 8.2. A Venn diagram showing the relation between frames and bases in a Hilbert space. Each rectangle shows a class, as indicated.

9. THE STFT: INVERTIBILITY, ORTHONORMALITY AND LOCALIZATION

In Sec. 8 we saw that a vector x in an infinite dimensional Hilbert space (e.g., a function $x(t)$ in L^2) can be expanded in terms of a sequence of vectors $\{f_n\}$ called a frame, that is $x = \sum_{n=1}^{\infty} \langle x, g_n \rangle f_n$. One of the most important features of frames is that the construction of the expansion coefficients $\langle x, g_n \rangle$ from x as well as the reconstruction of x from these coefficients are numerically stable operations because $A > 0$ and $B < \infty$, as explained in Sec. 8. Riesz basis and orthonormal basis, which are special cases of a frame (Fig. 8.2), also share this numerical stability.

In Sec. 3 we tried to represent an L^2 function in terms of the STFT. The STFT coefficients are constructed using the integral (3.3). Denote for simplicity

$$g_{kn}(t) = v^*(t - nT_s)e^{jk\omega_s t} \tag{9.1}$$

Then the computation of the STFT coefficients can be written as

$$X_{stft}(k\omega_s, nT_s) = \Big\langle x(t), g_{kn}(t) \Big\rangle \tag{9.2}$$

This is a linear transformation which converts $x(t)$ into a two dimensional sequence because k and n are integers. Our hope is to be able to reconstruct $x(t)$ using an inverse linear transformation (inverse STFT) of the form

$$x(t) = \sum_{k=-\infty}^{\infty} \sum_{n=-\infty}^{\infty} X_{stft}(k\omega_s, nT_s) f_{kn}(t). \tag{9.3}$$

We know that this can indeed be done in a numerically stable manner if $\{g_{kn}(t)\}$ is a frame in L^2 and $\{f_{kn}(t)\}$ the dual frame. The fundamental questions then are: under what conditions does $\{g_{kn}(t)\}$ constitute a frame? Under what further conditions does this become a Riesz basis, better still, an orthonormal basis? With such conditions, what are the time-frequency localization properties of the resulting STFT? The answers depend on the window $v(t)$, and the sample spacings ω_s and T_s.

We will first construct a very simple example which shows the existence of orthonormal STFT bases, and indicate a fundamental disadvantage in the example. We will then state the answers to the above general questions without proof. Details can be found in a number of references, e.g., [Heil and Walnut, 1989], [Daubechies, 1992], and [Benedetto and Frazier, 1994].

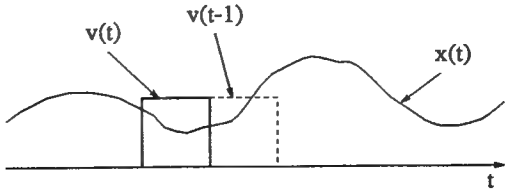

Fig. 9.1. The rectangular window in STFT.

Example 9.1. Orthonormal STFT Basis.

Suppose $v(t)$ is the rectangular window shown in Fig. 9.1, applied to an L^2 function $x(t)$. The product $x(t)v(t)$ therefore has finite duration. If we sample its Fourier transform at the rate $\omega_s = 2\pi$ we can recover $x(t)v(t)$ from these samples (this is like a Fourier series of the finite duration waveform $x(t)v(t)$). Shifting the window by successive integers, we can in this way recover successive pieces of $x(t)$ from the STFT, with sample spacing $\omega_s = 2\pi$ in the frequency domain. We see that the choice $T_s = 1$ and $\omega_s = 2\pi$ (so $\omega_s T_s = 2\pi$) leads to an STFT $X_{stft}(k\omega_s, nT_s)$, from which we can reconstruct $x(t)$ for all t. The quantity $g_{kn}(t)$ becomes

$$g_{kn}(t) = v(t-n)e^{jk\omega_s t} = v(t-n)e^{j2\pi kt} \tag{9.4}$$

Since the succcessive shifts of the window do not overlap, the functions $g_{kn}(t)$ are orthonormal for different values of n. The functions are also orthonormal for different values of k. Summarizing, the rectangular window of Fig. 9.1, with the time-frequency sampling durations $T_s = 1$ and $\omega_s = 2\pi$ produces an orthonormal STFT basis for L^2 functions. ◇

This example is reminiscent of the Nyquist sampling theorem in the sense that we can reconstruct $x(t)$ from (time-frequency) samples. But the difference is that $x(t)$ is an L^2 signal, not necessarily bandlimited. Note that T_s and ω_s cannot be arbitrarily interchanged (even if $\omega_s T_s = 2\pi$ preserved). Thus if we had chosen $T_s = 2$ and $\omega_s = \pi$ (preserving the product $\omega_s T_s$) we would not have obtained a basis because two successive positions of the window would be spaced too far apart and we would miss fifty percent of the signal $x(t)$.

9.1. Time-Frequency Sampling Density for Frames and Orthonormal Bases

Let us assume that $v(t)$ is normalized to have unit energy, that is $\int |v(t)|^2 dt = 1$ so that $\|g_{kn}(t)\| = 1$ for all k, n. If we impose the condition that $g_{kn}(t)$ be a frame, then it can be shown that the frame bounds satisfy the condition

$$A \leq \frac{2\pi}{\omega_s T_s} \leq B. \tag{9.5}$$

regardless of how $v(t)$ is chosen. Since an orthonormal basis is a tight frame with $A = B = 1$, *an STFT orthonormal basis must have* $\omega_s T_s = 2\pi$.

It can further be shown that if $\omega_S T_s > 2\pi$, then $\{g_{kn}(t)\}$ cannot be a frame. For $\omega_s T_s < 2\pi$ we can find frames by appropriate choice of window $v(t)$. The critical time-frequency sampling density is $(\omega_s T_s)^{-1} = (2\pi)^{-1}$. If the density is smaller we cannot have frames and if it is larger we cannot have orthonormal basis, but only frames.

Orthonormal STFT bases have poor time-frequency localization. Thus if we wish to have an orthonormal STFT basis, the time-frequency density is constrained to be such that $\omega_s T_s = 2\pi$. Under

this condition suppose we choose $v(t)$ appropriately to design such a basis. The time frequency localization properties of this system can be judged by computing the mean square durations D_t^2 and D_f^2 defined in (3.6). It has been shown by Balian and Low [Daubechies, 1992], [Benedetto and Frazier, 1994] that one of these is necessarily infinite no matter how we design $v(t)$. *Thus an orthonormal STFT basis always satisfies* $D_t D_f = \infty$. That is, either the time localization or the frequency resolution is very poor. This is summarized in the following theorem.

Theorem 9.1. Let the window $v(t)$ be such that $\{g_{kn}(t)\}$ in (9.1) is an orthonormal basis for L^2 (which means, in particular that $\omega_s T_s = 2\pi$). Define the rms durations D_t and D_f for the window $v(t)$ as usual [Eq. (3.6)]. Then either $D_t = \infty$ or $D_f = \infty$. ◇

Return now to Example 9.1 where we constructed an orthonormal STFT basis using the rectangular window of Fig. 9.1. Here $T_s = 1$ and $\omega_s = 2\pi$ (so that $\omega_s T_s = 2\pi$). The window $v(t)$ has finite mean square duation D_t^2. Its Fourier transform $V(\omega)$ has magnitude $|V(\omega)| = |\sin(\omega/2)/(\omega/2)|$ so that $\int \omega^2 |V(\omega)|^2 d\omega$ is not finite. This demonstrates the result of Theorem 9.1. One can try to replace the window $v(t)$ with something for which $D_t D_f$ is finite but this cannot be done without violating orthonormality.

Instability of the Gabor transform. Gabor constructed the STFT using the Gaussian window $v(t) = ce^{-t^2/2}$. In this case the sequence of functions $\{g_{kn}(t)\}$ can be shown to be complete in L^2 (in the sense defined in Sec. 7.2) as long as $\omega_s T_s \leq 2\pi$. However, if $\omega_s T_s = 2\pi$ then the system is not a frame because it can be shown that $A = 0$ in (8.1)! Thus the reconstruction of $x(t)$ from $X_{stft}(k\omega_s, nT_s)$ is unstable if $\omega_s T_s = 2\pi$ (see Sec. 8) even though $\{g_{kn}(t)\}$ is complete. So even though the Gabor transform has the ideal time frequency localization (minimum $D_t D_f$), it cannot provide a *stable basis,* hence certainly not an orthonormal basis, whenever $\omega_s T_s = 2\pi$.

Since orthonormal STFT basis is not possible if $\omega_s T_s \neq 2\pi$, this shows that we can *never* have an orthonormal basis with the Gabor transform (Gaussian windowed STFT), no matter how we choose ω_s and T_s. The Gabor example also demonstrates the fact that even if we successfully construct a complete set of functions (not necessarily a basis) to represent $x(t)$, it may not be useful because of instabilty of reconstruction. If we construct Riesz bases (e.g., orthonormal bases) or more generally frames, this disadvantage goes away. For example with the Gabor transform if we let $\omega_s T_s < 2\pi$ then all is well: we get a frame (so $A > 0$ and $B < \infty$ in (8.1)); we have stable reconstruction and good time frequency localization, but not orthonormality. Fig. 9.2 summarizes these results pertaining to the time-frequency product $\omega_s T_s$ in the STFT.

A major advantage of the wavelet transform over the STFT is that it is free from the above difficulties. For example we can obtain an orthonormal basis for L^2 with excellent time-frequency localization (finite,

controllable $D_t D_f$). We will also see how to constrain such a wavelet $\psi(t)$ to have the additional property of *regularity* or smoothness. Regularity is a property which is measured by the continuity and differentiability of $\psi(t)$. More precisely it is quantified by the Hölder index (to be defined in Sec. 13.1). In the next few sections where we construct wavelets based on paraunitary filter banks , we will see how to achieve all this systematically.

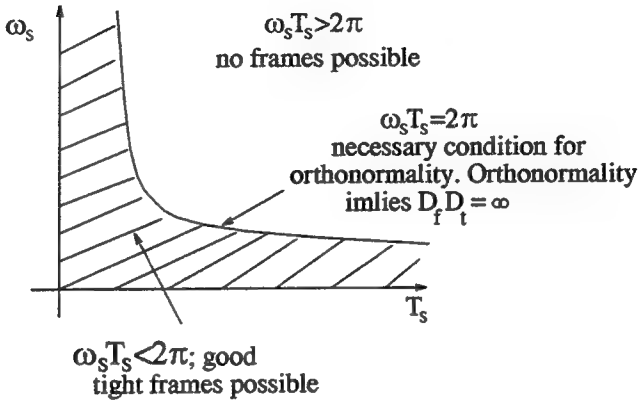

Fig. 9.2. Behavior of STFT representations for various regions of time-frequency sampling product $\omega_s T_s$. The curve $\omega_s T_s = 2\pi$ is critical; see text.

10. WAVELETS AND MULTIRESOLUTION

In Sec. 11–13 we will show how to construct compactly supported wavelets systematically to obtain orthonormal bases for L^2. The construction is such that excellent time-frequency localization is possible. Moreover the smoothness or regularity of the wavelets can be controlled. The construction is based on the two channel paraunitary filter bank described in Sec. 4. In that section the synthesis filters are denoted as $G_s(z)$ and $H_s(z)$ with impulse responses $g_s(n)$ and $h_s(n)$ respectively.

All constructions are based on obtaining the wavelet $\psi(t)$ and an auxilliary function $\phi(t)$ called the scaling function, from the impulse response sequences $g_s(n)$ and $h_s(n)$. We will do this by using time domain recursions of the form

$$\phi(t) = 2 \sum_{n=-\infty}^{\infty} g_s(n)\phi(2t-n), \quad \psi(t) = 2 \sum_{n=-\infty}^{\infty} h_s(n)\phi(2t-n), \tag{10.1}$$

called *dilation equations*. Equivalently in the frequency domain

$$\Phi(\omega) = G_s(e^{j\omega/2})\Phi(\omega/2), \quad \Psi(\omega) = H_s(e^{j\omega/2})\Phi(\omega/2) \tag{10.2}$$

It turns out that if $\{G_s(z), H_s(z)\}$ is a paraunitary pair with further mild conditions (e.g., that the lowpass filter $G_s(e^{j\omega})$ has a zero at π and no zeros in $[0, \pi/3]$) the recursions can be solved to obtain $\psi(t)$ which gives

rise to an orthonormal wavelet basis $\{2^{k/2}\psi(2^k t - n)\}$ for L^2. By constraining $G_s(e^{j\omega})$ to have a sufficient number of zeros at π we can further control the Hölder index (or regularity) of $\psi(t)$ as we see in Sec. 13.

Our immediate aim is to give an explanation for the occurence of the function $\phi(t)$, and the curious recursions (10.1) called the *dilation equations* or *two-scale equations*. These have origin in the beautiful theory of multiresolution for L^2 spaces [Meyer, 1986], [Mallat, 1989]. Since multiresolution theory lays the foundation for the construction of the most practical wavelets to date, we give a brief description of it here.

10.1. The Idea of Multiresolution

Return to Fig. 2.13(a) where we interpreted the wavelet transformation as a bank of continuous time analysis filters followed by samplers, and the inverse transformation as a bank of synthesis filters. Assume for simplicity the filters are ideal bandpass. Fig. 2.13(b) is a sketch of the frequency responses. The bandpass filters $F_k(\omega) = 2^{-k/2}\Psi(\omega/2^k)$ get narrower and narrower as k decreases (i.e., as k becomes more and more negative). Instead of letting k be negative, suppose we keep only $k \geq 0$ and include a lowpass filter $\Phi(\omega)$ to cover the low frequency region. Then we get the picture of Fig. 10.1. This is analogous to Fig. 2.12 where we used the pulse function $\phi(t)$ instead of using negative k in $\psi(2^k t - n)$.

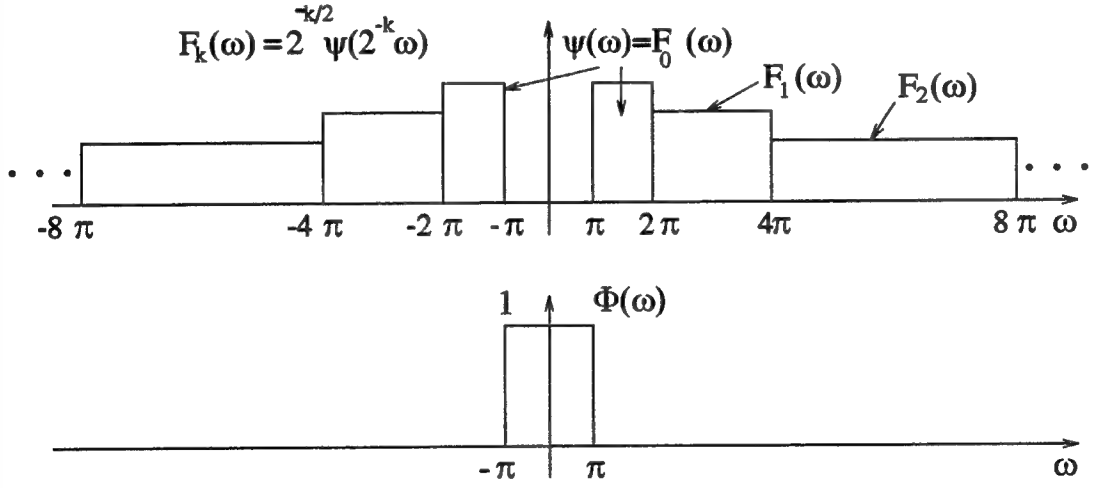

Fig. 10.1. The lowpass function $\Phi(\omega)$, bandpass function $\Psi(\omega)$, and the streched bandpass filters $F_k(\omega)$.

Imagine for a moment that $\Phi(\omega)$ is an ideal lowpass filter with cutoff $\pm\pi$. Then we can represent any L^2 function $F(\omega)$ with support restricted to $\pm\pi$ in the form $F(\omega) = \sum_{n=-\infty}^{\infty} a_n \Phi(\omega) e^{-j\omega n}$. This is simply the Fourier series expansion of $F(\omega)$ in $[-\pi, \pi]$, and it follows that $\sum_n |a_n|^2 < \infty$ (Theorem 6.1). In the

time domain this means

$$f(t) = \sum_{n=-\infty}^{\infty} a_n \phi(t-n). \tag{10.3}$$

Let us denote by V_0 the closure of the span of $\{\phi(t-n)\}$. Thus, V_0 is the class of L^2 signals that are bandlimited to $[-\pi, \pi]$. Since $\phi(t)$ is the sinc function, the shifted functions $\{\phi(t-n)\}$ form an orthonormal basis for V_0.

Consider now the subspace $W_0 \subset L^2$ of bandpass functions bandlimited to $\pi < |\omega| \leq 2\pi$. The bandpass sampling theorem (Sec. 2.1) allows us to reconstruct such a bandpass signal $g(t)$ from its samples $g(n)$ by using the ideal filter $\Psi(\omega)$. Denoting the impulse response of $\Psi(\omega)$ by $\psi(t)$ we see that $\{\psi(t-n)\}$ spans W_0. It can be verified that $\{\psi(t-n)\}$ is an orthonormal basis for W_0. Moreover, since $\Psi(\omega)$ and $\Phi(\omega)$ do not overlap, it follows from Parseval's theorem that W_0 is orthogonal to V_0.

Next consider the space of all signals of the form $f(t)+g(t)$ where $f(t) \in V_0$ and $g(t) \in W_0$. This space is called the direct sum (or orthogonal sum) of V_0 and W_0, and is denoted as $V_1 = V_0 \oplus W_0$. It is the space of all L^2 signals bandlimited to $[-2\pi, 2\pi]$. We can continue in this manner and define the spaces V_k and W_k for all k. Then V_k is the space of all L^2 signals bandlimited to $[-2^k\pi, 2^k\pi]$. And W_k is the space of L^2 functions bandlimited to $2^k\pi < |\omega| \leq 2^{k+1}\pi$. The general recursive relation is $V_{k+1} = V_k \oplus W_k$. Fig. 10.2 demonstrates this for the case where the filters are ideal bandpass. Only the positive half of the frequency axis is shown for simplicity.

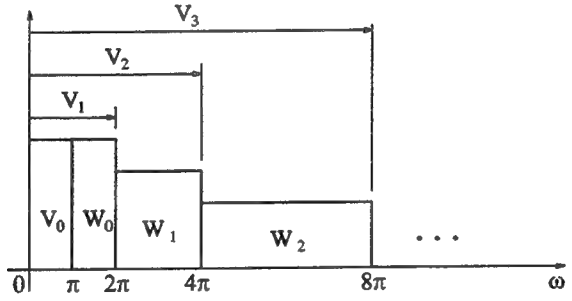

Fig. 10.2. Towards multiresolution analysis... The spaces $\{V_k\}$ and $\{W_k\}$ spanned by various filter responses.

It is clear that we could imagine V_0 itself to be composed of subspaces V_{-1} and W_{-1}. Thus $V_0 = V_{-1} \oplus W_{-1}$, $V_{-1} = V_{-2} \oplus W_{-2}$, and so forth. In this way we have defined a sequences of spaces $\{V_k\}$ and $\{W_k\}$ for all integers k such that the following conditions are true:

$$V_{k+1} = V_k \oplus W_k, \qquad \text{and} \qquad W_k \perp W_m,\ k \neq m. \tag{10.4}$$

where $\perp$ means "orthogonal". That is, the functions in W_k are orthogonal to those in W_m. It is clear that

$V_k \subset V_{k+1}$.

We will see later that *even if the ideal filters $\Phi(\omega)$ and $\Psi(\omega)$ are replaced with non ideal approximations*, we can sometimes define sequences of subspaces V_k and W_k satisfying the above conditions. The importance of this observation is this: *whenever $\Psi(\omega)$ and $\Phi(\omega)$ are such that we can construct such a subspace structure, the impulse response $\psi(t)$ of the filter $\Psi(\omega)$ can be used to generate an orthonormal wavelet basis!* While this might seem too complicated and roundabout, we will see that the construction of the function $\phi(t)$ is quite simple and elegant, and simplifies the constrution of orthonormal wavelet bases. A realization of these ideas based on paraunitary filter banks will be presented in Sec. 11. It is now time to be more precise with definitions as well as statements of the results.

Definition 10.1. Multiresolution analysis. Consider a sequence of closed subspaces $\{V_k\}$ in L^2, satisfying the following six properties.

1. *Ladder property.* $\ldots V_{-2} \subset V_{-1} \subset V_0 \subset V_1 \subset V_2 \ldots$
2. $\bigcap_{k=-\infty}^{\infty} V_k = \{0\}$
3. Closure of $\bigcup_{k=-\infty}^{\infty} V_k$ is equal to L^2.
4. *Scaling property.* $x(t) \in V_k$ if and only if $x(2t) \in V_{k+1}$. Since this implies "$x(t) \in V_0$ if and only if $x(2^k t) \in V_k$", all the spaces V_k are scaled versions of the space V_0. For $k > 0$, V_k is a *finer space* than V_0.
5. *Translation invariance.* If $x(t) \in V_0$ then $x(t-n) \in V_0$, that is, the space V_0 is invariant to translations by integers. By the previous property this means that V_k is invariant to translations by $2^{-k}n$.
6. *Special orthonormal basis.* There exists a function $\phi(t) \in V_0$ such that the integer shifted versions $\{\phi(t-n)\}$ form an orthonormal basis for V_0. By property 4 this means that $\{2^{k/2}\phi(2^k t - n)\}$ is an orthonormal basis for V_k. The function $\phi(t)$ is called the *scaling function* of multiresolution analysis. $\diamond$

Comments on the definition. Notice that the scaling function $\phi(t)$ determines V_0, hence all V_k. We say that $\phi(t)$ generates the entire multiresolution analysis $\{V_k\}$. The sequence $\{V_k\}$ is said to be a *ladder of subspaces* because of the inclusion property $V_k \subset V_{k+1}$. The technical terms *closed* and *closure* which originate from metric space theory, have simple meaning in our context (because L^2 is a Hilbert space). The subspace V_k is "closed" if the following is true: whenever a sequence of functions $\{f_n(t)\} \in V_k$ converges to a limit $f(t) \in L^2$ (i.e, $\|f(t) - f_n(t)\| \to 0$ as $n \to \infty$), the limit $f(t)$ is in V_k itself. In general an infinite union of closed sets is not closed, that is why we need to take "closure" in the third property above. The third property simply means that any element $x(t) \in L^2$ can be approximated arbitrary closely (in the L^2-norm sense) by an element in $\bigcup_{k=-\infty}^{\infty} V_k$.

General meaning of W_k. In the general setting of the above definition, the subspace W_k is defined as the orthogonal complement of V_k with respect to V_{k+1}. Thus the relation $V_{k+1} = V_k \oplus W_k$, which was valid in the ideal bandpass case (Fig. 10.2), continues to hold.

The Haar Multiresolution. A simple example of multiresolution where $\Phi(\omega)$ is not ideal lowpass is the Haar multiresolution, generated by the function $\phi(t)$ in Fig. 10.3(a). Here V_0 is the space of all functions that are piecewise constants on intervals of the form $[n, n+1]$. We will see later that the function $\psi(t)$ associated with this example is as in Fig. 10.3(b); the space W_0 is spanned by $\{\psi(t-n)\}$. The space V_k contains functions which are constants in $[2^{-k}n, 2^{-k}(n+1)]$. Fig. 10.3(c) and (d) show examples of functions belonging to V_0 and V_1. For this example, the six properties in the definition of multiresolution are particularly clear (except perhaps property 3, which can be proved too).

The multiresolution analysis generated by the ideal bandpass filters (Figs. 10.1, 10.2) is another simple example, where $\phi(t)$ is the sinc function. We see that the two elementary orthonormal wavelet examples (Haar wavelet and the ideal bandpass wavelet) also generate a corresponding multiresolution analysis. The connection between wavelets and multiresolution is deeper than this, and is elaborated in Sec. 10.2.

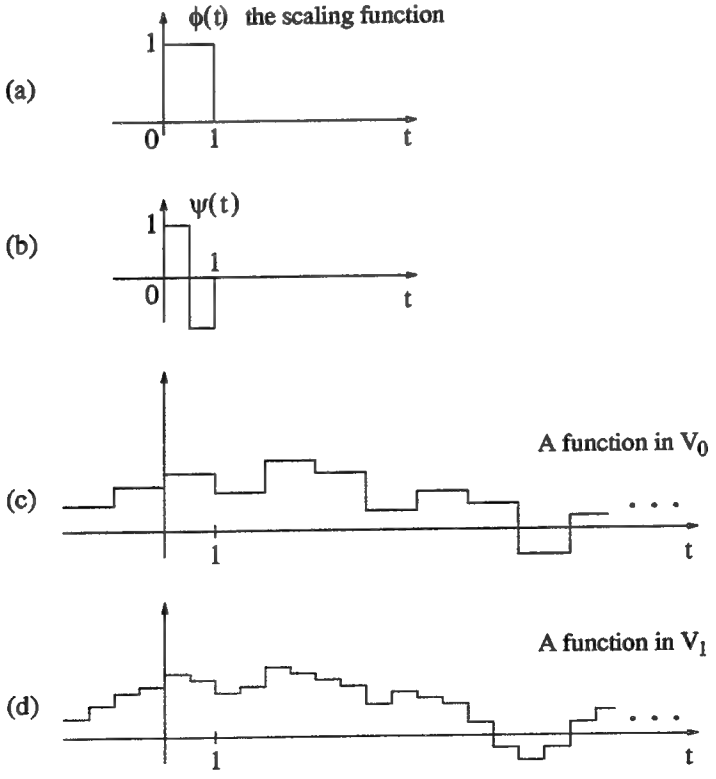

Fig. 10.3. The Haar multiresolution example. (a) The scaling function $\phi(t)$ that generates multiresolution, (b) the function $\psi(t)$ which generates W_0, (c) example of a memeber of V_0 and (d) example of a memeber of V_1.

Derivation of the Dilation Equation

Since $\{\sqrt{2}\phi(2t-n)\}$ is an orthonormal basis for V_1 (see property 6) and since $\phi(t) \in V_0 \subset V_1$ we see that $\phi(t)$ can be expressed as a linear combination of the functions $\{\sqrt{2}\phi(2t-n)\}$. Let us write

$$\phi(t) = 2\sum_{n=-\infty}^{\infty} g_s(n)\phi(2t-n) \qquad \text{(dilation equation)} \tag{10.5}$$

Thus the dilation equation arises naturally out of the multiresolution condition. For example, the Haar scaling function $\phi(t)$ satisfies the dilation equation

$$\phi(t) = \phi(2t) + \phi(2t-1). \tag{10.6}$$

The notation $g_s(n)$ and the factor 2 in the dilation equation might appear arbitrary now, but are convenient for future use. Orthonormality of $\{\phi(t-n)\}$ implies that $\|\phi(t)\| = 1$, and that $\{\sqrt{2}\phi(2t-n)\}$ are orthonormal. So $\sum_n |g_s(n)|^2 = 0.5$ from (10.5).

Example 10.1. Non orthonormal multiresolution.

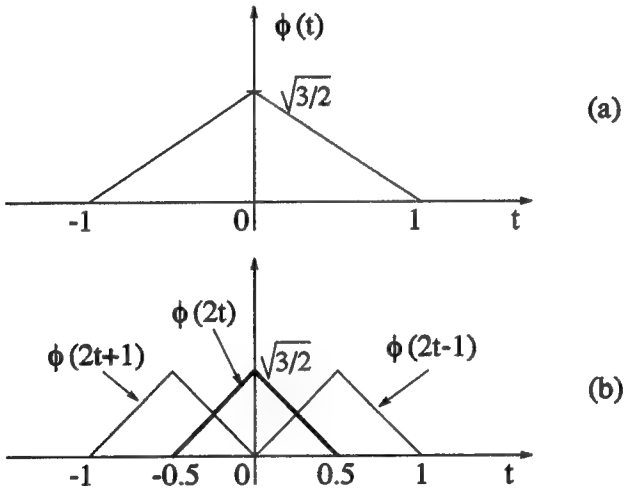

Fig. 10.4. Example of a scaling function $\phi(t)$ generating nonorthogonal multiresolution. (a) The scaling function, and (b) demonstrating the dilation equation.

Consider the triangular function shown in Fig. 10.4(a). This has $\|\phi(t)\| = 1$ and satisfies the dilation equation

$$\phi(t) = \phi(2t) + 0.5\phi(2t-1) + 0.5\phi(2t+1) \tag{10.7}$$

as demonstrated in Fig. 10.4(b). With V_k denoting the closure of the span of $\{2^{k/2}\phi(2^k t - n)\}$ it can be shown that the spaces $\{V_k\}$ satisfy all the conditions in the multiresolution definition, except one. Namely, $\{\phi(t-n)\}$ does not form an orthonormal basis [for example compare $\phi(t)$ and $\phi(t-1)$]. We will see later

(Example 10.2) that it does form a Riesz basis and that it can be converted into an orthonormal basis by orthonormalization. This example is a special case of family of scaling functions called *spline functions.* $\diamond$

We will see below that starting from an orthonormal multiresolution system (in particular from the function $\phi(t)$) one can generate an orthonormal wavelet basis for L^2. The wavelet bases generated from splines $\phi(t)$ (after orthonormalization) are called *spline wavelets* [Chui, 1992a,b]. These are also called the Battle-Lemarié family of wavelets. The link between multiresolution analysis and wavelets will be explained quantitatively in Sec. 10.2.

Multiresolution Approximation of L^2 Functions.

Given a multiresolution analysis, we know that $\bigcap_{k=-\infty}^{\infty} V_k = \{0\}$ and that the closure of $\bigcup_{k=-\infty}^{\infty} V_k = L^2$. From this it can be shown that the W_k's make up the entire L^2 space, that is

$$L^2 = \bigoplus_{k=-\infty}^{\infty} W_k. \tag{10.8a}$$

We can approximate an arbitrary L^2 function $x(t)$ to a certain degree of accuracy by projecting it onto V_k for appropriate k. Thus let $x_k(t)$ be this orthogonal projection (Sec. 2.2). Suppose we increase k to $k+1$. Since $V_{k+1} = V_k \oplus W_k$ and W_k is orthogonal to V_k, we see that the new approximation $x_{k+1}(t)$ (projection onto the finer space V_{k+1}) is given by $x_{k+1}(t) = x_k(t) + y_k(t)$ where $y_k(t)$ is in W_k.

Thus, when we go from scale k to scale $k+1$ we go to a bigger space $V_{k+1} \supset V_k$ which permits a finer approximation. This is nicely demonstrated in the two extreme examples mentioned above. For the example with ideal filters (Figs. 10.1, 10.2), the process of passing from scale k to $k+1$ is like admitting higher frequency components, which are orthogonal to the existing lowpass components. For the Haar example Fig. 10.3 where $\psi(t)$ and $\phi(t)$ are square pulses, when we pass from k to $k+1$ we permit finer pulses (i.e., highly localized finer variations in time domain). For this example, Figs. 10.3(c) and (d) demonstrate the projections $x_k(t)$ and $x_{k+1}(t)$ at two successive resolutions. The projections are piecewise-constant approximations of an L^2 signal $x(t)$.

By repeated application of $V_{k+1} = V_k \oplus W_k$ we can express V_0 as

$$V_0 = \bigoplus_{k=-\infty}^{-1} W_k, \tag{10.8b}$$

which, together with (10.8a) yields

$$L^2 = V_0 \oplus W_0 \oplus W_1 \oplus W_2 \oplus \ldots \tag{10.8c}$$

This has a nice interpretation based on Fig. 10.2. The L^2 signal $x(t)$ has been decomposed into orthogonal components belonging to V_0 (lowpass component), W_0 (bandpass component), W_1 (bandpass with higher bandwidth and center frequency), and so forth.

We can find an infinite number of multiresolution examples by choosing $\phi(t)$ appropriately. It is more important now to obtain systematic techniques for constructing such examples. The quality of the example is governed by the quality of $\psi(t)$ and $\phi(t)$, that is, the time localization and frequency resolution they can provide, the smoothness (regularity) of these functions, and the ease with which we can implement these approximations.

10.2. Relation between Multiresolution and Wavelets

Suppose $\phi(t) \in L^2$ generates an orthonormal multiresolution $\{V_k\}$ as defined in Sec. 10.1. We know $\phi(t) \in V_0$ and that $\{\phi(t-n)\}$ is an orthonormal basis for V_0. Moreover $\phi(t)$ satisfies the dilation equation (10.5), and the sequence $\{g_s(n)\} \in \ell^2$ defines the filter $G_s(e^{j\omega})$.

Now consider the finer space $V_1 = V_0 \oplus W_0$, where W_0 is orthonormal to V_0. If $f(t) \in W_0$ then $f(t) \in V_1$ so it is a linear combination of $\sqrt{2}\phi(2t-n)$ (property 6). Using this and the fact that W_0 is orthogonal to V_0 we can show that $F(\omega)$ (the L^2-FT of $f(t)$) has a special form. This is given by

$$F(\omega) = e^{j\omega/2} G_s^*(-e^{j\omega/2}) \Phi(\omega/2) H(e^{j\omega}),$$

where $H(e^{j\omega})$ is 2π-periodic. The special case of this with $H(e^{j\omega}) = 1$ will be denoted $\Psi(\omega)$, that is,

$$\Psi(\omega) = e^{j\omega/2} G_s^*(-e^{j\omega/2}) \Phi(\omega/2). \tag{10.9}$$

The above definition of $\Psi(\omega)$ is equivalent to

$$\psi(t) = 2 \sum_{n=-\infty}^{\infty} (-1)^{n+1} g_s^*(-n-1) \phi(2t-n) \qquad \text{(dilation equation for } \psi(t)\text{)}. \tag{10.10}$$

The function $\psi(t)$ satisfying this equation has some useful properties. First, it is in L^2. This follows from Theorem 6.2, since $\sum_n |g_s(n)|^2$ is finite. It can be shown that $\psi(t-n) \in W_0$ and that $\{\psi(t-n)\}$ is an orthonormal basis for W_0. This implies that $\{2^{k/2}\psi(2^k t - n)\}$ is an orthonormal basis for W_k (because $f(t) \in W_0$ if and only if $f(2^k t) \in W_k$, which is a property induced by the scaling property (property 4 in the definition of multiresolution). In view of (10.8a) we conclude that the sequence $\{2^{k/2}\psi(2^k t - n)\}$ with k and n varying over all integers, forms a basis for L^2. Summarizing we have the following result:

Theorem 10.1. Let $\phi(t) \in L^2$ generate an orthonormal multiresolution, i.e., a ladder of spaces $\{V_k\}$ satisfying the six properties in Definition 10.1. That is, in particular, $\{\phi(t-n)\}$ is an orthonormal basis for V_0. Then $\phi(t)$ satisfies the dilation equation (10.5) for some $g_s(n)$ with $\sum_n |g_s(n)|^2 = 0.5$. Define the function $\psi(t)$ according to the dilation equation (10.10). Then $\psi(t) \in W_0 \subset L^2$, and $\{\psi(t-n)\}$ is an orthonormal basis for W_0. Therefore $\{2^{k/2}\psi(2^k t - n)\}$ is an orthonormal basis for W_k, just as $\{2^{k/2}\phi(2^k t - n)\}$ is an

orthonormal basis for V_k (for fixed k). Moreover with k and n varying over all integers, the doubly indexed sequence $\{2^{k/2}\psi(2^k t - n)\}$ is an orthonormal wavelet basis for L^2. $\diamond$

Thus, to construct a wavelet basis for L^2 we only have to construct an orthonormal basis $\{\phi(t-n)\}$ for V_0. Everything else follows from that. All proofs can be found in a number of references, e.g., [Mallat, 1989], [Chui, 1992a], and [Daubechies, 1992].

10.3. Relation Between Multiresolution Analysis and Paraunitary Filter Banks

Denoting

$$h_s(n) = (-1)^{n+1} g_s^*(-1-n), \quad \text{i.e.,} \quad H_s(e^{j\omega}) = e^{j\omega} G_s^*(-e^{j\omega}),$$

we see that $\phi(t)$ and $\psi(t)$ satisfy the two dilation equations in (10.1). By construction $\psi(t) \in W_0$ and $\phi(t) \in V_0$. The fact that W_0 and V_0 are mutually orthogonal subspaces can be used to show that $H_s(e^{j\omega})$ and $G_s(e^{j\omega})$ satisfy

$$G_s^*(e^{j\omega}) H_s(e^{j\omega}) + G_s^*(-e^{j\omega}) H_s(-e^{j\omega}) = 0. \tag{10.11}$$

Moreover it can be shown that orthonormality of $\{\phi(t-n)\}$ leads to the power complementary property

$$|G_s(e^{j\omega})|^2 + |G_s(-e^{j\omega})|^2 = 1. \tag{10.12}$$

In other words, $G_s(e^{j\omega})$ is a power symmetric filter! That is, the filter $|G_s(e^{j\omega})|^2$ is a half band filter. Using $H_s(e^{j\omega}) = e^{j\omega} G_s^*(-e^{j\omega})$, we also have

$$|H_s(e^{j\omega})|^2 + |H_s(-e^{j\omega})|^2 = 1. \tag{10.13}$$

A compact way to express the above three equations is by defining the matrix

$$\mathbf{G}_s(e^{j\omega}) = \begin{bmatrix} G_s(e^{j\omega}) & H_s(e^{j\omega}) \\ G_s(-e^{j\omega}) & H_s(-e^{j\omega}) \end{bmatrix}$$

The three properties (10.11)-(10.13) are equivalent to $\mathbf{G}_s^\dagger(e^{j\omega})\mathbf{G}_s(e^{j\omega}) = \mathbf{I}$, that is the matrix $\mathbf{G}_s(e^{j\omega})$ is unitary for all ω. This matrix was defined in Sec. 4.4 in the context of paraunitary digital filter banks. Thus, the filters $G_s(e^{j\omega})$ and $H_s(e^{j\omega})$ constructed from a multiresolution setup as above constitute a paraunitary (CQF) synthesis bank.

Thus, *Orthonormal multiresolution automatically gives rise to paraunitary filter banks!* Starting from a multiresolution analysis we obtained two functions $\phi(t)$ and $\psi(t)$. These functions generate orthonormal bases $\{\phi(t-n)\}$ and $\{\psi(t-n)\}$ for the orthogonal subspaces V_0 and W_0. The functions $\phi(t)$ and $\psi(t)$ generated in this way satisfy the dilation equation (10.1). Defining the filters $G_s(z)$ and $H_s(z)$ from the coefficients $g_s(n)$ and $h_s(n)$ in an obvious way, we find that these filters form a paraunitary pair!

This raises the following fundamental question. If we start from a paraunitary pair $\{G_s(z), H_s(z)\}$ and define the functions $\phi(t)$ and $\psi(t)$ by (successfully) solving the dilation equations, do we obtain an orthonormal basis $\{\phi(t-n)\}$ for multiresolution, and a wavelet basis $\{2^{k/2}\psi(2^k t - n)\}$ for the space of L^2 functions? The answer, fortunately, is in the affirmative, subject to some minor requirements which can be trivially satisfied in practice. We return to this in Sec. 11.

Generating Wavelet and Multiresolution Coefficients From Paraunitary Filter Banks

Recall that the subspaces V_0 and W_0 have the orthonormal bases $\{\phi(t-n)\}$ and $\{\psi(t-n)\}$ respectively. By the scaling property, the subspace V_k has the orthonormal basis $\{\phi_{kn}(t)\}$, and similarly the subspace W_k has the orthonormal basis $\{\psi_{kn}(t)\}$, where, as usual, $\phi_{kn}(t) = 2^{k/2}\phi(2^k t - n)$ and $\psi_{kn}(t) = 2^{k/2}\psi(2^k t - n)$. The orthogonal projections of a signal $x(t) \in L^2$ onto V_k and W_k are given, respectively, by

$$P_k[x(t)] = \sum_{n=-\infty}^{\infty} \Big\langle x(t), \phi_{kn}(t) \Big\rangle \phi_{kn}(t), \qquad \text{and} \qquad Q_k[x(t)] = \sum_{n=-\infty}^{\infty} \Big\langle x(t), \psi_{kn}(t) \Big\rangle \psi_{kn}(t) \tag{10.14}$$

(see Sec. 2.2). Denote the scale-k projection coefficients as $d_k(n) = \langle x(t), \phi_{kn}(t) \rangle$ and $c_k(n) = \langle x(t), \psi_{kn}(t) \rangle$ for simplicity. (The notation c_{kn} was used in earlier sections, but $c_k(n)$ is convenient for the present discussion). We say that $d_k(n)$ are the *multiresolution coefficients* at scale k and $c_k(n)$ are the *wavelet coefficients* at scale k.

Assume that the projection coefficients $d_k(n)$ are known for some scale, say $k = 0$. We will then show that $d_k(n)$ and $c_k(n)$ for the coarser scales, i.e., $k = -1, -2, \ldots$ can be generated by using a paraunitary analysis filter bank $\{G_a(e^{j\omega}), H_a(e^{j\omega})\}$ corresponding to the synthesis bank $\{G_s(e^{j\omega}), H_s(e^{j\omega})\}$ (Sec. 4.4). We know $\phi(t)$ and $\psi(t)$ satisfy the dilation equations (10.1). By substituting the dilation equations into the righthand sides of $\phi_{kn}(t) = 2^{k/2}\phi(2^k t - n)$ and $\psi_{kn}(t) = 2^{k/2}\psi(2^k t - n)$, we obtain

$$\phi_{kn}(t) = \sqrt{2} \sum_{m=-\infty}^{\infty} g_s(m - 2n)\phi_{k+1,m}(t), \qquad \text{and} \qquad \psi_{kn}(t) = \sqrt{2} \sum_{m=-\infty}^{\infty} h_s(m - 2n)\phi_{k+1,m}(t). \tag{10.15}$$

A computation of the inner products $d_k(n) = \langle x(t), \phi_{kn}(t) \rangle$ and $c_k(n) = \langle x(t), \psi_{kn}(t) \rangle$ then yields

$$\begin{aligned} d_k(n) &= \sum_{m=-\infty}^{\infty} \sqrt{2} g_a(2n - m) d_{k+1}(m), \\ c_k(n) &= \sum_{m=-\infty}^{\infty} \sqrt{2} h_a(2n - m) d_{k+1}(m). \end{aligned} \tag{10.16}$$

where $g_a(n) = g_s^*(-n)$ and $h_a(n) = h_s^*(-n)$ are the analysis filters in the paraunitary filter bank.

The beauty of these equations is that they look like *discrete time convolutions!* Thus, if $d_{k+1}(n)$ is convolved with the impulse response $\sqrt{2}g_a(n)$ and the output decimated by two, the result is the sequence $d_k(n)$. A similar statement follows for $c_k(n)$. The above computation can therefore be interpreted in filter

bank form as in Fig. 10.5. Because of the perfect reconstruction property of the two channel system (Fig. 4.1), it follows that we can reconstruct the projection coefficients $d_{k+1}(n)$ from the projection coefficients $d_k(n)$ and $c_k(n)$.

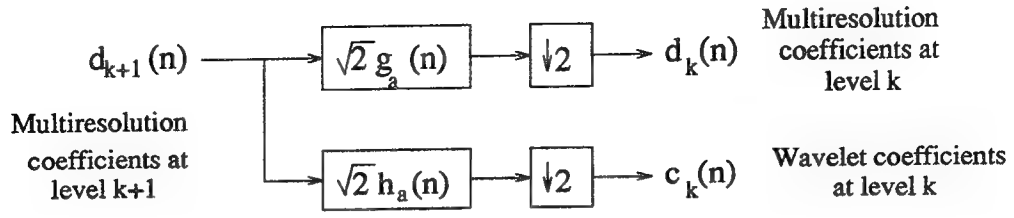

Fig. 10.5. Generating the wavelet and multiresolution coefficients at level k from level $k+1$.

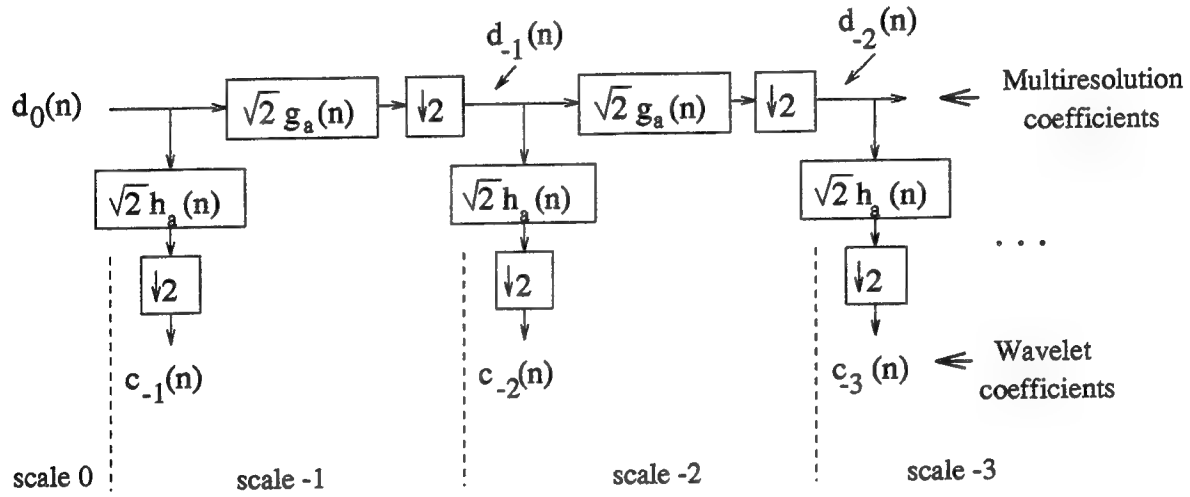

Fig. 10.6. Tree structured analysis bank generating wavelet coefficients $c_k(n)$ and multiresolution coefficients $d_k(n)$ recursively.

The Fast Wavelet Transform (FWT)

Repeated application of this idea results in Fig. 10.6 which is a tree structured paraunitary filter bank (Sec. 4.7) with analysis filters $\sqrt{2}g_a(n)$ and $\sqrt{2}h_a(n)$ at each stage. Thus, given the projection coefficients $d_0(n)$ for V_0, we can compute the projection coefficients $d_k(n)$ and $c_k(n)$ for the coarser spaces $V_{-1}, W_{-1}, V_{-2}, W_{-2}, \ldots$ This scheme is sometimes refered to as the *Fast Wavelet Transform (FWT)*. Fig. 10.7 shows a schematic of the computation. In this figure, each node (heavy dot) represents a decimated paraunitary analysis bank $\{\sqrt{2}g_a(n), \sqrt{2}h_a(n)\}$. The subspaces W_m and V_m are indicated in the nodes rather than the projection coefficients.

Computation of the initial projection coefficient. Everything depends on the computation of $d_0(n)$. Note that $d_0(n) = \langle x(t), \phi(t-n)\rangle$, which can be written as the integral $d_0(n) = \int x(t)\phi^*(t-n)dt$. An elaborate computation of this integral is avoided in practice. If the scale $k = 0$ is fine enough, that is,

if $x(t)$ does not change much within the duration where $\phi(t)$ is significant, we can approximate this integral with the sample value $x(n)$. That is, $d_0(n) \approx x(n)$. Improved approximations of $d_0(n)$ have been suggested by other authors, see references in [Djokovic and Vaidyanathan, 1994].

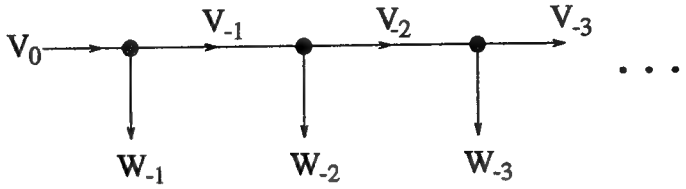

Fig. 10.7. A schematic of the tree structured filter-bank which generates the coefficients of the projections onto V_k and W_k.

Continuous-time Filter Banks and Multiresolution

The preceding discussions show the deep connection between orthonormal multiresolution ananlysis and discrete time paraunitary filter banks. As shown by Eq. (10.8c), any L^2 signal $x(t)$ can be written as a sum of its projections onto the mutually orthogonal spaces V_0, W_0, W_1 and so forth. That is,

$$x(t) = \sum_n d_0(n)\phi(t-n) + \sum_{k=0}^{\infty}\sum_n c_k(n)2^{k/2}\psi(2^k t - n).$$

This decomposition itself can be given a simple filter bank interpretation, with *continuous-time filters and samplers*. For this, first note that the V_0 component $\sum_n d_0(n)\phi(t-n)$ can be regarded as the output of a filter with impulse response $\phi(t)$, with the input chosen as the impulse train $\sum_n d_0(n)\delta_a(t-n)$. Similarly, the W_k component $\sum_n c_k(n)2^{k/2}\psi(2^k t - n)$ is the output of a filter with impulse response $f_k(t) = 2^{k/2}\psi(2^k t)$, in response to the input $\sum_n c_k(n)\delta_a(t - 2^{-k}n)$. This interpretation is shown by the synthesis bank of Fig. 10.8(a).

The projection coefficients $d_0(n)$ and $c_k(n)$ can also be interpreted in a nice way. For example, we have $d_0(n) = \langle x(t), \phi(t-n)\rangle$ by orthonormality. This inner product can be explicitly written out as

$$d_0(n) = \int x(t)\phi^*(t-n)dt.$$

The integral can be interpreted as a convolution of $x(t)$ with $\phi^*(-t)$. Thus consider the output of the filter with impulse response $\phi^*(-t)$, with the input chosen as $x(t)$. This output, sampled at time n, gives $d_0(n)$. Similarly, $c_k(n)$ can be interpreted as the output of the filter $h_k(t) = 2^{k/2}\psi^*(-2^k t)$, sampled at the time $2^{-k}n$. The analysis bank of Fig. 10.8(a) shows this interpretation. Thus, the projection coefficients $d_0(n)$ and $c_k(n)$ are the sampled versions of the outputs of an analysis filter bank.

Notice that all the filters in the filter bank are determined by the scaling function $\phi(t)$ and the wavelet function $\psi(t)$. Every synthesis filter $f_k(t)$ is the time reversed conjugate of the corresponding analysis filter

$h_k(t)$, that is, $f_k(t) = h_k^*(-t)$ (a consequence of orthonormality). In terms of frequency responses this means $F_k(\omega) = H_k^*(\omega)$. For completeness of the picture, Fig. 10.8(b) shows typical frequency response magnitudes of these filters.

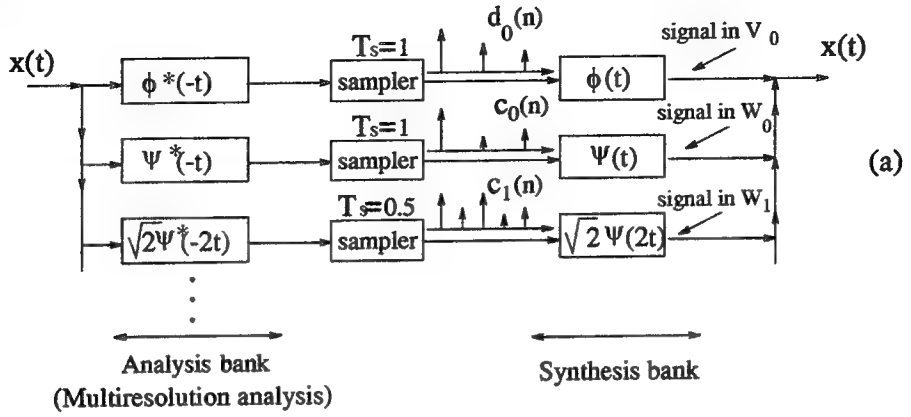

(a)

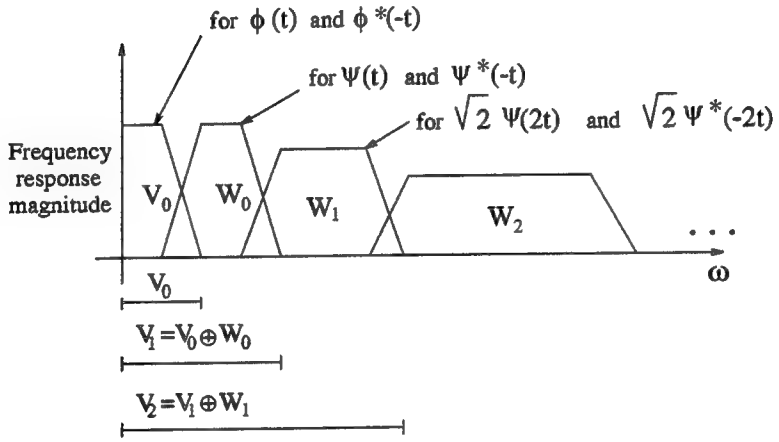

(b)

Fig. 10.8. (a) The multiresolution analysis and resynthesis in filter-bank form, and (b) typical frequency responses.

10.4. Further Manifestations of Orthonormality

The orthonormality of the basis functions $\{\phi(t-n)\}$ and $\{\psi(t-n)\}$ have further consequences which we summarize now. A knowledge of these will be useful when we generate the scaling function $\phi(t)$ and the wavelet function $\psi(t)$ systematically in Sec. 11 from paraunitary filter banks.

The Nyquist Property and Orthonormality

With $\phi(t) \in L^2$, the autocorrelation function $R(\tau) = \int \phi(t)\phi^*(t-\tau)dt$ exists for all τ because this is just an inner product of two elements in L^2. Clearly $R(0) = \|\phi(t)\|^2 = 1$. Moreover the orthonormality property

$\langle \phi(t), \phi(t-n) \rangle = \delta(n)$ can be rewritten as $R(n) = \delta(n)$. Thus, in particular, $R(\tau)$ has periodic zero crossings, at nonzero integer values of τ (Fig. 10.9). This is precisely the *Nyquist property* familiar to communication engineers. The autocorrelation of the scaling function $\phi(t)$ is a Nyquist function. The same holds for the wavelet function $\psi(t)$.

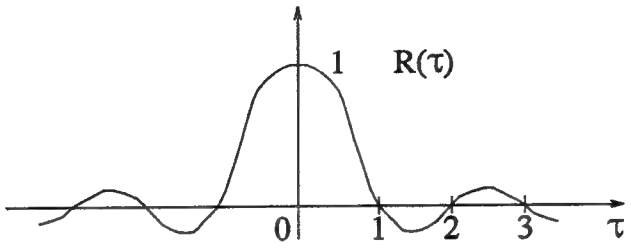

Fig. 10.9. Example of an autocorrelation of the scaling function $\phi(t)$.

Next, using Parseval's identity for L^2-FTs, we obtain $\langle \phi(t), \phi(t-n) \rangle = \int \Phi(\omega)\Phi^*(\omega)e^{j\omega n}d\omega/2\pi = \delta(n)$. If we decompose the integral into a sum of integrals over intervals of length 2π and use the 2π-periodicity of $e^{j\omega n}$ we obtain, after some simplification:

$$\sum_{k=-\infty}^{\infty} |\Phi(\omega + 2\pi k)|^2 = 1 \qquad \text{almost everywhere.} \tag{10.17}$$

This is the preceding Nyquist condition, now expressed in the frequency domain. The term *almost everywhere* (Sec. 6.1) arises from the fact that we have drawn a conclusion about an integrand from the value of the integral. Thus $\{\phi(t-n)\}$ *is orthonormal if and only if the preceding equation holds.* A similar result follows for $\Psi(\omega)$, that is orthonormality of $\{\psi(t-n)\}$ is equivalent to

$$\sum_{k=-\infty}^{\infty} |\Psi(\omega + 2\pi k)|^2 = 1, \qquad \text{almost everywhere.} \tag{10.18}$$

Case When Equalities Hold Pointwise

If we assume that all Fourier transforms are continuous, then equalities in the Fourier domain actually hold pointwise. This is the most common situation; in all examples to be seen here, the following are true: (i) the filters $G_s(e^{j\omega})$ and $H_s(e^{j\omega})$ are rational (FIR or IIR) so the frequency responses are continuous functions of ω, and (ii) $\phi(t)$ and $\psi(t)$ are not only in L^2 but also in L^1 i.e., $\phi(t), \psi(t) \in L^1 \cap L^2$. Thus, $\Phi(\omega)$ and $\Psi(\omega)$ are continuous functions (Sec. 6.3).

With the dilation equation $\Phi(\omega) = G_s(e^{j\omega/2})\Phi(\omega/2)$ holding pointwise, we have $\Phi(0) = G_s(e^{j0})\Phi(0)$. In all our applications $\Phi(0) \neq 0$ (it is a lowpass filter), so $G_s(e^{j0}) = 1$. The power symmetry property

$$|G_s(e^{j\omega})|^2 + |G_s(-e^{j\omega})|^2 = 1$$

then implies $G_s(e^{j\pi}) = 0$. Since the highpass synthesis filter is $H_s(e^{j\omega}) = e^{j\omega}G_s^*(-e^{j\omega})$ we conclude $H_s(e^{j0}) = 0$ and $H_s(e^{j\pi}) = -1$. Thus

$$G_s(e^{j0}) = 1,\ G_s(e^{j\pi}) = 0, \quad H_s(e^{j0}) = 0,\ H_s(e^{j\pi}) = -1. \tag{10.19}$$

In particular, the lowpass impulse response $g_s(n)$ therefore satisfies $\sum_n g_s(n) = 1$. Since we already have $\sum_n |g_s(n)|^2 = 0.5$ (Theorem 10.1), we have both of the following:

$$\sum_{n=-\infty}^{\infty} g_s(n) = 1, \qquad \text{and} \qquad \sum_{n=-\infty}^{\infty} |g_s(n)|^2 = 0.5. \tag{10.20}$$

From the dilation equation $\Phi(\omega) = G_s(e^{j\omega/2})\Phi(\omega/2)$ we obtain $\Phi(2\pi k) = G_s(e^{j\pi k})\Phi(\pi k)$. By using the fact that $G_s(e^{j\pi}) = 0$, and after elementary manipulations we can show that

$$\Phi(2\pi k) = 0,\ k \neq 0. \tag{10.21}$$

That is, $\Phi(\omega)$ is itself a Nyquist function of ω. If (10.17) is *assumed to hold pointwise,* then the above implies that $|\Phi(0)| = 1$. Without loss of generality we will let $\Phi(0) = 1$ i.e., $\int \phi(t)dt = 1$. The dilation equation for the wavelet function $\Psi(\omega)$ in (10.2) shows that $\Psi(0) = 0$ [since $H_s(e^{j0}) = 0$ by (10.19)]. That is, $\int \psi(t)dt = 0$. Summarizing, the scaling and wavelet functions satisfy

$$\int_{-\infty}^{\infty} \phi(t)dt = 1,\ \int_{-\infty}^{\infty} \psi(t)dt = 0, \qquad \text{and} \qquad \int_{-\infty}^{\infty} |\phi(t)|^2 dt = \int_{-\infty}^{\infty} |\psi(t)|^2 dt = 1, \tag{10.22}$$

where the third property follows from orthonormality. These integrals make sense because of the assumption $\phi(t) \in L^1 \cap L^2$. Another result that follows from $\Phi(2\pi k) = \delta(k)$ is that

$$\sum_{n=-\infty}^{\infty} \phi(t-n) = 1 \qquad \text{a.e.} \tag{10.23}$$

Thus the basis functions of the subspace V_0 themselves add up to unity. Return to the Haar basis, and notice how beautifully everything fits together!

10.5. Generating wavelet and multiresolution basis by design of $\phi(t)$

Most of the well-known wavelet basis families in recent times have been generated by first finding a scaling function $\phi(t)$ such that it is a valid generator of multiresolution, and then generating $\psi(t)$ from $\phi(t)$. The first step therefore is to identify the conditions under which a function $\phi(t)$ will be a valid scaling function (i.e., it will generate a multiresolution). Once this is done, and we successfully identify the coefficients $g_s(n)$ in the dilation equation for $\phi(t)$, then we can identify the wavelet function $\psi(t)$ using the second dilation equation in (10.1). From Theorem 10.1 we know that if $\psi(t)$ is computed in this way, then $\{2^{k/2}\psi(2^k t - n)\}$

is an orthonormal wavelet basis for L^2. The following results can be deduced from the many detailed results presented in [Daubechies, 1992].

Theorem 10.2. Let $\phi(t)$ satisfy the following three conditions: (a) $\phi(t) \in L^1 \cap L^2$, (b) $\int \phi(t)dt \neq 0$ (i.e., $\Phi(0) \neq 0$), (c) $\phi(t) = 2\sum_n g_s(n)\phi(2t-n)$ for some $\{g_s(n)\}$, and (d) $\{\phi(t-n)\}$ is an orthonormal sequence. Then the following are true.

1. $\phi(t)$ generates a multiresolution. That is, if we define the space V_k to be the closure of the span of $\{2^{k/2}\phi(2^k t-n)\}$, then the set of spaces $\{V_k\}$ satisfies the six conditions in Definition 10.1.
2. Define $\psi(t) = 2\sum_n (-1)^{n+1} g_s^*(-n-1)\phi(2t-n)$. Then $\psi(t)$ generates an orthonormal wavelet basis for L^2. That is, $\{2^{k/2}\psi(2^k t-n)\}$, with k *and* n *varying over all integers,* is an orthonormal basis for L^2. In fact, for fixed k, the functions $\{2^{k/2}\psi(2^k t-n)\}$ form an orthonormal basis for the subspace W_k defined in Sec. 10.1. ♢

Comments. In many examples $\phi(t) \in L^2$, and it is compactly supported. Then it is naturally in L^1 as well (Eq. (6.1)), so the assumption $\phi(t) \in L^2 \cap L^1$ is not too restrictive. Since $L^1 \cap L^2$ is dense in L^2, the above construction still gives a wavelet basis for L^2. Notice also that the orthonormality of $\{\phi(t-n)\}$ implies orthonormality of $\{\sqrt{2}\phi(2t-n)\}$. So the recursion $\phi(t) = 2\sum_n g_s(n)\phi(2t-n)$ is a Fourier series for $\phi(t)$ in L^2. Thus the condition $\sum_n |g_s(n)|^2 = 0.5$ is automatically implied. This, therefore, is not explicitly stated as part of the conditions in the theorem.

Orthnormalization

From Sec. 10.4 we know that orthonormality of $\{\phi(t-n)\}$ is equivalent to

$$\sum_{k=-\infty}^{\infty} |\Phi(\omega + 2\pi k)|^2 = 1. \tag{10.24}$$

Suppose now that this is not satisfied but the weaker condition

$$a \leq \sum_{k=-\infty}^{\infty} |\Phi(\omega + 2\pi k)|^2 \leq b \tag{10.25}$$

holds for some $a > 0$ and $b < \infty$. Then it can be shown that we can at least obtain a Riesz basis (Sec. 7.3) of the form $\{\phi(t-n)\}$ for V_0. We can also normalize it to obtain an orthonormal sequence $\{\widehat{\phi}(t-n)\}$ from which an orthonormal wavelet basis can be generated in the usual way. The following theorem summarizes the main results.

Theorem 10.3. Let (a) $\phi(t) \in L^1 \cap L^2$, (b) $\int \phi(t)dt \neq 0$ (i.e., $\Phi(0) \neq 0$), and (c) $\phi(t) = 2\sum_n g_s(n)\phi(2t-n)$ with $\sum_n |g_s(n)|^2 < \infty$. Instead of the orthonormality condition (10.24), let (10.25) hold for some $a > 0$ and $b < \infty$. Then the following are true.

1. $\{\phi(t-n)\}$ is a Riesz basis for the closure V_0 of its span.
2. $\phi(t)$ generates a multiresolution. That is, if we define the space V_k to be the closure of the span of $\{2^{k/2}\phi(2^k t-n)\}$, then the set of spaces $\{V_k\}$ satisfies the six conditions in Definition 10.1. ◇

Orthonormalization. If we define a new function $\widehat{\phi}(t)$ in terms of its Fourier transform as follows:

$$\widehat{\Phi}(\omega)=\frac{\Phi(\omega)}{\left(\sum_k|\Phi(\omega+2\pi k)|^2\right)^{0.5}} \tag{10.26}$$

then $\widehat{\phi}(t)$ generates an orthonormal multiresolution. It satisfies a dilation equation similar to (10.1). From this we can define a corresponding wavelet function $\widehat{\psi}(t)$ in the usual way. That is, if $\widehat{\phi}(t)=2\sum_n g_s(n)\widehat{\phi}(2t-n)$, then choose $\widehat{\psi}(t)=2\sum_n h_s(n)\widehat{\phi}(2t-n)$, where $h_s(n)=(-1)^{n+1}g_s^*(-n-1)$. This wavelet $\widehat{\psi}(t)$ then generates an orthonormal wavelet basis for L^2. Note that the basis is not necessarily compactly supported if we start with compactly supported $\phi(t)$. An example will be seen in Fig. 13.2(b) later.

Example 10.2. Battle-Lemarié orthonormal wavelets from splines. In Example 10.1 we considered a triangular $\phi(t)$ (Fig. 10.4) which generates a nonorthonormal multiresolution. In this example we have

$$\Phi(\omega)=\sqrt{\frac{3}{2}}\left(\frac{\sin(\omega/2)}{(\omega/2)}\right)^2 \tag{10.27}$$

and it can be shown that

$$\sum_{k=-\infty}^{\infty}|\Phi(\omega+2\pi k)|^2=\frac{2+\cos\omega}{2} \tag{10.28}$$

The inequality (10.25) is satisfied with $a=1/2$ and $b=3/2$. Thus we have a Riesz basis $\{\phi(t-n)\}$ for V_0. From this scaling function we can obtain the normalized function $\widehat{\Phi}(\omega)$ as above and then generate the wavelet function $\widehat{\psi}(t)$ as explained above. This gives an orthonormal wavelet basis for L^2. But $\widehat{\phi}(t)$ does not have compact support (unlike $\phi(t)$). That is the wavelet function $\widehat{\psi}(t)$ generating the orthonormal wavelet basis is not compactly supported either. ◇

11. ORTHONORMAL WAVELET BASIS FROM PARAUNITARY FILTER BANKS

The wisdom gained from the multiresolution viewpoint (Sec. 10) tells us there is a close connection between wavelet bases and two channel digital filter banks. In fact we obtained the equations of a paraunitary filter bank just by imposing the orthonormality condition on the multiresolution basis functions $\{\phi(t-n)\}$. In this section we will present the complete story: suppose we start from a two channel digital filter bank with the paraunitary property. Can we derive an orthonormal wavelet basis from this? To be more specific, return to the dilation equations (10.1) or equivalently (10.2). Here $g_s(n)$ and $h_s(n)$ are the impulse response

coefficients of the two synthesis filters $G_s(e^{j\omega})$ and $H_s(e^{j\omega})$ in the digital filter bank. Given these two filters, can we "solve" for $\phi(t)$ and $\psi(t)$? If so, does this $\psi(t)$ generate an orthonormal basis for L^2 space? In this section we will answer some of these questions. Unlike in any other section, we will also indicate a sketch of the proof for each major result, in view of the importance of these in modern signal processing theory.

Recall first that under some mild conditions (Sec. 10.4) we can prove that the filters have to satisfy (10.19),(10.20), if we need to generate wavelet and multiresolution bases successfully. We will impose these at the outset. By repeated application of the dilation equation we get $\Phi(\omega) = G_s(e^{j\omega/2})G_s(e^{j\omega/4})\Phi(\omega/4)$. Further indefinite repetition yields an infinite product. Using the condition $\Phi(0) = 1$ which we justified at the end of Sec. 10.4, we obtain the infinite products

$$\Phi(\omega) = \prod_{k=1}^{\infty} G_s(e^{j\omega/2^k}) = G_s(e^{j\omega/2}) \prod_{k=2}^{\infty} G_s(e^{j\omega/2^k}), \tag{11.1a}$$

$$\Psi(\omega) = H_s(e^{j\omega/2}) \prod_{k=2}^{\infty} G_s(e^{j\omega/2^k}). \tag{11.1b}$$

The first issue to be addressed is the convergence of the infinite products above. For this we need to review some preliminaries on infinite products [Apostol, 1974], [Rudin, 1966].

The ideal bandpass wavelet re-derived from the digital filter bank. Before we address the mathematical details, let us consider a simple example. Suppose the pair of filters $G_s(e^{j\omega})$ and $H_s(e^{j\omega})$ are ideal brickwall lowpass and highpass filters as in Fig. 4.8(a). Then we can verify, by making simple sketches of a few terms in (11.1), that the above infinite products yield the functions $\Phi(\omega)$ and $\Psi(\omega)$ shown in Fig. 10.1. That is, the ideal bandpass wavelet is indeed related to the ideal paraunitary filter bank by means of the above infinite product!

11.1. Convergence of Infinite Products

To define convergence of a product of the form $\prod_{k=1}^{\infty} a_k$, consider the sequence $\{p_n\}$ of partial products $p_n = \prod_{k=1}^{n} a_k$. If this converges to a (complex) number A with $0 < |A| < \infty$ we say that the infinite product converges to A. Convergence to zero should be defined more carefully to avoid degenerate situations (e.g., if $a_1 = 0$, then $p_n = 0$ for all n regardless of the remaining terms $a_k, k > 1$). We use the definition in [Apostol, 1974]. The infinite product is said to converge to zero if and only if $a_k = 0$ for a finite nonzero number of values of k, *and* if the product with these a_k's deleted converges to a nonzero value.

Useful Facts About Infinite Products

1. Whenever $\prod_{k=1}^{\infty} a_k$ converges, it can be shown that $a_k \to 1$ as $k \to \infty$. For this reason it is convenient to write $a_k = 1 + b_k$.

2. We say that $\prod_{k=1}^{\infty}(1+b_k)$ converges absolutely if $\prod_{k=1}^{\infty}(1+|b_k|)$ converges. Absolute convergence of $\prod_{k=1}^{\infty}(1+b_k)$ implies its convergence.
3. It can be shown that the product $\prod_{k=1}^{\infty}(1+|b_k|)$ converges if and only if the sum $\sum_{k=1}^{\infty}|b_k|$ converges. That is, $\prod_{k=1}^{\infty}(1+b_k)$ converges absolutely if and only if $\sum_{k=1}^{\infty}b_k$ converges absolutely.

Examples. The product $\prod_{k=1}^{\infty}(1+k^{-2})$ converges because $\sum_{k=1}^{\infty}1/k^2$ converges. Similarly $\prod_{k=1}^{\infty}(1-k^{-2})$ converges because it converges absolutely, by the preceding example. The product $\prod_{k=1}^{\infty}(1+k^{-1})$ does not converge because $\sum_{k=1}^{\infty}1/k$ diverges. Products such as $\prod_{k=1}^{\infty}(1/k^2)$ do not converge because the terms do not approach unity as $k \to \infty$. ◇

Uniform Convergence

A sequence $\{p_n(z)\}$ of functions of the complex variable z converges *uniformly* to a function $p(z)$ on a set $\mathcal{S}$ in the complex plane if the convergence rate is the same everywhere in $\mathcal{S}$. More precisely, if we are given $\epsilon > 0$, we can find N such that $|p_n(z) - p(z)| < \epsilon$ for every $z \in \mathcal{S}$, as long as $n \geq N$. The crucial thing is that N depends only on ϵ and not on z, as long as $z \in \mathcal{S}$. A similar definition applies for functions of real variables.

We say that an infinite product of functions $\prod_{k=1}^{\infty}a_k(z)$ converges at a point z if the sequence of partial products $p_n(z) = \prod_{k=1}^{n}a_k(z)$ converges as described previously. If this convergence of $p_n(z)$ is uniform in a set $\mathcal{S}$ we say that the infinite product converges *uniformly* on $\mathcal{S}$. Uniform convergence has similar advantages as in the case of infinite summations. For example, if each of the functions $a_k(\omega)$ is continuous on the real interval $[\omega_1, \omega_2]$, then uniform convergence of the infinite product $A(\omega) = \prod_{k=1}^{\infty}a_k(\omega)$ on $[\omega_1, \omega_2]$ implies that the limit $A(\omega)$ is continuous on $[\omega_1, \omega_2]$. We saw above that convergence of infinite products can be related to that of infinite summations. The following theorem [Rudin, 1966] makes the connection between uniform convergence of summations and uniform convergence of products.

Theorem 11.1. Let $b_k(z), k \geq 1$ be a sequence of bounded functions of the complex variable z, such that $\sum_{k=1}^{\infty}|b_k(z)|$ converges uniformly on a compact set† $\mathcal{S}$ in the complex z plane. Then the infinite product $\prod_{k=1}^{\infty}(1+b_k(z))$ converges uniformly on $\mathcal{S}$. Moreover, this product is zero for some z_0 if and only if $1 + b_k(z_0) = 0$ for some k. ◇

Uniform convergence and analyticity. We know that if a sequence of continuous functions converges uniformly to a function, then the limit is also continuous. A similar result is true for analytic functions. That is, if a sequence $\{f_n(s)\}$ of analytic functions converges uniformly to a function $f(s)$ then $f(s)$ is analytic as

† For us, a compact set means any closed bounded set in the complex plane or on the real line. Examples (i) all points on and inside a circle in the complex plane, and (ii) the closed interval $[a, b]$ on the real line.

well. For a more precise statement of this result see Theorem 10.28 in Rudin [1966].

11.2. Infinite Product Defining the Scaling Function

Return now to the infinite product (11.1a). As justified in Sec. 10.4, we assume $G_s(e^{j\omega})$ to be continuous, $G_s(e^{j0}) = 1$, and $\Phi(0) \neq 0$. Note that $G_s(e^{j0}) = 1$ is necessary for the infinite product to converge (because convergence of $\prod_k a_k$ implies that $a_k \to 1$; apply this for $\omega = 0$). The following convergence result is fundamental.

Theorem 11.2. Convergence of the infinite product. Let $G_s(e^{j\omega}) = \sum_{n=-\infty}^{\infty} g_s(n)e^{-j\omega n}$. Assume that $G_s(e^{j0}) = 1$, and $\sum_n |ng_s(n)| < \infty$. Then

1. The infinite product (11.1a) converges pointwise for all ω. In fact it converges absolutely for all ω, and uniformly on compact sets (i.e., closed bounded sets, e.g., sets of the form $[\omega_1, \omega_2]$).
2. The quantity $G_s(e^{j\omega})$, as well as the limit $\Phi(\omega)$ of the infinite product (11.1a) are continuous functions of ω.
3. $G_s(e^{j\omega})$ is in L^2. ◇

Since the condition $\sum_n |ng_s(n)| < \infty$ implies $\sum_n |g_s(n)| < \infty$, the filter $G_s(e^{j\omega})$ is restricted to be stable. But the above result holds whether $g_s(n)$ is FIR or IIR.

Sketch of proof. Theorem 11.1 allows us to reduce the convergence of the product to the convergence of an infinite sum. For this we have to write $G_s(e^{j\omega})$ in the form $1 - F(e^{j\omega})$ and then consider the summation $\sum_{k=1}^{\infty} |F(e^{j\omega/2^k})|$. Since $G_s(e^{j0}) = 1 = \sum_n g_s(n)$, we can write $G_s(e^{j\omega}) = 1 - (1 - G_s(e^{j\omega})) = 1 - \sum_n g_s(n)(1 - e^{-j\omega n})$. But $|\sum_n g_s(n)(1 - e^{-j\omega n})| \leq 2\sum_n |g_s(n)\sin(\omega n/2)| \leq |\omega| \sum_n |ng_s(n)|$ (use $|\sin x/x| \leq 1$). Since $\sum_n |ng_s(n)|$ is assumed to converge, we have $|\sum_n g_s(n)(1 - e^{-j\omega n})| \leq c|\omega|$. Using this, and the fact that $\sum_{k=1}^{\infty} 2^{-k}$ converges, we can complete the proof of part 1 (apply Theorem 11.1). Since $\sum_n |ng_s(n)| < \infty$ implies in particular that $g_s(n) \in \ell^1$, its ℓ^1-FT $G_s(e^{j\omega})$ is continuous (Sec. 6.3). The continuity of $G_s(e^{j\omega})$ together with uniform convergence of the infinite product implies that the pointwise limit $\Phi(\omega)$ is also continuous. Finally, since $\ell^1 \subset \ell^2$ (Sec. 6.2), we have $g_s(n) \in \ell^2$, that is, $G_s(e^{j\omega}) \in L^2[0, 2\pi]$ as well. ▽▽▽

11.3. Orthonormal Wavelet Basis From Paraunitary Filter Bank

We now consider the behavior of the infinite product $\prod_{k=1}^{\infty} G_s(e^{j\omega/2^k})$ when $G_s(e^{j\omega})$ comes from a paraunitary filter bank. The paraunitary property implies that $G_s(e^{j\omega})$ is power symmetric. If we impose some further mild conditions on $G_s(e^{j\omega})$ then the scaling function $\phi(t)$ generates an orthonormal multiresolution basis $\{\phi(t - n)\}$. We can then obtain an orthonormal wavelet basis $\{\psi_{kn}(t)\}$ (Theorems 10.1, 10.2). The

main results will be given in theorems 11.3–11.6 and 12.1.

First let us define the truncated partial products $P_n(\omega)$. Since $G_s(e^{j\omega})$ has period 2π, the term $G_s(e^{j\omega/2^k})$ has period $2^{k+1}\pi$. For this reason the partial product $\prod_{k=1}^{n} G_s(e^{j\omega/2^k})$ has period $2^{n+1}\pi$, and we can regard the region $[-2^n\pi, 2^n\pi]$ to be the fundamental period. Let us truncate the partial product to this region, and define

$$P_n(\omega) = \begin{cases} \prod_{k=1}^{n} G_s(e^{j\omega/2^k}), & \text{for } -2^n\pi \le \omega \le 2^n\pi \\ 0 & \text{otherwise.} \end{cases} \tag{11.2}$$

This quantity will be useful later. We will see that this is in $L^2(R)$, and we can talk about $p_n(t)$, its inverse L^2-FT.

Theorem 11.3. Let $G_s(e^{j\omega})$ be as in Theorem 11.2. In addition let it be power symmetric, that is $|G_s(e^{j\omega})|^2 + |G_s(-e^{j\omega})|^2 = 1$. (Notice in particular that this implies $G_s(e^{j\pi}) = 0$, since $G_s(e^{j0}) = 1$). Then the following are true.

1. $\int_0^{2\pi} |G_s(e^{j\omega})|^2 d\omega/2\pi = 0.5$.
2. The truncated partial product $P_n(\omega)$ is in L^2, and $\int_{-\infty}^{\infty} |P_n(\omega)|^2 d\omega/2\pi = 1$ for all n. Morover the inverse L^2-FT, denoted as $p_n(t)$, gives rise to an orthonormal sequence $\{p_n(t-k)\}$, that is $\langle p_n(t-k), p_n(t-i)\rangle = \delta(k-i)$ for any $n \ge 1$.
3. The limit $\Phi(\omega)$ of the infinite product (11.1a) is in L^2, hence it has an inverse L^2-FT, $\phi(t) \in L^2$. Moreover $\|\phi(t)\|_2 \le 1$. ◇

Sketch of proof. Part 1 follows by integrating both sides of $|G_s(e^{j\omega})|^2 + |G_s(-e^{j\omega})|^2 = 1$. The integral in part 2 is $\int_0^{2^{n+1}\pi} \prod_{k=1}^{n} |G_s(e^{j\omega/2^k})|^2 d\omega/2\pi$ which we can split into two terms like $\int_0^{2^n\pi} + \int_{2^n\pi}^{2^{n+1}\pi}$. Using the 2π-periodicity and the power symmetric property of $G_s(e^{j\omega})$, we obtain $\int |P_n|^2 d\omega = \int |P_{n-1}|^2 d\omega$. Repeated application of this, used together with part 1, yields $\int_{-\infty}^{\infty} |P_n(\omega)|^2 d\omega/2\pi = 1$. The proof of orthonormality of $\{p_n(t-k)\}$ follows essentially in a similar way by working with the modified integral $\int_{-\infty}^{\infty} |P_n(\omega)|^2 e^{j\omega(k-i)} d\omega/2\pi$, and using the half-band property of $|G_s(e^{j\omega})|^2$.

The third part is the most subtle one, and uses Fatou's Lemma for Lebesgue integrals (Sec. 6.1). For this, define $g_n(\omega) = |P_n(\omega)|^2$. Then $\{g_n(\omega)\}$ is a sequence of nonnegative integrable functions such that $g_n(\omega) \to |\Phi(\omega)|^2$ pointwise for each ω. Moreover, since $\int g_n(\omega) d\omega = 2\pi$ (from part 2), Fatou's lemma assures us that $|\Phi(\omega)|^2$ is integrable with integral $\le 2\pi$. This proves part 3. ▽▽▽

It is most interesting that the truncated partial products $P_n(\omega)$ give rise to orthonormal sequences $\{p_n(t-k)\}$. This orthonormality is induced by the paraunitary property, more precisely the power symmetry property of $G_s(e^{j\omega})$. This is consistent with the fact that the filter-bank type of basis introduced in Sec. 4.8 for the discrete time functions $x(n) \in \ell^2$ is an orthonormal basis for ℓ^2 whenever the filter bank is

paraunitary.

Since the scaling function $\Phi(\omega)$ is the pointwise limit of $\{P_n(\omega)\}$ as $n \to \infty$, this leads to the hope that $\{\phi(t-k)\}$ is also an orthonormal sequence (so that we can generate a multiresolution and then a wavelet basis as in Theorems 10.1,10.2). This however is not always true!

The crux of the reason is that $\Phi(\omega)$ is only the pointwise limit of $\{P_n(\omega)\}$, and not necessarily the L^2 limit! The distinction is subtle (see below). The pointwise limit property means that, for any fixed ω, the function $P_n(\omega)$ approaches $\Phi(\omega)$. The L^2 limit property means that $\int |P_n(\omega) - \Phi(\omega)|^2 d\omega \to 0$. Neither of these limit properties implies the other, that is neither is stronger than the other. It can be shown that it is the L^2 limit which propagates the orthonormality property, and this is what we want.

Theorem 11.4. Let $\{p_n(t-k)\}$ be an orthonormal sequence for each n, that is, $\langle p_n(t-k), p_n(t-i)\rangle = \delta(k-i)$. Suppose $p_n(t) \to \phi(t)$ in the L^2 sense. Then $\{\phi(t-k)\}$ is an orthonormal sequence. ◇

Proof. If we take limits as $n \to \infty$, we can write

$$\lim_{n\to\infty} \langle p_n(t-k), p_n(t-i)\rangle = \langle \lim_{n\to\infty} p_n(t-k), \lim_{n\to\infty} p_n(t-i)\rangle \tag{11.3}$$

This movement of the "limit" sign past the inner product sign is allowed (by continuity of inner products, Sec. 6.2) provided the limits in the second expression are L^2 limits. By the conditions of the theorem, the left side of the above equation is $\delta(k-i)$ whereas the right side is $\langle \phi(t-k), \phi(t-i)\rangle$. So the result follows.

▽▽▽

L^2 Convergence Versus Pointwise Convergence.

The fact that L^2 limits are not necessarily pointwise limits is obvious from the fact that differences at a countable set of points do not affect integrals. The fact that pointwise limits are not necessarily L^2 limits is demonstrated by the sequence of L^2 functions $\{f_n(t)\}$, with $f_n(t)$ as in Fig. 11.1.

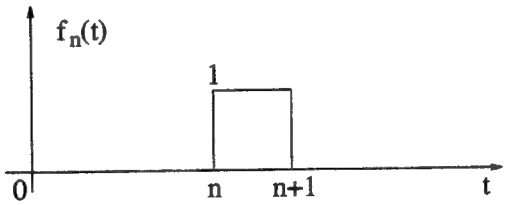

Fig. 11.1. A sequence $\{f_n(t)\}$ whose pointwise limit is not a limit in the L^2-sense.

Note that $f_n(t) \to 0$ pointwise for each t, that is, the pointwise limit is $f(t) \equiv 0$. So $\|f_n(t) - f(t)\| = \|f_n(t)\| = 1$ for all n, hence $\|f_n(t) - f(t)\|$ does not go to zero as $n \to \infty$. Thus $f(t)$ is not the L^2 limit of $f_n(t)$. Notice in this example that $1 = \lim_{n\to\infty} \int |f_n(t)|^2 dt \neq \int \lim_{n\to\infty} |f_n(t)|^2 dt = 0$. This is consistent

with the fact that Lebesgue dominated convergence theorem cannot be applied here – there is no integrable function that dominates $|f_n(t)|^2$ for all n. In this example, the sequence $\{f_n(t)\}$ does not converge in the L^2 sense (in fact $\|f_n(t) - f_m(t)\|^2 = 2$ for $n \neq m$. So $\{f_n\}$ is not a Cauchy sequence in L^2).

Some facts pertaining to pointwise and L^2 convergences: It can be shown that if $f_n(t) \to f(t)$ in L^2 sense and $f_n(t) \to g(t) \in L^2$ pointwise as well, then $f(t) = g(t)$ a.e. In particular $\|f(t) - g(t)\| = 0$ and $\|f(t)\| = \|g(t)\|$. It can also be shown that if $f_n(t) \to f(t)$ in L^2 sense, then $\|f_n(t)\| \to \|f(t)\|$. Finally if $f_n(t) \to f(t) \in L^2$ pointwise a.e., and $\|f_n(t)\| \to \|f(t)\|$ then $f_n(t) \to f(t)$ in L^2 sense as well [Rudin, 1966].

Theorem 11.5. Orthonormal wavelet basis. Let the filter $G_s(e^{j\omega}) = \sum_{n=-\infty}^{\infty} g_s(n)e^{-j\omega n}$ satisfy the following properties.

1. $G_s(e^{j0}) = 1$,
2. $\sum_n |ng_s(n)| < \infty$,
3. $|G_s(e^{j\omega})|^2 + |G_s(-e^{j\omega})|^2 = 1$ (power-symmetry), and
4. $G_s(e^{j\omega}) \neq 0$ for $\omega \in [-0.5\pi, 0.5\pi]$.

Then the infinite product (11.1a) converges to a limit $\Phi(\omega) \in L^2$, and its inverse FT $\phi(t)$ is such that $\{\phi(t-n)\}$ is an orthonormal sequence. Defining the wavelet function $\psi(t)$ as usual, i.e., as in (10.10), the sequence $\{2^{k/2}\psi(2^k t - n)\}$ (with k and n varying over all integers) forms an orthonormal wavelet basis for L^2. ◇

Sketch of proof. We will show that the sequence $\{P_n(\omega)\}$ of partial products converges to $\Phi(\omega)$ in the L^2 sense, that is $\int |P_n(\omega) - \Phi(\omega)|^2 d\omega \to 0$, so that $p_n(t) \to \phi(t)$ in L^2 sense. The desired result then follows in view of Theorems 11.3 and 11.4. The key tool in the proof is the dominated convergence theorem for Lebesgue integrals (Sec. 6.1). First, the condition $G(e^{j\omega}) \neq 0$ in $[-0.5\pi, 0.5\pi]$ implies that $\Phi(\omega) \neq 0$ in $[-\pi, \pi]$. Since $|\Phi(\omega)|^2$ is continuous (Theorem 11.2) it has a minimum value $c^2 > 0$ in $[-\pi, \pi]$. Now the truncated partial product $P_n(\omega)$ can always be written as $P_n(\omega) = \Phi(\omega)/\Phi(\omega/2^n)$ in its region of support. Since $|\Phi(\omega/2^n)|^2 \geq c^2$ in $[-2^n\pi, 2^n\pi]$, we have $|P_n(\omega)|^2 \leq |\Phi(\omega)|^2/c^2$ for all ω. Define $Q_n(\omega) = |P_n(\omega) - \Phi(\omega)|^2$. Then using $|P_n(\omega)|^2 \leq |\Phi(\omega)|^2/c^2$ we can show that $Q_n(\omega) \leq \alpha|\Phi(\omega)|^2$ for some constant α. Since the right hand side is integrable, and since $Q_n(\omega) \to 0$ pointwise (Theorem 11.2) we can use the dominated convergence theorem (Sec. 6.1) to conclude that $\lim_n \int Q_n(\omega)\, d\omega = \int \lim_n Q_n(\omega)\, d\omega = 0$. This completes the proof. ▽▽▽

Computing the Scaling and Wavelet Functions

Given the coefficients $g_s(n)$ of the filter $G_s(e^{j\omega})$, how do we compute the scaling function $\phi(t)$ and the wavelet function $\psi(t)$? Since we can compute $\psi(t)$ using $\psi(t) = 2\sum_{n=-\infty}^{\infty}(-1)^{n+1}g_s^*(-n-1)\phi(2t-n)$, the key

issue is the computation of $\phi(t)$. In the preceding theorems, $\phi(t)$ was defined only as an inverse L^2 FT of the infinite product $\Phi(\omega)$ given in (11.1a). Since an L^2 function is determined only in the a.e. sense, this way of defining $\phi(t)$ itself does not fully determine $\phi(t)$. Recall however, that the infinite product for $\Phi(\omega)$ was only a consequence of the more fundamental equation, namely the dilation equation $\phi(t) = 2\sum_{n=-\infty}^{\infty} g_s(n)\phi(2t-n)$. In practice, $\phi(t)$ is computed using this equation (which is often a finite sum, see Sec. 12). The procedure is recursive, that is we assume an initial solution for the function $\phi(t)$, substitute it into the right hand side of the dilation equation, thereby recompute $\phi(t)$, and then repeat the process. Details of this, and discussions on convergence of this procedure can be found in [Daubechies, 1992], [Chui, 1992a], [Daubechies and Lagarias, 1991], and [Rioul, 1991].

Eigenfunction Condition for Orthonormality [Lawton, 1990]

Recall that Eq. (10.17) is equivalent to the orthonormality of $\{\phi(t-n)\}$. Let $S(e^{j\omega})$ denote the left hand side of (10.17), which evidently has period 2π in ω. Using the frequency domain version of the dilation equation (10.2), it can be shown that the scaling function $\phi(t)$ generated from $G_s(e^{j\omega})$ is such that

$$|G_s(e^{j\omega})|^2 S(e^{j\omega})\Big|_{\downarrow 2} = 0.5S(e^{j\omega}) \tag{11.4}$$

where the notation $\downarrow 2$ indicates decimation (Sec. 4.1). Thus the function $S(e^{j\omega})$ can be regarded as an eigenfunction (with eigenvalue = 0.5) of the operator $\mathcal{F}$ which performs filtering by $|G_s(e^{j\omega})|^2$ followed by decimation.

Now consider the case where the digital filter bank is paraunitary, so that $G_s(e^{j\omega})$ is power symmetric, that is satisfies (10.12). The power symmetric condition can be rewritten in the form $|G_s(e^{j\omega})|^2\Big|_{\downarrow 2} = 0.5$. Thus in the power symmetric case, the identity function is an eigenfunction of the operator $\mathcal{F}$. If the only eigenfunction of the operator $\mathcal{F}$ is the identity function, it then follows that $S(e^{j\omega}) = 1$, that is (10.17) holds and $\{\phi(t-n)\}$ is orthonororrmal.

The FIR case. In Sec. 12 we will see that restricting $G_s(z)$ to be FIR ensures that $\phi(t)$ has finite duration. For the FIR case, Lawton and Cohen independently showed that the above eigenfunction condition also works in the other direction. That is, if $\{\phi(t-n)\}$ has to be orthonororrmal, then the trignometric polynomial $S(e^{j\omega})$ satisfying (11.4) has to be unique up to a scale factor.† Details can be found in [Daubechies, 1992].

† A finite sum of the form $\sum_{n=N_1}^{N_2} p_n e^{j\omega n}$ is said to be a trignometric polynomial. If $G_s(e^{j\omega})$ is FIR, it can be show that the left hand side of (10.17) is not only periodic in ω, but is in fact a trignometric polynomial.

Examples and Counter Examples

We already indicated after the introduction of Eq. (11.1), that the example of the ideal bandpass wavelet can be generated formally by starting from the ideal brickwall paraunitary filter bank. We now discuss some other examples.

Example 11.1. Haar basis from filter banks. A filter bank of the form Fig. 4.1(a) with filters

$$G_a(z) = \frac{1+z^{-1}}{2},\ H_a(z) = \frac{z^{-1}-1}{2},\quad G_s(z) = \frac{1+z^{-1}}{2},\ H_s(z) = \frac{1-z^{-1}}{2},$$

is paraunitary. The magnitude responses of the synthesis filters, $|G_s(e^{j\omega})| = |\cos(\omega/2)|$ and $|H_s(e^{j\omega})| = |\sin(\omega/2)|$ are shown in Fig. 11.2(a). $G_s(z)$ satisfies all the conditions of Theorem 11.5. In this case we can evaluate the infinite products for $\Phi(\omega)$ and $\Psi(\omega)$ explicitly by using the identity $\prod_{m=1}^{\infty} \cos(2^{-m}\omega) = \sin\omega/\omega$. The resulting $\phi(t)$ and $\psi(t)$ are as shown in Fig. 11.2 (b) and (c). These are precisely the functions that generate the Haar orthonormal basis. ♢

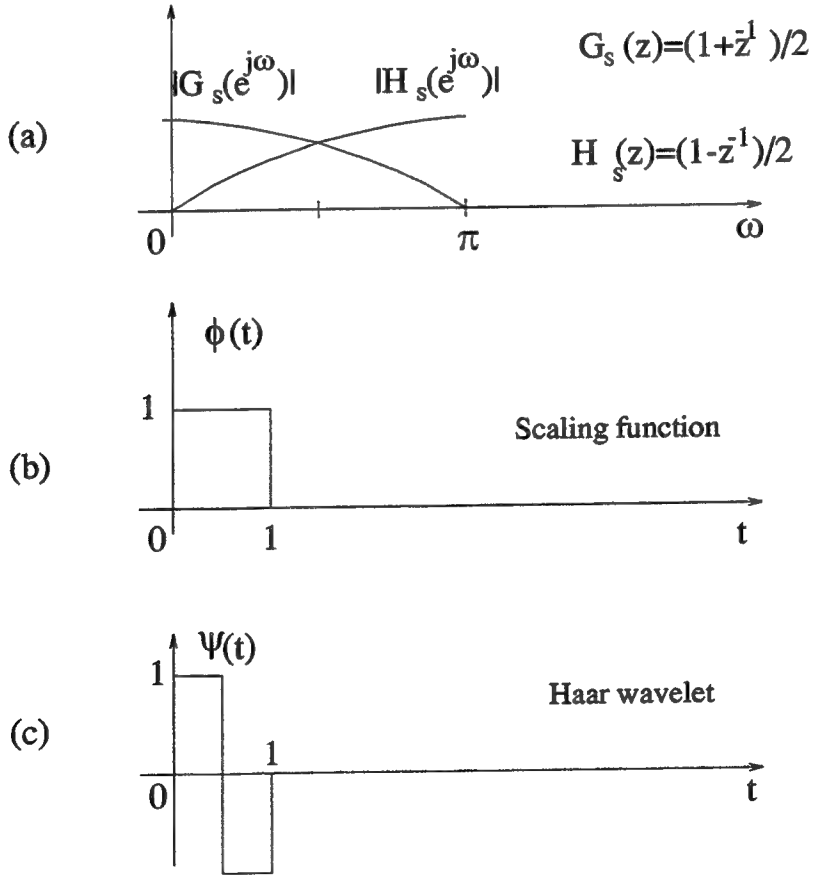

Fig. 11.2. Haar basis generated from paraunitary filter bank.

(a) The synthesis filters in the paraunitary filter bank,

(b) the scaling function and (c) the wavelet function generated using dilation equation.

Example. 11.2. Paraunitary filter bank which does not give orthonormal wavelets. Consider the filter bank with analysis filters $G_a(z) = (1 + z^{-3})/2$, $H_a(z) = -(1 - z^{-3})/2$, and synthesis filters $G_s(z) = (1 + z^{-3})/2$, $H_s(z) = (1 - z^{-3})/2$. Since this is obtained from the preceding example by the substitution $z \to z^3$, it remains paraunitary and satisfies the perfect reconstruction property. $G_s(z)$ satisfies all the properties of Theorem 11.5, except the fourth condition. With $\phi(t)$ and $\psi(t)$ obtained from $G_s(e^{j\omega})$ using the usual dilation equations, the functions $\{\phi(t - n)\}$ are *not orthonormal.* Moreover the wavelet functions $\{2^{k/2}\psi(2^k t - n)\}$ do not form an orthonormal basis either. These statements can be verified from the sketches of the functions $\phi(t)$ and $\psi(t)$ shown in Fig. 11.3. Clearly $\phi(t)$ and $\phi(t-1)$ are not orthogonal, and $\psi(t)$ and $\psi(t-2)$ are not orthogonal. In this example, $\|P_n(\omega)\| = 1$ for all n whereas $\|\Phi(\omega)\| = 1/\sqrt{3}$. Since the limit of $\|P_n(\omega)\|$ does not agree with $\|\Phi(\omega)\|$, we conclude that $\Phi(\omega)$ is not the L^2 limit of $P_n(\omega)$. The L_2 limit of $P_n(\omega)$ does not exist in this example. ◇

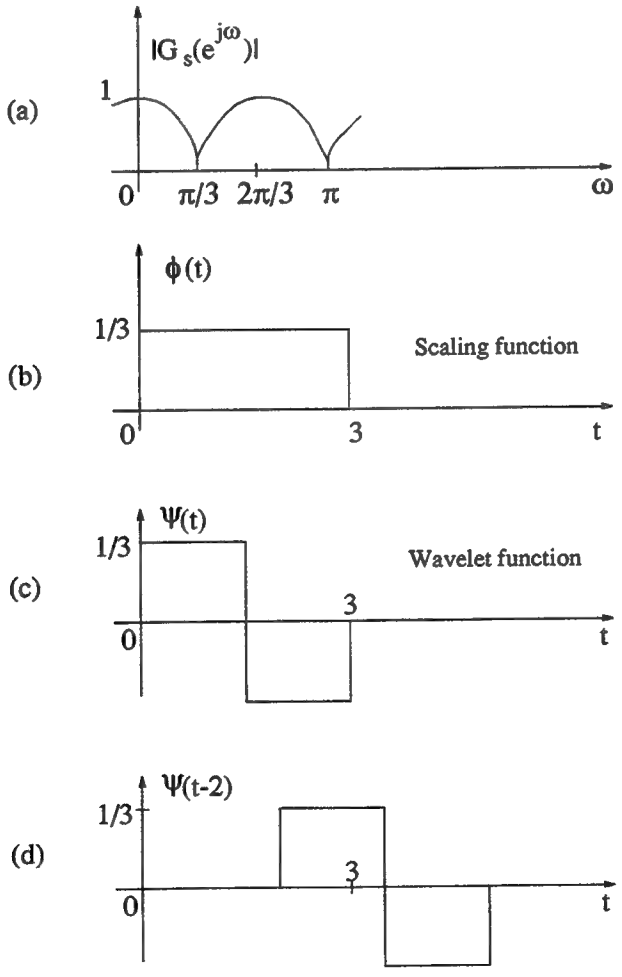

Fig. 11.3. Example 11.2. A paraunitary filter bank generating nonorthonormal $\{\phi(t - n)\}$
(a) The synthesis filter response, (b) the scaling function, (c) the wavelet function, and (d) a shifted version.

Thus, a paraunitary filter bank may not generate an orthonormal wavelet basis if the fourth condition in Theorem 11.5 is violated. However this is hardly of concern in practice, since any reasonable lowpass filter designed for a two channel filter bank will be free from zeros in the region $[-0.5\pi, 0.5\pi]$! In fact a stronger result has been proved by Cohen who derived necessary and sufficient conditions for an FIR paraunitary filter bank to generate an orthonormal wavelet basis. One outcome of Cohen's analysis is that the fourth condition in Theorem 11.4 can be replaced by the even milder condition that $G_s(e^{j\omega})$ be not zero in $[-\frac{\pi}{3}, \frac{\pi}{3}]$. In this sense the condition for obtaining an orthonormal wavelet basis is trivially satisfied in practice. The case where the fourth condition fails is primarily of theoretical interest; a very cute result in this context is Lawton's tight frame theorem presented next.

11.4. Wavelet Tight Frames

Even though the wavelet functions $\{2^{k/2}\psi(2^k t - n)\}$ generated from a paraunitary filter bank may not form an orthonormal basis (when the fourth condition of Theorem 11.5 is violated), they always form a tight frame for L^2. Thus any L^2 function can still be expressed as an infinite linear combination of the functions $\{2^{k/2}\psi(2^k t - n)\}$. More precisely we have the following result [Lawton, 1990].

Theorem 11.6. Tight frames from paraunitary filter banks. Let $G_s(e^{j\omega}) = \sum_{n=0}^{N} g_s(n)e^{-j\omega n}$ be a filter satisfying the following properties.

1. $G_s(e^{j0}) = 1$, and
2. $|G_s(e^{j\omega})|^2 + |G_s(-e^{j\omega})|^2 = 1$ (power-symmetry).

Then $\phi(t) \in L^2$. Defining the wavelet function $\psi(t)$ as usual, i.e., as in (10.10), the sequence $\{2^{k/2}\psi(2^k t - n)\}$ (with k and n varying over all integers) forms a tight frame for L^2, with frame bound unity (i.e., $A = B = 1$, see Sec. 8). ◇

Thus, the functions $\psi_{kn}(t)$ in Example 11.2 constitute a tight frame for L^2. From Sec. 8.3 we know that this tight frame property means that any $x(t) \in L^2$ can be expressed as

$$x(t) = \sum_{k=-\infty}^{\infty} \sum_{n=-\infty}^{\infty} \langle x(t), \psi_{kn}(t) \rangle \, \psi_{kn}(t), \tag{11.5}$$

where $\psi_{kn}(t) = 2^{k/2}\psi(2^k t - n)$. This expression is pretty much like an expansion into an orthonormal basis. We can find the wavelet coefficients $c_{kn} = \langle x(t), \psi_{kn}(t) \rangle$ exactly as in the orthonormal case. We also know that frames offer stability of reconstruction (Sec. 8.1). Thus, in every respect this resembles an orthonormal basis, with the only difference that the functions are not linearly independent. That is, there is redundancy in the wavelet tight frame $\{\psi_{kn}(t)\}$.

12. COMPACTLY SUPPORTED ORTHONORMAL WAVELETS

In Sec. 11 we showed how to construct an orthonormal wavelet basis for L^2 space by starting from a paraunitary filter bank. Essentially we defined two infinite products $\Phi(\omega)$ and $\Psi(\omega)$ starting from the digital lowpass filter $G_s(e^{j\omega})$. Under some mild conditions on $G_s(e^{j\omega})$, the products converge (Theorem 11.2). Under the further condition that $G_s(e^{j\omega})$ be power symmetric and nonzero in $[-0.5\pi, 0.5\pi]$ we saw that $\{\phi(t-k)\}$ forms an orthonormal set, and the corresponding $\{2^{k/2}\psi(2^k t - n)\}$ forms an orthonormal wavelet basis for L^2 (Theorem 11.5). We will now see that if we further constrain $G_s(e^{j\omega})$ to be FIR, that is $G_s(z) = \sum_{n=0}^{N} g_s(n) z^{-n}$, then the scaling function $\phi(t)$ and the wavelet function $\psi(t)$ have finite duration [Daubechies, 1988, 1992].

Theorem 12.1. Let $G_s(z) = \sum_{n=0}^{N} g_s(n) z^{-n}$, with $G_s(e^{j0}) = 1$ and $H_s(e^{j\omega}) = e^{j\omega} G_s^*(-e^{j\omega})$. Define the infinite products as in (11.1a),(11.1b), and assume that the limits $\Phi(\omega)$ and $\Psi(\omega)$ are L^2 functions (for example, by imposing power symmetry condition on $G_s(z)$ as in Theorem 11.3). Then $\phi(t)$ and $\psi(t)$ (the inverse L^2 FTs) are compactly supported, with support in $[0, N]$. ◇

The time-decay of the wavelet $\psi(t)$ is therefore excellent. In particular, all the basis functions $2^{k/2}\psi(2^k t - n)$ are compactly supported. By further restricting the lowpass filter $G_s(z)$ to have sufficient number of zeros at $\omega = \pi$, we will also ensure (Sec. 13) that the Fourier transform $\Psi(\omega)$ has excellent decay (equivalently $\psi(t)$ is regular or smooth in the sense to be quantified in Sec. 13).

The rest of this section is devoted to the technical details of the above result. The reader not interested in these details can skip to Sec. 13 without loss of continuity. The Theorem might seem "obvious" at first sight, and indeed a simple engineering argument based on Dirac delta functions can be given (p. 521 [Vaidyanathan, 1993]). However the correct mathematical justification relies on a number of deep results in function theory. One of these is the celebrated Paley-Wiener theorem for bandlimited functions.

The Paley-Wiener Theorem

A beautiful result in the theory of signals is that if an L^2 function $f(t)$ is bandlimited, that is $F(\omega) = 0, |\omega| \geq \sigma$, then $f(t)$ is the "real-axis restriction of an entire function." Let us first explain the meaning of this phrase. We say that a function $f(s)$ of the complex variable s is *entire* if it is analytic for all s. Examples are polynomials in s, exponentials such as e^s, and simple combinations of these. The function $f(t)$ obtained from $f(s)$ for real values of s ($s = t$) is the real-axis restriction of $f(s)$.

Thus if $f(t)$ is a bandlimited signal then there exists an entire function $f(s)$ such that its real axis restriction is $f(t)$. In particular, therefore a bandlimited function $f(t)$ is continuous and infinitely differentiable with respect to the time variable t. The entire function $f(s)$ associated with the bandlimited function

has the further property $|f(s)| \leq ce^{\sigma|s|}$ for some $c > 0$. We express this by saying that $f(s)$ is *exponentially bounded* or of the exponential type. What is even more interesting is that the converse of this result is true, that is, if $f(s)$ is an entire function of the exponential type, and the real axis restriction $f(t)$ is in L^2, then $f(t)$ is bandlimited. By interchanging the time and frequency variables we can obtain similar conclusions for time-limited signals; this is what we need in the discussion of time limited (compactly supported) wavelets.

Theorem 12.2 (Paley-Wiener). Let $W(s)$ be an entire function such that (a) for all s, we have $|W(s)| \leq c\exp(A|s|)$ for some $c, A > 0$, and (b) the real axis restriction $W(\omega)$ is in L^2. Then there exists a function $w(t)$ in L^2 such that $W(s) = \int_{-A}^{A} w(t)e^{-jts}dt$. ◇

A proof can be found in [Rudin, 1966]. Thus $w(t)$ can be regarded as a compactly supported function with support in $[-A, A]$. Recall [Eq. (6.1)] that $L^2[-A, A] \subset L^1[-A, A]$, so $w(t)$ is in $L^1[-A, A]$ *and* $L^2[-A, A]$. So $W(\omega)$ is the L^1-FT of $w(t)$, and agrees with the L^2-FT a.e.

Our aim is to show that the infinite product for $\Phi(\omega)$ satisfies the conditions of the Paley-Wiener theorem, and therefore that $\phi(t)$ is compactly supported. A modified version of the above result is more convenient for this. The modification allows the support to be more general, namely $[-A_1, A_2]$, and permits us to work with the imaginary part of s rather than the absolute value.

Theorem 12.3 (Paley-Wiener, modified). Let $W(s)$ be an entire function such that

$$|W(s)| \leq \begin{cases} c_1 \exp\Big(A_1|\text{Im } s|\Big), & \text{Im } s \geq 0 \\ c_2 \exp\Big(A_2|\text{Im } s|\Big), & \text{Im } s \leq 0 \end{cases} \tag{12.1}$$

for some $c_1, c_2, A_1, A_2 > 0$, and such that the real axis restriction $W(\omega)$ is in L^2. Then there exists a function $w(t)$ in L^2 such that $W(s) = \int_{-A_2}^{A_1} w(t)e^{-jts}dt$. We can regard $W(\omega)$ as the Fourier transform of the function $w(t)$ supported in $[-A_2, A_1]$. ◇

This result can be made more general; the condition (12.1) can be replaced with one where the right hand sides have the form $P_i(s)\exp(A_i|\text{Im } s|)$ where $P_i(s)$ are polynomials. We are now ready to sketch the proof that $\phi(t)$ and $\psi(t)$ have the compact support $[0, N]$.

1. Using the fact that $G_s(z)$ is FIR and that $G_s(e^{j0}) = 1$, show that the product $\prod_{k=1}^{\infty} G_s(e^{js/2^k})$ converges uniformly on any compact set of the complex s-plane. (For real s, namely $s = \omega$ this holds even for the IIR case as long as $\sum_n |ng_s(n)|$ converges. This was shown in Theorem 11.2.)
2. Uniformity of convergence of the product guarantees that its limit $\Phi(s)$ is an entire function of the complex variable s (Theorem 10.28, [Rudin, 1966]).
3. The FIR nature of $G_s(z)$ allows us to establish the exponential bound (12.1) for $\Phi(s)$ with $A_2 = 0$ and $A_1 = N$. This shows that $\phi(t)$ is compactly supported in $[0, N]$. Since $\psi(t)$ is obtained from the dilation equation (10.10), the same result follows for $\psi(t)$ as well.

13. WAVELET REGULARITY

From the preceding section we know that if we construct the power-symmetric FIR filter $G_s(z)$ properly, then we can get an orthonormal multiresolution basis $\{\phi(t-n)\}$, and an orthonormal wavelet basis $\{2^{k/2}\psi(2^k t-n)\}$ for the L^2. Both of these bases are compactly supported. These are solutions to the two-scale dilation equations

$$\phi(t) = 2\sum_{n=0}^{N} g_s(n)\phi(2t-n), \tag{13.1}$$

$$\psi(t) = 2\sum_{n=0}^{N} h_s(n)\phi(2t-n), \tag{13.2}$$

where $h_s(n) = (-1)^{n+1}g_s^*(-n-1)$. In the frequency domain we have the explicit infinite product expressions (11.1) connecting the filters $G_s(z)$ and $H_s(z)$ to the L^2 Fourier transforms $\Phi(\omega)$ and $\Psi(\omega)$.

Fig. 13.1(a) shows two cases of a 9th order FIR filter $G_s(e^{j\omega})$ used to generate the compactly supported wavelet. The resulting wavelets are shown in Figs. 13.1(b) and (c). In both cases, all conditions of Theorem 11.5 are satisfied so we obtain orthonormal wavelet bases for L^2. The filter $G_s(e^{j\omega})$ has more zeros at π for Case 2 than for Case 1. The corresponding wavelet looks much smoother or "regular" — this is an example of a Daubechies wavelet (Sec. 13.4). It turns out that, by designing $G_s(z)$ to have a sufficient number of zeros at π we can make the wavelet "as regular as we please." A quantitative discussion of the connection between the number of zeros at π and the smoothness of $\psi(t)$ will be given in the following sections.

Qualitatively, the idea is this. If $G_s(e^{j\omega})$ has a large number of zeros at π, then the function $\Phi(\omega)$ given by the infinite product (11.1a) decays "fast" as $\omega \to \infty$. This fast asymptotic decay in the frequency domain implies that the time function $\phi(t)$ is "smooth". And since $\psi(t)$ is derived from $\phi(t)$ using a finite sum (13.2), the smoothness of $\phi(t)$ is transmitted to $\psi(t)$. In the next few sections we will make the ideas more quantitative. References for this section include [Daubechies and Lagarias, 1991], [Daubechies, 1992] and [Rioul, 1992].

Why regularity?

The point made above was that if we design an FIR paraunitary filter bank with the additional constraint that the lowpass filter $G_s(e^{j\omega})$ have a sufficient number of zeros at π, the wavelet basis functions $\psi_{kn}(t)$ are sufficiently smooth. The smoothness requirement is perhaps the main new component brought into the filter bank theory from the wavelet theory. Its importance can be understood in a number of ways.

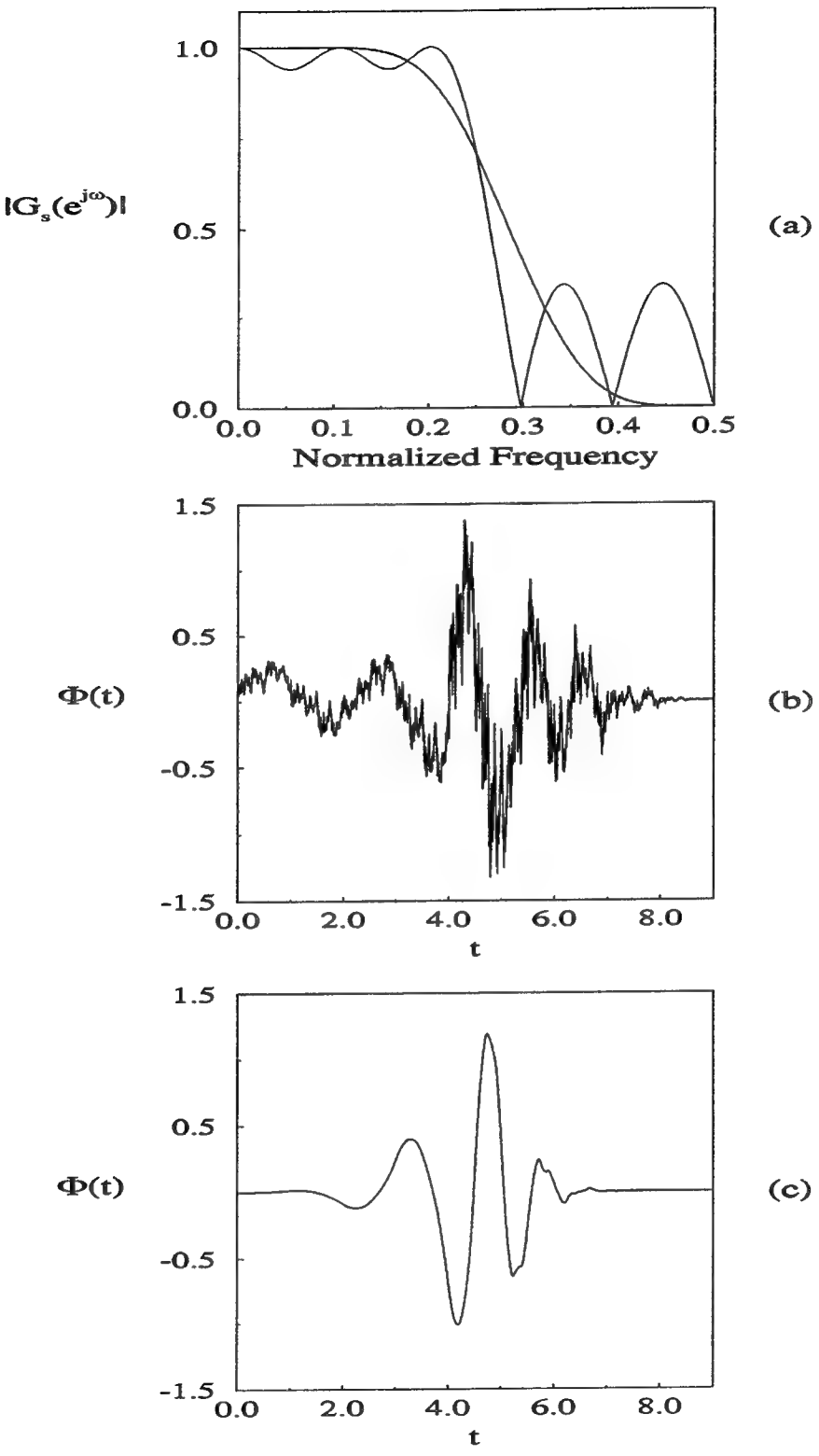

Fig. 13.1. Demonstrating the importance of zeros at π. (a) The response of the FIR filter $G_s(z)$ for two cases, and (b), (c) the corresponding wavelet functions.

Consider the expansion $x(t) = \sum_{k,n} c_{k,n}\psi_{kn}(t)$. Suppose we truncate this to a finite number of terms as is often done in practice. If the basis functions are not smooth, then the error can produce perceptually annoying effects in applications such as audio and image coding, even though the L^2 norm of the error might be small.

Consider next a tree structured filter bank. An example is shown in Fig. 4.6. In the synthesis bank, the first path can be regarded as an effective interpolation filter, that is, an expander (e.g., $\uparrow 8$ in Fig. 4.6) followed by a filter of the form $G_s(e^{j\omega})G_s(e^{2j\omega})G_s(e^{4j\omega})\ldots G_s(e^{2^L j\omega})$. This same finite product can be obtained by truncating to $L+1$ terms the infinite product defining $\Phi(\omega)$ [Eq. (11.1)], and making a change of variables. Similarly the remaining paths can be related to interpolation filters which are various truncated versions of the infinite product defining $\Psi(\omega)$ in Eq. (11.1). Imagine now that we use the tree structured system in subband coding. The quantization error in each subband is filtered through an interpolation filter. If the impulse response of the interpolation filter is not smooth enough (e.g., if it resembles Fig. 13.1(b)), then the filtered noise tends to show severe perceptual effects, for example in image reconstruction. This explains, qualitatively, the importance of having "smooth impulse responses" for the synthesis filters.

13.1. Smoothness and Hölder Regularity Index

We are familiar with the notion of continuous functions. We say that $f(t)$ is continuous at t_0 if, for any $\epsilon > 0$ we can find a $\delta > 0$ such that $|f(t) - f(t_0)| < \epsilon$ for all t satisfying $|t - t_0| < \delta$. A stronger type of continuity, called Hölder continuity, is defined as follows: $f(t)$ is Hölder continuous in a region $\mathcal{S}$ if $|f(t_0) - f(t_1)| \leq c|t_0 - t_1|^\beta$ for some $c, \beta > 0$, for all $t_0, t_1 \in \mathcal{S}$. This implies, in particular, continuity in the ordinary sense. If $\beta > 1$ the above would imply that $f(t)$ is constant on $\mathcal{S}$. For this reason, we have the restriction $0 < \beta \leq 1$. As β increases from 0 to 1, the function becomes "smoother and smoother". The constant β is called the *Lipschitz constant* of the function $f(t)$.

Suppose the function $f(t)$ is n times differentiable in some region $\mathcal{S}$ and the nth derivative $f^{(n)}(t)$ is Hölder continuous with Lipschitz constant β. Define $\alpha = n + \beta$. We say that $f(t)$ belongs to the class C^α. The coefficient α is called the *Hölder regularity index* of $f(t)$. For example, $C^{3.4}$ is the class of functions that are three times differentiable and the third derivatives are Hölder continuous with Lipschitz constant equal to 0.4.

The Hölder regularity index α is taken as a quantitative measure of regularity or smoothness of the function $\psi(t)$. We sometimes say $\psi(t)$ has regularity α. Qualitatively speaking, a function with a large Hölder index is regarded as more "smooth" or "well-behaved". Since the dilation equations in the FIR case are finite summations, the Hölder indices of $\phi(t)$ and $\psi(t)$ are identical.

There exist functions which are differentiable infinite number of times. That is, they belong to C^∞. Examples are e^t, $\sin t$, and polynomials. There even exist C^∞ functions that are compactly supported (i.e., have finite duration); however we will not have occassion to encounter these.

13.2. Frequency-Domain Decay and Time-Domain Smoothness

We can obtain time-domain smoothness of a certain degree by imposing certain conditions on the Fourier transform $\Psi(\omega)$. This is made possible by the fact that the rate of decay of $\Psi(\omega)$ as $\omega \to \infty$ (i.e., the asymptotic decay) governs the Hölder regularity index α of $\psi(t)$. Suppose $\Psi(\omega)$ decays faster than $(1 + |\omega|)^{-(1+\alpha)}$. That is,

$$|\Psi(\omega)| \leq \frac{c}{(1+|\omega|)^{1+\alpha+\epsilon}} \qquad \text{for all } \omega, \tag{13.3}$$

for some $c > 0, \epsilon > 0$. Then $\Psi(\omega)(1 + |\omega|)^\alpha$ is bounded by the integrable function $c/(1 + |\omega|)^{1+\epsilon}$, and is therefore (Lebesgue) integrable. It can be shown using standard Fourier theory that this implies $\psi(t) \in C^\alpha$. In the wavelet construction of Sec. 11 which begins with a digital filter bank, the above decay of $\Psi(\omega)$ can be accomplished by designing the digital filter $G_s(e^{j\omega})$ such that it has a sufficient number of zeros at $\omega = \pi$ (Sec. 13.4).

Thus, the decay in the frequency domain translates into regularity in the time domain. Similarly one can regard time-domain decay as an indication of smoothness in frequency. When comparing two kinds of wavelets, we can usually compare them in terms of time domain regularity (frequency domain decay) and time domain decay (frequency domain smoothness). An extreme example is where $\psi(t)$ is bandlimited. This means that $\Psi(\omega)$ is zero outside the passband, and so the "decay" is the best possible. Correspondingly the smoothness of $\psi(t)$ is excellent; in fact $\psi(t) \in C^\infty$. However, the *decay* of $\psi(t)$ may not be excellent (certainly it cannot be time limited if it is band limited).

Return to the two familiar wavelet examples, namely the Haar wavelet (Fig. 2.12) and the bandpass wavelet (Figs. 2.9, 2.11). We see that the Haar wavelet has poor decay in the frequency domain since $\Psi(\omega)$ decays only as ω^{-1}. Correspondingly the time domain signal $\psi(t)$ is not even continuous, hence not differentiable.† The bandpass wavelet on the other hand is band limited (so the decay in frequency is excellent). Thus $\psi(t) \in C^\infty$, but it decays slowly, behaving like t^{-1} for large t. These two examples represent two extremes of orthonormal wavelet bases for L^2.

The game, therefore, is to construct wavelets that have good *decay in time* as well as good *regularity in time*. An extreme hope is where $\psi(t) \in C^\infty$ and has compact support as well. It can be shown that such

† It is true that $\psi(t)$ is differentiable almost everywhere. But the discontinuities at the points $t = 0, 0.5, 1.0$ will be very noticable if we take linear combinations like $\sum_{k,n} c_{kn}\psi_{kn}(t)$.

$\psi(t)$ can never give rise to an orthonormal basis (see Sec. 13.3 for more precise statement) so we have to strike a compromise between *regularity in time* and *decay in time.*

Regularity and Decay in Early Wavelet Constructions

In 1982 Stromberg showed how to construct wavelets such that $\psi(t)$ has exponential decay, and at the same time has arbitrary regularity (i.e., $\psi(t) \in C^k$ for any chosen integer k). In 1985 Meyer constructed wavelets with bandlimited $\psi(t)$ (so $\psi(t) \in C^\infty$ as for the bandpass wavelet), but he also showed how to design this $\psi(t)$ to decay faster than any chosen inverse polynomial, as $t \to \infty$. Figure 13.2(a) shows an example of a Meyer wavelet; a detailed description of this wavelet can be found in [Daubechies, 1992]. In both of the above constructions, the wavelets gave rise to orthonromal bases for L^2.

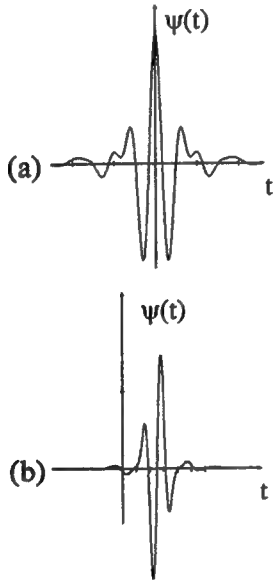

Fig. 13.2. (a) An example of the Meyer wavelet, and
(b) an example of the Battle-Lemarie wavelet.

In 1987 and 1988, Battle and Lemarié constructed, independently, wavelets with similar properties as Stromberg's wavelets, namely $\psi(t) \in C^k$ for arbitrary k, and $\psi(t)$ decays exponentially. Their construction is based on spline functions and an orthonormalization step, as described in Sec. 10.5. The resulting wavelets, while not compactly supported, decay exponentially and generate orthonormal bases. Fig. 13.2(b) shows an example of the Battle-Lemarié wavelet.

Table 13.1 gives a summary of the main features of these early wavelet constructions (first three entries). When these examples were constructed, the relation between wavelets and digital filter banks was not known. The constructions were not systematic, or unified by a central theory. Moreover it was not clear whether

one could get a compactly supported (i.e., finite-duration) wavelet $\psi(t)$ which at the same time has arbitrary regularity (i.e., $\psi(t) \in C^k$ for any chosen k), *and generates an orthonormal wavelet basis.* This was made possible for the first time when the relation between wavelets and digital filter banks was observed by Daubechies [1988]. Simultaneously and independently Mallat invented the multiresolution framework and observed the relation between his framework, wavelets, and paraunitary digital filter banks (the CQF bank, Sec. 4). These discoveries have made the wavelet construction easy and sytematic, as described earlier in Sec. 11–12. The way to obtain arbitrary wavelet regularity with this scheme is described next.

Type of wavelet	Decay of ψ (t) in time	Regularity of ψ(t) in time	Type of wavelet basis
Stromberg, 1982	Exponential	ψ(t) in C^k, k can be chosen arbitrarily large	Orthonormal
Meyer, 1985	Faster than any chosen inverse polynomial	ψ(t) in C^∞ (bandlimited)	Orthonormal
Battle-Lemarie, 1987, 88 (SPLINES)	Exponential	ψ(t) in C^k, k can be chosen arbitrarily large	Orthonormal
Daubechies, 1988	Compactly supported	ψ(t) in C^α, α can be chosen as large as we please	Orthonormal

Table 13.1. Summary of several types of wavelet bases for $L^2(\mathcal{R})$.

13.3. Time-Domain Decay and Time-Domain Regularity

We will now state a fundamental limitation which arises when trying to impose regularity and decay simultaneously [Daubechies, 1992].

Theorem 13.1. Vanishing Moments. Let $\{2^{k/2}\psi(2^k t - n)\}, -\infty \leq k, n \leq \infty$ be an orthonormal set in L^2. Suppose the wavelet $\psi(t)$ satisfies the following properties.

1. $|\psi(t)| \leq c(1+|t|)^{-(m+1+\epsilon)}$ for some integer m and some $\epsilon > 0$. That is, the wavelet decays faster than $(1+|t|)^{-(m+1)}$.

2. $\psi(t) \in C^m$ (i.e., $\psi(t)$ differentiable m times), and the m derivatives are bounded.

Then the first m moments of $\psi(t)$ are zero, that is, $\int t^i \psi(t) dt = 0$ for $0 \leq i \leq m$. ◇

Impossibility of Compact Support, Infinite Differentiability, and Orthonormality. Suppose we have an orthonormal wavelet basis such that $\psi(t)$ is compactly supported, and infinitely differentiable (i.e., $\psi(t) \in C^\infty$). Then all the conditions of Theorem 13.1 are satisfied. So the moments of $\psi(t)$ are zero, and therefore $\psi(t) = 0$ for all t violating the unit-norm property of $\psi(t)$. We cannot, therefore, design compactly supported orthonormal wavelets which are infinitely differentiable; only a finite Hölder index can be accomplished. A similar observation can be made even when $\psi(t)$ is not compactly supported as long as it decays faster than any inverse polynomial (e.g., exponential decay).

The vanishing moment condtion $\int t^i \psi(t) dt = 0, 0 \leq i \leq m$ implies that the L^2 Fourier transform $\Psi(\omega)$ has $m+1$ zeros at $\omega = 0$. This follows by using standard theorems on the L^1-FT [Rudin, 1966].† Thus, the first m derivatives of $\Psi(\omega)$ vanish at $\omega = 0$. This implies a certain degree of flatness at $\omega = 0$. Summarizing, we have:

Theorem 13.2. Flatness in Frequency and Regularity in Time. Suppose we have a compactly supported $\psi(t)$ generating an orthonormal wavelet basis $\{2^{k/2}\psi(2^k t - n)\}$, and let $\psi(t) \in C^m$, with m derivatives bounded. Then $\Psi(\omega)$ has $m+1$ zeros at $\omega = 0$. ◇

Return now to the wavelet construction technique described in Sec. 11. We started from a paraunitary FIR filter bank (Fig. 4.1(a)) and obtained the scaling function $\phi(t)$ and wavelet function $\psi(t)$ as in (13.1) and (13.2). The FIR nature implies that $\psi(t)$ has compact support (Sec. 12). With the mild conditions of Theorem 11.5 satisfied, we have an orthonormal wavelet basis for L^2. We see that if the wavelet $\psi(t)$ has Hölder index α, then it satisfies all the conditions of Theorem 13.2 where m is the integer part of α. Thus $\Psi(\omega)$ has $m+1$ zeros at $\omega = 0$. But since $\Phi(0) \neq 0$ (Section 10.4), we conclude from the dilation equation $\Psi(\omega) = H_s(e^{j\omega/2})\Phi(\omega/2)$ that the highpass FIR filter $H_s(z)$ has $m+1$ zeros at $\omega = 0$ (i.e., at $z = 1$). Using the relation $H_s(e^{j\omega}) = e^{j\omega} G_s^*(-e^{j\omega})$ we conclude that $G_s(e^{j\omega})$ has $m+1$ zeros at $\omega = \pi$. That is, the lowpass FIR filter $G_s(z)$ has the form $G_s(z) = (1 + z^{-1})^{m+1} F(z)$ where $F(z)$ is FIR. Summarizing, we have:

Theorem 13.3. Zeros at π and regularity. Suppose we wish to design a compactly supported orthonormal wavelet basis for L^2 by designing an FIR filter $G_s(z)$ satisfying the conditions of Theorem 11.5. If $\psi(t)$ has to have the Hölder regularity index α then it is necessary that $G_s(z)$ have the form $G_s(z) = (1 + z^{-1})^{m+1} F(z)$ where $F(z)$ is FIR, and m is the integer part of α. ◇

One zero at π is essential. From Theorem 11.2 we know that we need to have $G_s(e^{j0}) = 1$ for the

† Since $\psi(t) \in L^2$ and has compact support, $\psi(t) \in L^1$ as well.

infinite product (11.1a) to converge. Theorem 11.5 imposes further conditions which enables us to obtain an orthonormal wavelet basis for L^2. One of these conditions is the power symmetric property $|G_s(e^{j\omega})|^2 + |G_s(-e^{j\omega})|^2 = 1$. Together with $G_s(e^{j0}) = 1$ this implies $G_s(e^{j\pi}) = 0$. Thus, it is necessary to have at least one zero of $G_s(e^{j\omega})$ at π. The filter which generates the Haar basis (Example 11.1) has exactly one zero at π. But the Haar wavelet $\psi(t)$ is not even continuous. If we desire increased regularity (continuity, differentiability ...), we need to put additional zeros at π, as the above theorem shows.

Design techniques for paraunitary filter banks do not automatically yield filters which have zeor(s) at π. This condition has to be incorporated separately. The maximally flat filter bank solution (Sec. 4.6) does satisfy this property, and in fact even allows us to specify the number of zeros at π.

13.4. Wavelets With Specified Regularity

The fundamental connection between digital filter banks and continuous time wavelets, elaborated in the preceding sections, allows us to construct the scaling function $\phi(t)$ and the wavelet function $\psi(t)$ with specified regularity index α. If $G_s(z)$ has a certain number of zeros at π, this translates into the Hölder regularity index α. We will see that what really matters is not only the number of zeros at π, but also the order of the FIR filter $G_s(z)$.

For a given order N of the filter $G_s(z)$, suppose we wish to put as many of its zeros as possible at π. Let this number be K. What is the largest possible K? We can't have all N zeros at π because we have imposed the power symmetric condition on $G_s(z)$. The best we can do is to put all the unit-circle zeros at π. The power symmetric condition says that $G(z) \triangleq \widetilde{G}_s(z)G_s(z)$ is a half-band filter. This filter has order $2N$, with $2K$ zeros at π. Since we wish to maximize K for fixed N, the solution for $G(z)$ is the maximally flat FIR filter (Fig. 4.5), given in (4.23). As the filter in (4.23) has $2K$ zeros at π and order $2N = 4K - 2$ we conclude that $K = (N+1)/2$. For example if $G_s(z)$ is a fifth order power symmetric filter it can have at most three zeros at π.

The 20% Regularity Rule

Suppose $G_s(z)$ has been designed to be FIR power symmetric of order N, with the number K of zeros at π adjusted to be maximum (i.e., $K = (N+1)/2$). Then it can be shown that the corresponding scaling and wavelet functions have a Hölder regularity index $\alpha \approx 0.2K$. This approximate estimate is poor for small K but improves as K grows. Thus every additional zero at π contributes to $\approx 20\%$ improvement in regularity.

For $K = 4$ (i.e., 7th order $G_s(z)$) we have $\alpha = 1.275$ which means that the wavelet $\psi(t)$ is once differentiable and the derivative is Hölder continuous with Lipschitz constant 0.275. For $K = 10$ (19th order $G_s(z)$) we have $\alpha = 2.9$, so the wavelet $\psi(t)$ is twice differentiable and the second derivative has Hölder

regularity index 0.9.

Design procedure. The design procedure is therefore very simple. For a specified regularity index α, we can estimate K and hence $N = 2K - 1$. For this K, we compute the coefficients of the FIR half band maximally flat filter $G(z)$ using (4.23). From this we compute a spectral factor $G_s(z)$ of the filter $G(z)$. Tables of the filter coefficients $g_s(n)$ for various values of N can be found in [Daubechies, 1992]. From the coefficients $g_s(n)$ of the FIR filter $G_s(z)$, the compactly supported scaling and wavelet functions are fully determined via the dilation equations. These wavelets are called Daubechies wavelets and were first generated in [Daubechies, 1988]. Fig. 13.1(c) is an example, generated with a 9th order FIR filter $G_s(z)$, whose response is shown as Case 2 in Fig. 13.1(a).

The above regularity estimates, based on frequency domain behavior, give a single number α that represents the regularity of $\psi(t)$ for all t. It is also possible to define *pointwise* or *local* regularity of the function $\psi(t)$ so that its smoothness can be estimated as a function of time t. These estimation methods, based on time domain iterations, are more sophisticated but give a detailed view of the behavior of $\psi(t)$. Detailed discussions on obtaining various kinds of estimates for regularity can be found in [Daubechies and Lagarias, 1991], [Daubechies, 1992] and [Rioul, 1992].

14. CONCLUDING REMARKS

We introduced the wavelet transform, and studied its connection to filter banks and short time Fourier transforms. A number of mathematical concepts such as frames and Riesz bases were reviewed and used later for a more careful study of wavelets. We introduced the idea of multiresolution analysis, and explained the connections both to filter banks and wavelets. This connection was then used to generate orthonormal wavelet bases from paraunitary filter banks. Such wavelets have compact support when the filter bank is FIR. The regularity or smoothness of the wavelet was quantified in terms of the Hölder exponent. We showed that we can achieve any specified Hölder exponent for compactly supported wavelets by restricting the lowpass filter of the FIR paraunitary filter bank to be a maximally flat power-symmetric filter, with a sufficient number of zeros at π.

Why Wavelets?

Discussions comparing wavelets with other types of time frequency transforms appear at several places in this chapter. Here is a list of these discussions:

1. Sec. 2.5 discusses basic properties of wavelets, and Sec. 2.7 gives an elementary comparison of wavelet basis with the Fourier basis.

2. Sec. 3.2 compares the wavelet transform with the short time Fourier transform, and shows the time frequency tilings for both cases.
3. Sec. 9 gives a deeper comparison with the STFT in terms of stability properties of the inverse, existence of frames, and so forth.
4. Sec. 13 shows a comparison to the traditional filter bank design approach. In traditional designs, the appearance of zero(s) at π is not considered important. At the beginning of Sec. 13 (under "Why regularity"), we discuss the importance of these zeros in wavelets as well as in tree structured filter banks

Further reading

The literature on wavelet theory and applications is enormous. This chapter is only a brief introduction, concentrating on one dimensional orthonormal wavelets. There exist many results on the topics of multidimensional wavelets, biorthogonal wavelets, and wavelets based on IIR filter banks. Two special issues of the IEEE Transactions have appeared on the topic so far [IEEE, 1992] and [IEEE, 1993], covering some of these topics. Multidimensional wavelets are treated by several authors in the edited volume [Chui 1992b], and the filter bank perspective can be found in [Kovačević and Vetterli, 1992]. Advanced results on multidimensional wavelets can be found in [Cohen and Daubechies, 1993], and the theory of biorthogonal wavelets is treated in [Cohen, et al., 1992]. Sampling theorems for wavelet and multiresolution subspaces have been introduced by Walter [1992], and extended by other authors. See Djokovic and Vaidyanathan [1994], and references therein. Advanced results on wavelets constructed from M-channel filter banks can be found in the chapter by Gopinath and Burrus (see [Chui, 1992b]), and in [Steffen, et al., 1993]. The reader can also refer to the collections of chapters in Chui [1992b] and [Benedetto and Frazier, 1994], and many references therein.

Acknowledgement.

The authors are grateful to Dr. Ingrid Daubechies, Princeton University, for many useful e-mail discussions on wavelets.

APPENDIX A. DISTRIBUTIONS AND THEIR FOURIER TRANSFORMS

There are many commonly used examples such as $x(t) = 1$, which are not in L^p for any finite p. For these we cannot define the Fourier transform in the sense of Sec. 6.3. However, in electrical sciences (even in physics) we often make statements like

$$\begin{aligned} x(t) = 1 \quad &\text{implies} \quad X(\omega) = 2\pi\delta(\omega) \\ \text{and } x(t) = \delta(t) \quad &\text{implies} \quad X(\omega) = 1 \text{ for all } \omega. \end{aligned} \tag{A.1}$$

The Dirac delta $\delta(t)$ is actually a fictitious function, assumed to be zero everywhere except at $t = 0$ (where it is undefined), and satisfying $\int \delta(t)dt = 1$. It is often regarded as the limit of a sequence of functions $f_n(t)$ with $\int f_n(t)dt = 1$ and such that $f_n(t) \to 0$ pointwise for all $t \neq 0$. If the Dirac delta were a function in the usual sense, its Lebesgue integral would be zero rather than one, since the "function" is zero a.e. There are many such mathematical difficulties in dealing with Dirac delta.

In mathematics, the delta function is regarded as a linear mapping that takes a function $s(t)$ as an "input", and produces the number $s(0)$ as an output (compare with the statement $\int s(t)\delta(t)dt = s(0)$, which can be found in engineering texts, e.g., [Oppenheim, et al., 1983]). Of course, we have to define the class of allowed inputs $s(t)$ carefully. For example, if $s(t)$ is not continuous at $t = 0$ then the Dirac delta cannot be properly defined. With appropriate restrictions on the class of allowed "inputs," such mappings are called *distributions* (all precise definitions will be given below).

The space $\mathcal{D}$ from which the inputs $s(t)$ are drawn is usually restricted to be the set of all functions which have two properties: (a) compact support (finite duration), and (b) infinite differentiability everywhere. In particular they are continuous everywhere. We will see below that this allows us to define "derivatives of distributions," and so forth. It has been found that a slightly larger class of functions $\mathcal{S} \supset \mathcal{D}$ is more useful. The class $\mathcal{S}$ is defined similar to $\mathcal{D}$ with the exception that the "compact support" requirement is replaced with the milder condition that the functions decay faster than any inverse polynomial (i.e., faster than $|t|^{-n}$ for any integer n), as $|t| \to \infty$. It can be shown that, while $\mathcal{D} \subset \mathcal{S}$, the set $\mathcal{S}$ is itself smaller than L^1. That is,

$$\mathcal{D} \subset \mathcal{S} \subset L^1. \tag{A.2}$$

Recall that the FT of an L^1 function may not be in L^1 (Sec. 6.3). Similarly the FT of a nonzero function in $\mathcal{D}$ is not in $\mathcal{D}$, because $s(t)$ and its FT cannot both be of finite duration. However, the set $\mathcal{S}$ sandwiched between $\mathcal{D}$ and L^1 has this beautiful property: the L^1-FT of any function in $\mathcal{S}$ still belongs to $\mathcal{S}$ [Rudin, 1973]. This will be useful in defining Fourier transforms of tempered distributions (see below).

Definitions

1. A *functional* $\lambda[.]$, defined on a set $\mathcal{R}$ of functions, takes an element $s(t) \in \mathcal{R}$ as input and produces a complex number $\lambda[s(t)]$ as the output. A *linear functional* is a functional that satisfies the usual meaning of linearity, that is, $\lambda[a_1 s_1(t) + a_2 s_2(t)] = a_1 \lambda[s_1(t)] + a_2 \lambda[s_2(t)]$.
2. Linear functionals on $\mathcal{D}$ are called *distributions*, whereas linear functionals on $\mathcal{S}$ are called *tempered distributions*.

For example, if λ is the Dirac delta distribution, $\lambda[s(t)] = s(0)$. Fig. A.1 shows a schematic of distributions in general, and the Dirac delta in particular.

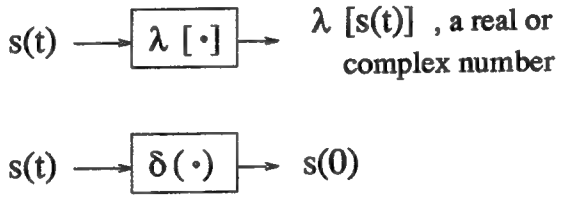

Fig. A.1. (a) Schematic of a distribution $\lambda[\cdot]$ and (b) the example of delta function as a distribution.

Regular and irregular distributions. Let $x(t)$ be a locally integrable function (i.e., the Lebesgue $\int_a^b x(t)dt$ exists for every finite a, b), not growing faster than polynomials as $|t| \to \infty$. We can use it to define a linear functional λ on $\mathcal{S}$ (or $\mathcal{D}$) as follows: for any $s(t) \in \mathcal{S}$ define

$$\lambda[s(t)] = \int x(t)s(t)dt. \tag{A.3}$$

We then say that the distribution λ is induced by the function $x(t)$. One can view the Dirac delta distribution as being described by

$$\lambda[s(t)] = \int \delta(t)s(t)dt = s(0) \tag{A.4}$$

but it is not an induced distribution because $\delta(t)$ is only a fictitious function. Distributions that are induced by locally integrable functions as in (A.3) are said to be *regular*. Dirac delta is not a regular distribution.

Fourier transforms of tempered distributions. We define the Fourier transform of a tempered distribution λ as another tempered distribution Λ such that

$$\Lambda[s(t)] = \lambda[S(\omega)]. \tag{A.5}$$

Thus the FT of the distribution λ is the same distribution operating on $S(\omega)$ rather than $s(t)$, as shown schematically in Fig. A.2. This definition makes sense because the domain of tempered distributions is the class $\mathcal{S}$ and, as already stated, if $s(t) \in \mathcal{S}$ then $S(\omega) \in \mathcal{S}$.

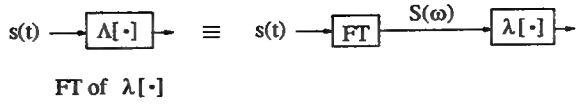

Fig. A.2. The Fourier transform (FT) of a tempered distribution, shown schematically.

For example let λ be the Dirac delta distribution. Then

$$\Lambda[s(t)] = \lambda[S(\omega)] = S(0) = \int s(v)dv. \tag{A.6}$$

The extreme right hand side represents a regular distribution induced by the locally integrable function $X(\omega) = 1$. (Note that v in (A.6) is just a dummy variable of integration; you can replace it with ω). So we say that the FT of the Dirac delta distribution is the constant function ($X(\omega) = 1$ everywhere). *What we really mean is that the FT of the Dirac delta distribution λ is the distribution Λ induced by the constant function.* Fig. A.3 gives a schematic summary of this.

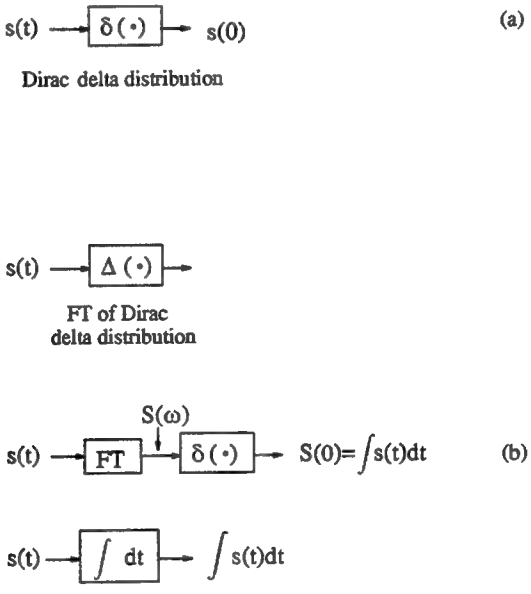

Fig. A.3. (a) The Dirac delta distribution, and (b) its Fourier transform, shown schematically.

By a dual argument we can show that the FT of the constant function is the delta function. Again the real meaning of this statement is: the FT of the regular distribution induced by the constant function is the Dirac delta distribution. We can give similar meaning to the FT of a polynomial, and conversely interpret

a polynomial as the FT of a distribution. Example: the FT of the polynomial t is the distribution that extracts derivatives at the origin (why?).

Many other operations on distributions can be defined similarly. For example the derivative of a distribution is the distribution of the derivative (except for a sign): $\lambda'[s(t)] = -\lambda[s'(t)]$, as schematically shown in Fig. A.4. This definition opens up a whole theory of calculus for distributions, but we will not require them here. An introduction to distributions can be found in [Kolmogorov and Fomin, 1970]. Advanced results can be found in [Rudin, 1973].

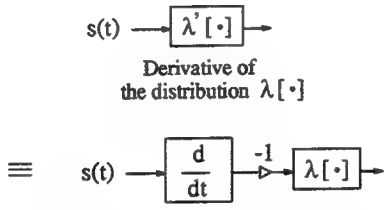

Fig. A.4. The derivative of a distribution $\lambda[\cdot]$.

15. BIBLIOGRAPHY

Akansu, A.N., and Haddad, R.A., *Multiresolution signal decomposition: transforms, subbands, and wavelets,* Academic Press, Inc., 1992.

Anderson, B. D. O., and Moore, J. B. *Optimal filtering,* Prentice Hall, Inc., Englewood Cliffs, NJ, 1979.

Apostol, T.M. *Mathematical analysis,* Addison-Wesley, 1974.

Allen, J. B., and Rabiner, L. R. "A unified theory of short-time spectrum analysis and synthesis," Proc. IEEE, vol. 65, pp. 1558–1564, Nov. 1977.

Belevitch, V. *Classical network theory,* Holden Day, Inc., San Francisco, 1968.

Bellanger, M., Bonnerot, G., and Coudreuse, M. "Digital filtering by polyphase network: application to sample rate alteration and filter banks," *IEEE Trans. on Acoust. Speech and Signal Proc.,* vol. ASSP-24, pp. 109-114, April 1976.

Benedetto, J. J., and Frazier, M. W. *Wavelets: mathematics and applications,* CRC Press, Inc., 1994.

Brune, O. "Synthesis of a finite two terminal network whose driving point imped- ance is a prescribed function of frequency," *J. Math., and Phys.,* vol. 10, pp. 191-235, 1931.

Chui, C. K. *An introduction to wavelets,* Academic Press, 1992a.

Chui, C. K. (edited), *Wavelets: a tutorial in theory and applications,* Academic Press, 1992b.

Cohen, A., Daubechies, I., and Feauveau, J. C. "Biorthogonal bases of compactly supported wavelets," *Comm. on Pure and Appl. Math.,* vol. 45, pp. 485-560, 1992.

Cohen, A and Daubechies, I. "Non-separable Bidimensional Wavelet Bases", Rev. Mat. Eberu. Americana, v. 9, pp. 51–137, 1993.

Crochiere, R. E., and Rabiner, L. R. *Multirate digital signal processing,* Englewood Cliffs, NJ: Prentice Hall, 1983.

Croisier, A., Esteban, D., and Galand, C. "Perfect channel splitting by use of interpolation/decimation/tree decomposition techniques," Int. Symp. on Info., Circuits and Systems, Patras, Greece, 1976.

Daubechies, I. "Orthonormal bases of compactly supported wavelets," *Comm. on Pure and Appl. Math.,* vol. 41, pp. 909-996, Nov. 1988.

Daubechies, I. *Ten lectures on wavelets,* SIAM, CBMS series, April 1992.

Daubechies, I., and Lagarias, J. "Two-scale difference equations: existence and global regularity of solutions," SIAM J. Math. Anal., vol. 22, pp. 1388-1410, 1991.

Djokovic, I., and Vaidyanathan, P.P. "Generalized sampling theorems in multiresolution subspaces," Tech. Rep.,

Caltech, August 1994.

Duffin, R. J., and Schaeffer, A. C. "A class of nonharmonic Fourier series," Trans. Amer. Math. Soc., vol. 72, pp. 341–366, 1952.

Flanagan, J. L., and Golden, R. M. "Phase vocoder", Bell Syst. Tech, J., vol. 45, pp. 1493–1509, 1966.

Gabor, D. "Theory of communications," *J. Inst. Elec. Eng.,* (London), vol. 93, pp. 429-457, 1946.

Grossman, A., and Morlet, J. *Decomposition of Hardy functions into square integrable wavelets of constant shape, SIAM J. Math. Anal.,* vol. 15, pp. 723-736, 1984.

Gopinath, R. A., and Burrus, C. S., "A tutorial overview of filter banks, wavelets, and interrelations," Proc. IEEE Int. Symp. on Circuits and Systems, pp. 104–107, May 1993.

Haar, A. "Zur theorie der orthogonalen funktionen systeme, Math. Ann., vol. 69, pp. 331–371, 1910.

Haaser, N. B., and Sullivan, J. A. *Real analysis,* Dover Publ. Inc., 1971.

Heil, C. E., and Walnut, D. F. "Continuous and discrete wavelet transforms," SIAM review, vol. 31, pp 628–666, Dec. 1989.

Herrmann, O. "On the approximation problem in nonrecursive digital filter design," *IEEE Trans. Circuit theory,* vol. CT-18, pp. 411-413, May 1971.

IEEE, 1992, Special issue on wavelet transforms and multiresolution signal analysis, IEEE Trans. Info. Th., vol. 38, March 1992.

IEEE, 1993, Special issue on wavelets and signal processing, IEEE Trans. Signal Proc., vol. 41, Dec. 1993.

Kolmogorov, A. N., and Fomin, S. V., *Introductory real analysis,* Dover Publ. Inc., 1970.

Kovačević, J., and Vetterli, M. "Nonseparable multidimensional perfect reconstruction filter banks and wavelet bases for R^n," *IEEE Trans. on Info. Theory,* vol. IT-38, Feb. 1992.

Lawton, W. M., "Tight frames of compactly supported affine wavelets," J. Math. Phys., vol. 31, pp. 1898–1901, Aug. 1990.

Mallat, S. "A theory for multiresolution signal decomposition: the wavelet representation," *IEEE Trans. on Pattern Anal., and Machine Intell.,* vol. 11, pp. 674-693, July 1989a.

Mallat, S. "Multiresolution approximations and wavelet orthonormal bases of $L^2(R)$," *Trans. of Amer. Math. Soc.,* vol. 315, pp. 69-87, Sept. 1989b.

Malvar, H. S. *Signal processing with lapped transforms,* Artech House, Norwood, MA, 1992.

Meyer, Y. *Ondelettes et fonctions splines* Seminaire EDP, Ecole Polytechnique, Paris, 1986.

Mintzer, F. "Filters for distortion-free two-band multirate filter banks," *IEEE Trans. on Acoustics, Speech and Signal Proc.,* vol. ASSP-33, pp. 626-630, June 1985.

Naylor, A. W., and Sell, G. R. *Linear operator theory in engineering sciences,* Springer-Verlag, 1982.

Oppenheim, A. V., and Schafer, R. W. *Discrete-time signal processing,* Prentice Hall, Inc., Englewood Cliffs, NJ, 1989.

Oppenheim, A. V., Willsky, A. S., and Young, I. T. *Signals and systems,* Prentice Hall, Inc., 1983.

Papoulis, A. *The Fourier integral and its applications,* McGraw Hill Book Co., 1962.

Portnoff, M. R. "Time-frequency representation of digital signals and systems based on short-time Fourier Analysis," *IEEE Trans. on Acoust. Speech and Signal Proc.,* vol. ASSP-28, pp. 55-69, Feb. 1980.

Riesz and Nagy, *Functional analysis,* Dover Publ. Inc., 1955.

Rioul, O. "Simple regularity criteria for subdivision schemes," Siam J. Math. Anal., vol. 23, pp. 1544-1576, Nov. 1992.

Rioul, O., and Vetterli, M. "Wavelets and signal processing," *IEEE Signal Processing magazine,* pp. 14-38, Oct. 1991.

Rudin, W. *Real and complex analysis,* McGraw-Hill, Inc., 1966.

Rudin, W. *Functional analysis,* McGraw-Hill, Inc., 1973.

Schafer, R. W., and Rabiner L. R., "Design and simulation of a speech analysis-synthesis system based on short-time Fourier analysis, IEEE Trans. Audio and Electroacoust. vol. 21, pp. 165–174, June 1973.

Smith, M. J. T., and Barnwell III, T. P. "A procedure for designing exact reconstruction filter banks for tree structured subband coders," Proc. IEEE Int. Conf. Acoust. Speech, and Signal Proc., pp. 27.1.1-27.1.4, San Diego, CA, March 1984.

Soman, A. K., and Vaidyanathan, P. P. "On orthonormal wavelets and paraunitary filter banks," *IEEE Trans. on Signal Processing,* vol. SP-41, March 1993.

Steffen, P., Heller, P. N., Gopinath, R. A., and Burrus, C. S., "Theory of regular M-band wavelet bases," IEEE Trans. Signal Processing, vol. 41, pp. 3497–3511, Dec. 1993.

Strang, G. "Wavelet transforms versus Fourier transforms," Bull. Amer. Math. Soc., vol. 28, pp. 288–305, April 1993.

Vaidyanathan, P. P. "Theory and design of M-channel maximally decimated quad-rature mirror filters with arbitrary M, having perfect reconstruction property," *IEEE Trans. on Acoustics, Speech and Signal Processing,* vol. ASSP-35, pp. 476-492, April 1987.

Vaidyanathan, P. P. *Multirate systems and filter banks,* Prentice Hall, Inc., Englewood Cliffs, NJ, 1993.

Van Valkenburg, M. E. *Introduction to Modern Network Synthesis,* John Wiley & Sons, Inc., 1960.

Veldhuis, R. N. J., Breeuwer, M., and Van der wall, R. G. "Subband coding of digital audio signals" Philips J.

Res., vol. 44, pp. 329-343, 1989.

Vetterli, M. "A theory of multirate filter banks," *IEEE Trans. on Acoustics, Speech and Signal Processing,* vol. ASSP-35, pp. 356-372, March 1987.

Vetterli, M., and Herley, C. "Wavelets and filter banks," *IEEE Trans. on Signal Processing,* vol. SP-40, 1992.

Walter, G. G. "A sampling theorem for wavelet subspaces," IEEE Trans. on Info. Th., vol. 38, pp. 881-884, March 1992.

Woods, J. W. *Subband image coding,* Kluwer Academic Publishers, Inc., 1991.

Young, R. M. *An introduction to nonharmonic Fourier series,* Academic Press, Inc., 1980.